

Supporting Information

for

Electrochemical Hydrogenation of α -
Ketoesters and Benzoxazinones Using
Carbon Electrodes and a Sustainable
Brønsted Acid

Dion B. Nemez, Baldeep K. Sidhu, Patrick K. Giesbrecht, Jason D. Braun and David E.

*Herbert**

^aDepartment of Chemistry and the Manitoba Institute for Materials, University of

Manitoba, 144 Dysart Road, Winnipeg, Manitoba, R3T 2N2, Canada;

*david.herbert@umanitoba.ca

TABLE OF CONTENTS

GENERAL EXPERIMENTAL DETAILS.....	6
CYCLIC VOLTAMMETRY.....	7
Table S1. Tabulated Cyclic Voltammetry (CV) Data ^a	7
Figure S1. CV of 10 mM 1a before (red) and after (black) the addition of 3 equivalents of acetic acid, taken at 100 mVs ⁻¹ in CH ₃ CN containing 0.1 M <i>n</i> Bu ₄ NPF ₆	8
Figure S2. CV of 8 mM 1b before (red) and after (black) the addition of 3 equivalents of acetic acid, taken at 100 mVs ⁻¹ in CH ₃ CN containing 0.1 M <i>n</i> Bu ₄ NPF ₆	8
Figure S3. CV of 8 mM 1c before (red) and after (black) the addition of 3 equivalents of acetic acid, taken at 100 mVs ⁻¹ in CH ₃ CN containing 0.1 M <i>n</i> Bu ₄ NPF ₆	9
Figure S4. CV of 15 mM 1d before (red) and after (black) the addition of 3 equivalents of acetic acid, taken at 100 mVs ⁻¹ in CH ₃ CN containing 0.1 M <i>n</i> Bu ₄ NPF ₆	9
Figure S5. CV of 4 mM 1e before (red) and after (black) the addition of 3 equivalents of acetic acid, taken at 100 mVs ⁻¹ in CH ₃ CN containing 0.1 M <i>n</i> Bu ₄ NPF ₆	10
Figure S6. CV of 3 mM 1f before (red) and after (black) the addition of 3 equivalents of acetic acid, taken at 100 mVs ⁻¹ in CH ₃ CN containing 0.1 M <i>n</i> Bu ₄ NPF ₆	10
Figure S7. CV of 10 mM 1g before (red) and after (black) the addition of 3 equivalents of acetic acid, taken at 100 mVs ⁻¹ in CH ₃ CN containing 0.1 M <i>n</i> Bu ₄ NPF ₆	11
Figure S8. CV of 10 mM 1h before (red) and after (black) the addition of 3 equivalents of acetic acid, taken at 100 mVs ⁻¹ in CH ₃ CN containing 0.1 M <i>n</i> Bu ₄ NPF ₆	11
Figure S9. CV of 15 mM 1i before (red) and after (black) the addition of 3 equivalents of acetic acid, taken at 100 mVs ⁻¹ in CH ₃ CN containing 0.1 M <i>n</i> Bu ₄ NPF ₆	12
Figure S10. CV of 6 mM 1j before (red) and after (black) the addition of 3 equivalents of acetic acid, taken at 100 mVs ⁻¹ in CH ₃ CN containing 0.1 M <i>n</i> Bu ₄ NPF ₆	12
Figure S11. CV of 10 mM 1k before (red) and after (black) the addition of 3 equivalents of acetic acid, taken at 100 mVs ⁻¹ in CH ₃ CN containing 0.1 M <i>n</i> Bu ₄ NPF ₆	13
Figure S12. CV of 15 mM 2a before (red) and after (black) the addition of 3 equivalents of acetic acid, taken at 100 mVs ⁻¹ in CH ₃ CN containing 0.1 M <i>n</i> Bu ₄ NPF ₆	13
Figure S13. CV of 3 mM 2b before (red) and after (black) the addition of 3 equivalents of acetic acid, taken at 100 mVs ⁻¹ in CH ₃ CN containing 0.1 M <i>n</i> Bu ₄ NPF ₆	14
Figure S14. CV of 1 mM 2c before (red) and after (black) the addition of 3 equivalents of acetic acid, taken at 100 mVs ⁻¹ in CH ₃ CN containing 0.1 M <i>n</i> Bu ₄ NPF ₆	14
Figure S15. CV of 3 mM 2d before (red) and after (black) the addition of 3 equivalents of acetic acid, taken at 100 mVs ⁻¹ in CH ₃ CN containing 0.1 M <i>n</i> Bu ₄ NPF ₆	15
Figure S16. CV of 2 mM 2e before (red) and after (black) the addition of 3 equivalents of acetic acid, taken at 100 mVs ⁻¹ in CH ₃ CN containing 0.1 M <i>n</i> Bu ₄ NPF ₆	15
Figure S17. CV of 4 mM 2f before (red) and after (black) the addition of 3 equivalents of acetic acid, taken at 100 mVs ⁻¹ in CH ₃ CN containing 0.1 M <i>n</i> Bu ₄ NPF ₆	16
Figure S18. CV of 8 mM 2g before (red) and after (black) the addition of 3 equivalents of acetic acid, taken at 100 mVs ⁻¹ in CH ₃ CN containing 0.1 M <i>n</i> Bu ₄ NPF ₆	16
POTENTIOSTATIC ELECTROLYSIS	17
Figure S19. Photographs showing three views of the electrochemical set-up.....	17
Figure S20. CPE plot for hydrogenation of 1a	18
Figure S21. CPE plot for hydrogenation of 1b	19
Figure S22. CPE plot for hydrogenation of 1c	19
Figure S23. CPE plot for hydrogenation of 1d	20
Figure S24. CPE plot for hydrogenation of 1e	20

Figure S25. CPE plot for hydrogenation of 1f	21
Figure S26. CPE plot for hydrogenation of 1g	21
Figure S27. CPE plot for hydrogenation of 1h	22
Figure S28. CPE plot for hydrogenation of 1i	22
Figure S29. CPE plot for hydrogenation of 1j	23
Figure S30. CPE plot for hydrogenation of 2a	23
Figure S31. CPE plot for hydrogenation of 2b	24
Figure S32. CPE plot for hydrogenation of 2c	24
Figure S33. CPE plot for hydrogenation of 2d	25
Figure S34. CPE plot for hydrogenation of 2e	25
Figure S35. CPE plot for hydrogenation of 2f	26
Figure S36. CPE plot for hydrogenation of 2g	26
Figure S37. Charge vs. time plots of controlled potential electrolysis of 1a . Conditions: 3.5 mM 1a , $E_{app} = -0.90$ vs Ag/AgCl (-1.23 V vs FcH ^{0/+}), 90% v/v CH ₃ CN/H ₂ O, 0.1 M LiClO ₄ , reticulated vitreous carbon (RVC) working electrode (~ 700 cm ²), graphite rod counter electrode in a fritted tube, Ag/AgCl quasi-reference electrode, constant sparge with Ar (1 atm).	27
Table S2. Average current consumption during controlled potential electrolysis of 1d in 90% v/v CH ₃ CN/H ₂ O compared with in neat CH ₃ CN.....	27
Preparation of Novel Ketoester and Benzoxazinone Substrates	28
General Procedure for Electrochemical Hydrogenation and Product Isolation.....	31
Hydrogenated Product Characterization	31
¹H NMR/¹³C NMR SPECTRA.....	40
Figure S38. ¹ H NMR (300 MHz, 22 °C, CDCl ₃) of 1a-H₂ . Unreacted starting material 1a is denoted with an asterisk (*).	40
Figure S39. ¹³ C{ ¹ H} NMR (75 MHz, 22 °C, CDCl ₃) of 1a-H₂ . Unreacted starting material 1a is denoted with an asterisk (*).	40
Figure S40. ¹ H NMR (300 MHz, 22 °C, CDCl ₃) of 1b-H₂ . Unreacted starting material 1b is denoted with an asterisk (*).	41
Figure S41. ¹³ C{ ¹ H} NMR (75 MHz, 22 °C, CDCl ₃) of 1b-H₂ . Unreacted starting material 1b is denoted with an asterisk (*).	41
Figure S42. ¹ H NMR (300 MHz, 22 °C, CDCl ₃) of 1c-H₂ . Unreacted starting material 1c is denoted with an asterisk (*).	42
Figure S43. ¹³ C{ ¹ H} NMR (75 MHz, 22 °C, CDCl ₃) of 1c-H₂ . Unreacted starting material 1c is denoted with an asterisk (*).	42
Figure S44. ¹ H NMR (300 MHz, 22 °C, CDCl ₃) of 1d-H₂ . Unreacted starting material 1d is denoted with an asterisk (*).	43
Figure S45. ¹³ C{ ¹ H} NMR (75 MHz, 22 °C, CDCl ₃) of 1d-H₂ . Unreacted starting material 1d is denoted with an asterisk (*).	43
Figure S46. ¹ H NMR (300 MHz, 22 °C, CDCl ₃) of 1e-H₂ . Unreacted starting material 1e is denoted with an asterisk (*).	44
Figure S47. ¹³ C{ ¹ H} NMR (75 MHz, 22 °C, CDCl ₃) of 1e-H₂ . Unreacted starting material 1e is denoted with an asterisk (*).	44
Figure S48. ¹ H NMR (300 MHz, 22 °C, CDCl ₃) of 1f-H₂ . Unreacted starting material 1f is denoted with an asterisk (*).	45
Figure S49. ¹³ C{ ¹ H} NMR (75 MHz, 22 °C, CDCl ₃) of 1f-H₂ . Unreacted starting material 1f is denoted with an asterisk (*).	45
Figure S50. ¹ H NMR (300 MHz, 22 °C, CDCl ₃) of 1g-H₂ . Unreacted starting material 1g is denoted with an asterisk (*).	46
Figure S51. ¹³ C{ ¹ H} NMR (75 MHz, 22 °C, CDCl ₃) of 1g-H₂ . Unreacted starting material 1g is denoted with an asterisk (*).	46

Figure S52. ^1H NMR (300 MHz, 22 °C, CDCl_3) of 1h-H₂ . Unreacted starting material 1h is denoted with an asterisk (*).	47
Figure S53. ^{13}C NMR (75 MHz, 22 °C, CDCl_3) of 1h-H₂ . Unreacted starting material 1h is denoted with an asterisk (*).	47
Figure S54. ^1H NMR (300 MHz, 22 °C, CDCl_3) of 1i-H₂ . Unreacted starting material 1i is denoted with an asterisk (*).	48
Figure S55. $^{13}\text{C}\{^1\text{H}\}$ NMR (75 MHz, 22 °C, CDCl_3) of 1i-H₂ . Unreacted starting material 1i is denoted with an asterisk (*).	48
Figure S56. ^1H NMR (300 MHz, 22 °C, CDCl_3) of 1j-H₂ .	49
Figure S57. $^{13}\text{C}\{^1\text{H}\}$ NMR (75 MHz, 22 °C, CDCl_3) of 1j-H₂ .	49
Figure S58. ^1H NMR (300 MHz, 22 °C, CDCl_3) of 1j .	50
Figure S59. $^{13}\text{C}\{^1\text{H}\}$ NMR (75 MHz, 22 °C, CDCl_3) of 1j .	50
Figure S60. ^1H NMR (300 MHz, 22 °C, CDCl_3) of 2a-H₂ . Unreacted starting material 2a is denoted with an asterisk (*).	51
Figure S61. $^{13}\text{C}\{^1\text{H}\}$ NMR (75 MHz, 22 °C, CDCl_3) of 2a-H₂ .	51
Figure S62. ^1H NMR (500 MHz, 22 °C, CDCl_3) of 2b-H₂ . Unreacted starting material 2b is denoted with an asterisk (*).	52
Figure S63. $^{13}\text{C}\{^1\text{H}\}$ NMR (126 MHz, 22 °C, CDCl_3) of 2b-H₂ .	52
Figure S64. ^1H NMR (300 MHz, 22 °C, CDCl_3) of 2c-H₂ . Unreacted starting material 2c is denoted with an asterisk (*).	53
Figure S65. $^{13}\text{C}\{^1\text{H}\}$ NMR (75 MHz, 22 °C, CDCl_3) of 2c-H₂ .	53
Figure S66. ^1H NMR (500 MHz, 22 °C, CDCl_3) of 2d-H₂ . Unreacted starting material 2d is denoted with an asterisk (*).	54
Figure S67. $^{13}\text{C}\{^1\text{H}\}$ NMR (126 MHz, 22 °C, CDCl_3) of 2d-H₂ . Unreacted starting material 2d is denoted with an asterisk (*).	54
Figure S68. ^1H NMR (300 MHz, 22 °C, CDCl_3) of 2e .	55
Figure S69. $^{13}\text{C}\{^1\text{H}\}$ NMR (75 MHz, 22 °C, CDCl_3) of 2e .	55
Figure S70. ^1H NMR (300 MHz, 22 °C, CDCl_3) of 2e-H₂ .	56
Figure S71. $^{13}\text{C}\{^1\text{H}\}$ NMR (75 MHz, 22 °C, CDCl_3) of 2e-H₂ .	56
Figure S72. ^1H NMR (300 MHz, 22 °C, CDCl_3) of 2f-H₂ . Unreacted starting material 2f is denoted with an asterisk (*).	57
Figure S73. $^{13}\text{C}\{^1\text{H}\}$ NMR (75 MHz, 22 °C, CDCl_3) of 2f-H₂ .	57
Figure S74. ^1H NMR (300 MHz, 22 °C, CDCl_3) of 2g .	58
Figure S75. $^{13}\text{C}\{^1\text{H}\}$ NMR (75 MHz, 22 °C, CDCl_3) of 2g .	58
Figure S76. ^{19}F NMR (282 MHz, 22 °C, CDCl_3) of 2g .	59
Figure S77. ^1H NMR (300 MHz, 22 °C, CDCl_3) of 2g-H₂ . Unreacted starting material 2g is denoted with an asterisk (*).	59
Figure S78. $^{13}\text{C}\{^1\text{H}\}$ NMR (75 MHz, 22 °C, CDCl_3) of 2g-H₂ . Unreacted starting material 2g is denoted with an asterisk (*).	60
Electrolysis Using a Pt Mesh Working Electrode	61
Figure S79. CPE plot of 2d using the standard electrochemical hydrogenation conditions and a Pt mesh working electrode.	61
Figure S80. ^1H NMR (300 MHz, 22 °C, CDCl_3) of 2d using a Pt mesh working electrode. No conversion to product is observed.	62
Figure S81. CPE plot for attempted hydrogenation of 1d using a Pt mesh working electrode.	62
Figure S82. ^1H NMR (300 MHz, 22 °C, CDCl_3) of 1d using a Pt mesh working electrode. No conversion to product is observed.	63
Electrochemical Hydrogenation of 1d in Neat CH₃CN	64
Figure S83. CPE plot for hydrogenation of 1d in neat CH_3CN .	64
Figure S84. ^1H NMR (500 MHz, 22 °C, CDCl_3) of 1d-H₂ produced in neat CH_3CN .	64
pH Changes During Electrolytic Hydrogenation of 1b	65

Electrochemical Hydrogenation of 1a at Lower Electrolyte Concentration	65
Figure S85. CPE plot for electrochemical hydrogenation of 1a using the standard electrochemical hydrogenation conditions but with 1.1 M LiClO ₄	66
Figure S86. ¹ H NMR (300 MHz, 22 °C, CDCl ₃) of 1a , using the standard electrochemical hydrogenation conditions but with 1.1 M LiClO ₄ . Unreacted starting material 1a is denoted with an asterisk (*).	66
Electrochemical Hydrogenation Using Alternative Electrolytes	67
Figure S87. CPE plot of 2d , using the standard electrochemical hydrogenation conditions but with [nBu ₄ N][PF ₆] as the electrolyte.	68
Figure S88. ¹ H NMR (500 MHz, 22 °C, CDCl ₃) of 2d , using the standard electrochemical hydrogenation conditions but with [nBu ₄ N][PF ₆] as the electrolyte. Unreacted starting material 1a is denoted with an asterisk (*). The major species present is [nBu ₄ N][PF ₆].....	68
Attempted Electrochemical Hydrogenation of Alkylated Ketoester 1k	69
Figure S89. CPE plot of the attempted formation of <i>tert</i> -butyl 2-hydroxypropanoate 1k	69
Figure S90. ¹ H NMR (300 MHz, 22 °C, CDCl ₃) of 1k	70
Figure S91. ¹ H NMR (600 MHz, 22 °C, CDCl ₃) of aliquot from attempted electrochemical hydrogenation of 1k	70
X-RAY CRYSTALLOGRAPHY EXPERIMENTAL	71
Figure S92. Solid-state structure of 1j (CCDC 2024463) with thermal ellipsoids shown at 50% probability levels. Selected bond distances (Å) and angles (°): C1-C7 1.4789(19), C7-C8 1.531(2), C7-O1 1.2147(17), C8-O2 1.1999(17), C8-O3 1.3290(16), C9-O3 1.4728(17); C1-C7-C8 119.33(12), O1-C7-C1 122.85(13), O1-C7-C8 117.73(13), O2-C8-C7 122.96(13), O2-C8-O3 126.18(13), O3-C8-C7 110.67(11).	74
Figure S93. (a) Solid-state structure of 2a (CCDC 2026013) with thermal ellipsoids shown at 50% probability levels. Selected bond distances (Å) and angles (°): N(1)-C(7) 1.292(5), N(1)-C(4) 1.394(5), C(7)-C(8) 1.494(5), C(7)-C(9) 1.475(6); C(4)-N(1)-C(7) 118.2(3), N(1)-C(7)-C(8) 122.9(3), N(1)-C(7)-C(9) 119.8(3), C(9)-C(7)-C(8) 117.3(3). (b) View along N1-O1 vector showing the 43° angle between the plane formed by C1-C8/O1/N1 and the plane formed by C9-C14.....	74
Figure S94. (a) Solid-state structure of 2b (CCDC 2026014) with thermal ellipsoids shown at 50% probability levels. Selected bond distances (Å) and angles (°): N(1)-C(7) 1.290(3), N(1)-C(4) 1.393(3), C(7)-C(8) 1.500(3), C(7)-C(9) 1.484(3); C(4)-N(1)-C(7) 119.27(18), N(1)-C(7)-C(8) 122.43(19), N(1)-C(7)-C(9) 118.47(19), C(9)-C(7)-C(8) 119.07(19). (b) View along N1-O1 vector showing the 29° angle between the plane formed by C1-C8/O1/N1 and the plane formed by C9-C14.....	75
REFERENCES	76

GENERAL EXPERIMENTAL DETAILS

All chemicals and reagents were used as received unless otherwise noted. Solutions for electrochemical experiments were made using MilliQ water ($18.2 \Omega \cdot \text{cm}$) and HPLC grade CH_3CN (Sigma Aldrich), with LiClO_4 (98%, Sigma Aldrich) as the supporting electrolyte. Substrates **1a-I**,¹ **1k**² and **2a-g**³ were synthesized following literature procedures and spectroscopic data matched that reported. Substrate **1j** was prepared as described below, and full characterized by multinuclear NMR, HR-MS and single-crystal X-ray diffraction. The substrates were used in 1 to 15 mM concentrations in mixed solutions (10% (v/v) $\text{H}_2\text{O}/\text{CH}_3\text{CN}$). Acetic acid (AA; Fischer Scientific) was used as received in 3 to 30 mM concentrations. NMR spectra were recorded on a Bruker Avance 300 MHz or Bruker Avance-III 500 MHz spectrometer as noted. High-resolution mass spectra were collected on a Bruker microOTOF-QIII.

CYCLIC VOLTAMMETRY

CV experiments were performed using a CHI 760c bipotentiostat, freshly polished (0.05 μm alumina paste) glassy carbon (GCE) disc working electrodes, a Pt wire counter electrode, and a Ag/AgCl aqueous quasi-reference electrode. Electrochemical grade $n\text{Bu}_4\text{NPF}_6$ was used as electrolyte (Sigma Aldrich, 0.1 M). Ferrocene (FcH) was added as an internal standard to each solution upon completion of each set of cyclic voltammetry experiments, allowing potentials to be referenced to the ferrocene/ferrocenium ($\text{FcH}^{0/+}$) redox couple.⁴

Table S1. Tabulated Cyclic Voltammetry (CV) Data^a

Compound	$E / V (i_a/i_c)^b$	$E / V (i_a/i_c)^c$	ΔE (conditions <i>b</i> vs <i>c</i>)
1a	-1.66 (0.50), -2.58	-1.61	0.05
1b	-1.79 (0.81)	-1.66	0.13
1c	-1.84 (0.59), -3.03	-1.66	0.19
1d	-1.87 (0.19), -2.75	-1.81	0.06
1e	-1.69 (0.47), -2.45	-1.55	0.14
1f	-1.69 (0.29), -2.50	-1.54	0.15
1g	-1.60 (0.023)	-1.54	0.06
1h	-1.77 (0.79), -2.73	-1.53	0.24
1i	-1.87 (0.018), -2.82	-1.86	0.01
1j	-1.75 (0.88), -2.57	-1.52	0.23
1k	-2.10 (0.21)	-1.90 ^d	0.20
2a	-1.54 (0.81), -2.27	-1.24	0.30
2b	-1.65 (0.082)	-1.40	0.25
2c	-1.66 (0.76)	-1.31	0.35
2d	-1.59 (0.98), -2.27	-1.34	0.26
2e	-1.56 (0.94)	-1.14	0.42
2f	-1.57 (0.91)	-1.18	0.38
2g	-1.46 (0.48)	-1.30	0.16

^a Cyclic voltammograms were performed in CH_3CN with 0.1 M $n\text{Bu}_4\text{NPF}_6$ both before (conditions *b*) and after (conditions *c*) the addition of 30 mM aqueous CH_3COOH . GCE disk working electrode, Ag/AgCl reference electrode, Pt wire counter electrode, scan rate = 100 mV s^{-1} . All reported $E_{1/2}$ values are referenced to the $\text{FcH}^{0/+}$ (FcH = ferrocene) redox couple.

^d Small shoulder on larger reduction peak of CH_3COOH .

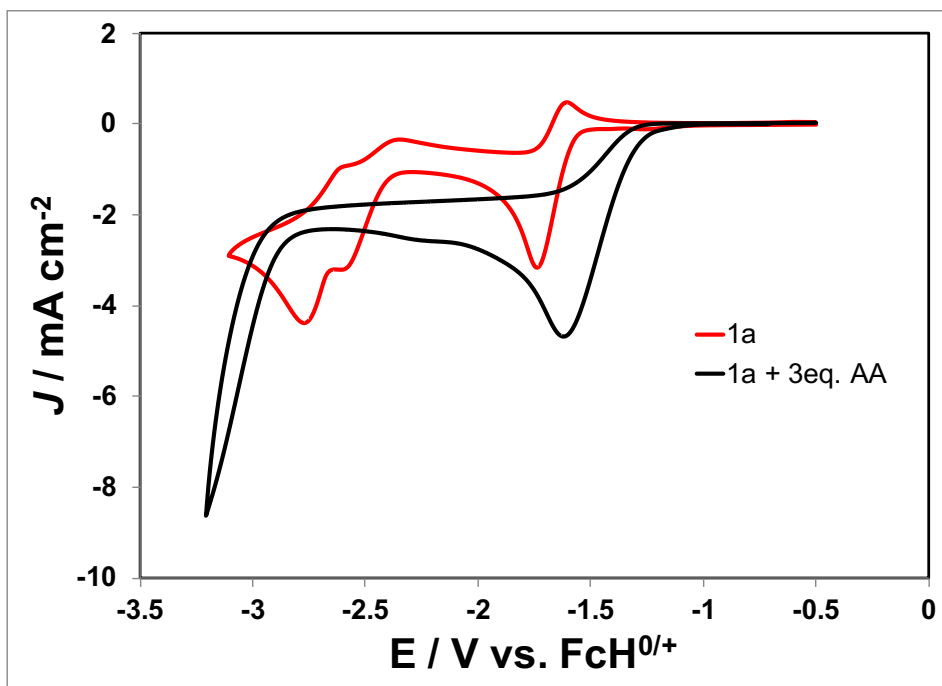


Figure S1. CV of 10 mM **1a** before (red) and after (black) the addition of 3 equivalents of acetic acid, taken at 100 mVs^{-1} in CH_3CN containing 0.1 M $n\text{Bu}_4\text{NPF}_6$.

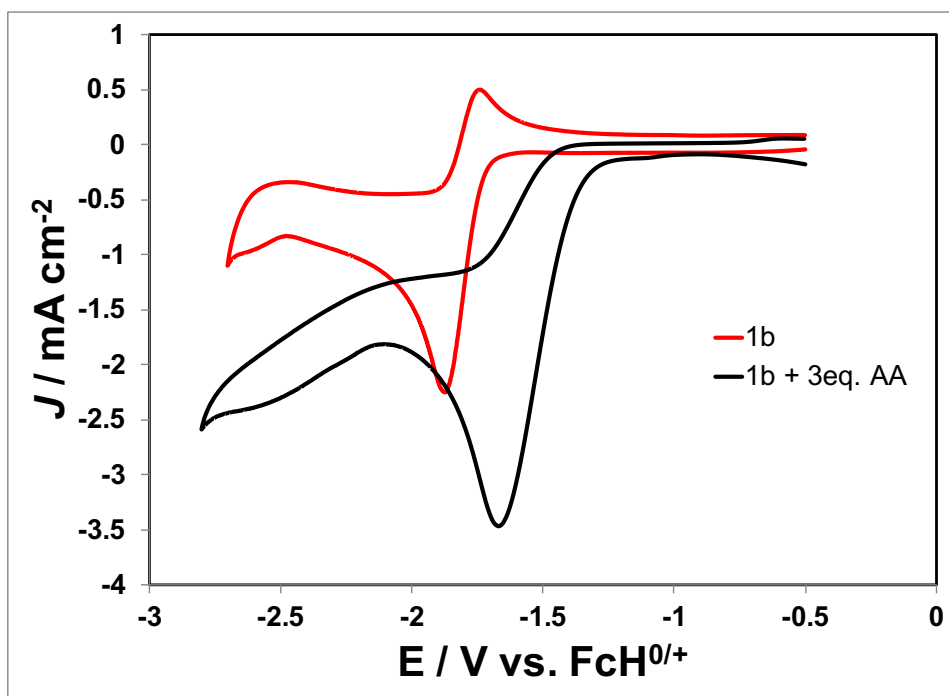


Figure S2. CV of 8 mM **1b** before (red) and after (black) the addition of 3 equivalents of acetic acid, taken at 100 mVs^{-1} in CH_3CN containing 0.1 M $n\text{Bu}_4\text{NPF}_6$.

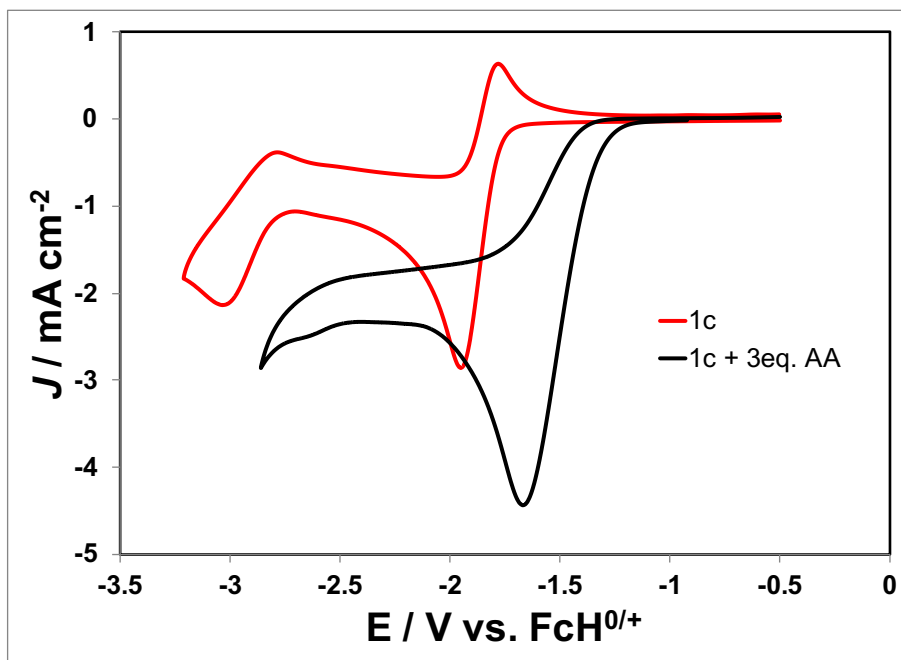


Figure S3. CV of 8 mM **1c** before (red) and after (black) the addition of 3 equivalents of acetic acid, taken at 100 mVs^{-1} in CH_3CN containing 0.1 M $n\text{Bu}_4\text{NPF}_6$.

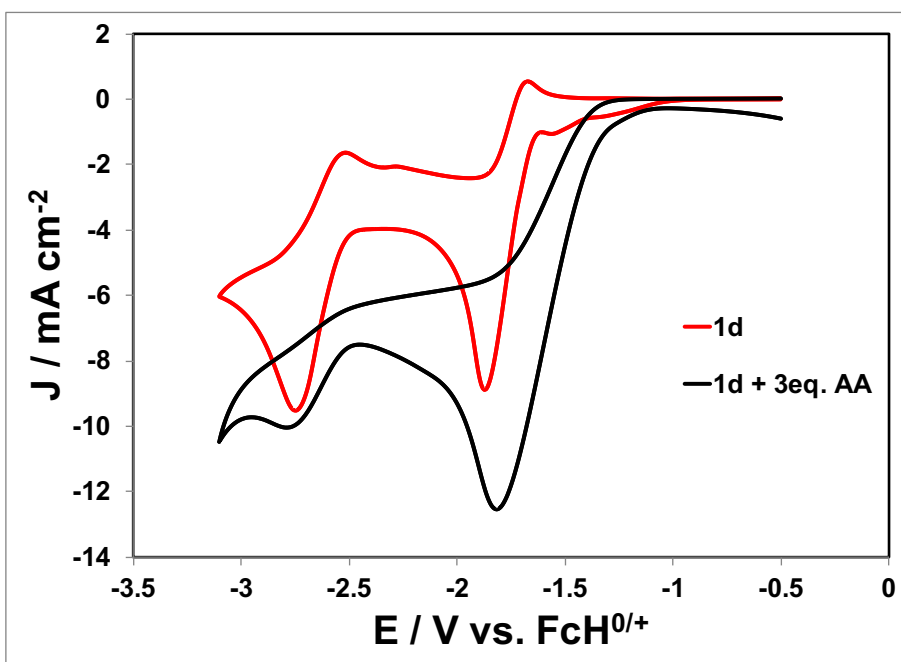


Figure S4. CV of 15 mM **1d** before (red) and after (black) the addition of 3 equivalents of acetic acid, taken at 100 mVs^{-1} in CH_3CN containing 0.1 M $n\text{Bu}_4\text{NPF}_6$.

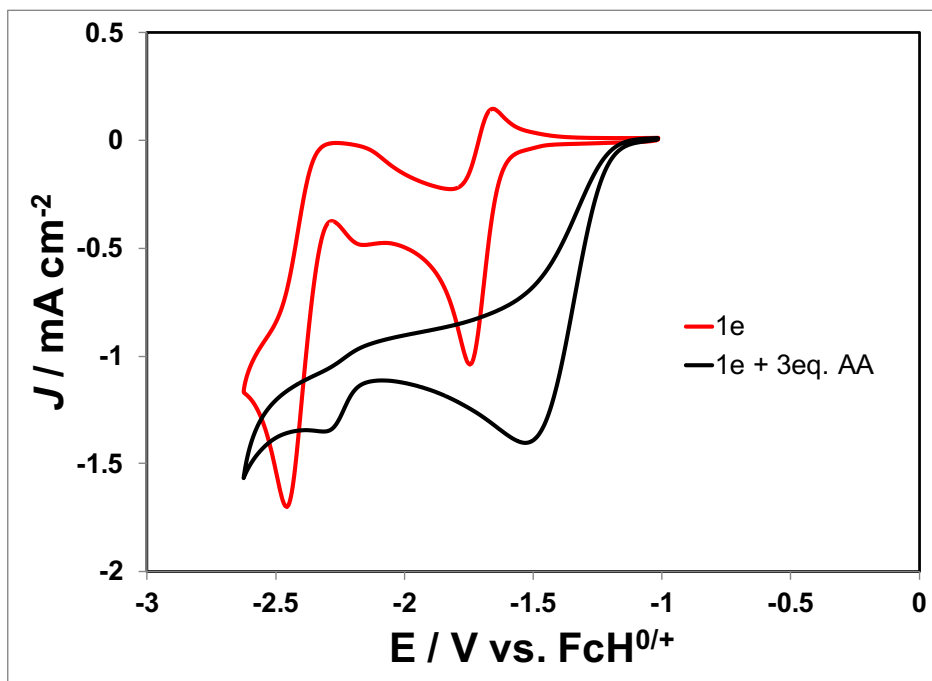


Figure S5. CV of 4 mM **1e** before (red) and after (black) the addition of 3 equivalents of acetic acid, taken at 100 mVs^{-1} in CH_3CN containing 0.1 M $n\text{Bu}_4\text{NPF}_6$.

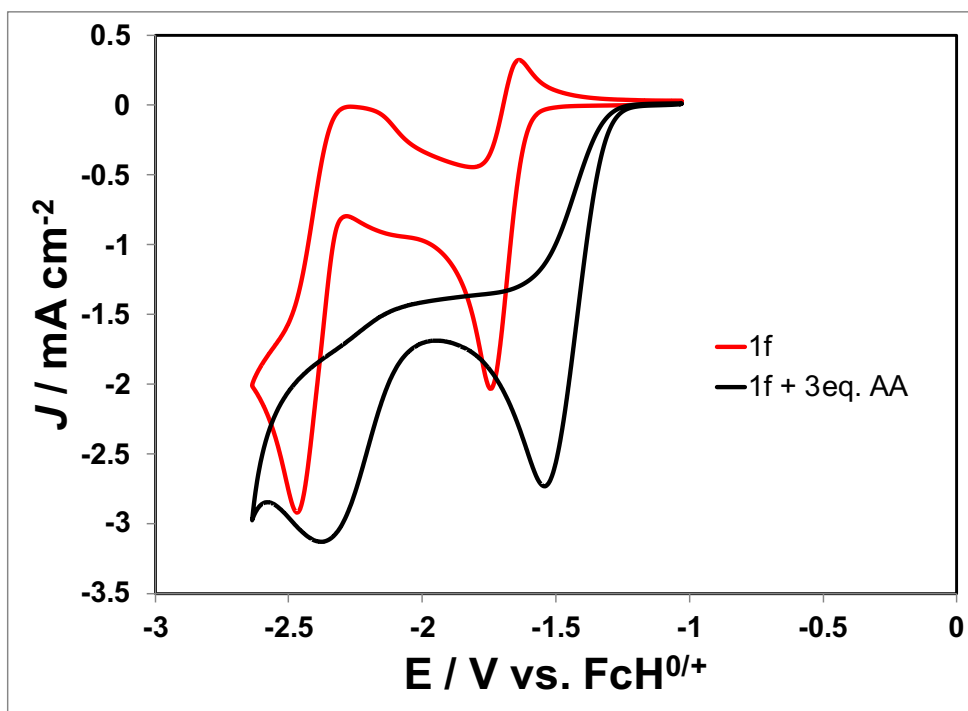


Figure S6. CV of 3 mM **1f** before (red) and after (black) the addition of 3 equivalents of acetic acid, taken at 100 mVs^{-1} in CH_3CN containing 0.1 M $n\text{Bu}_4\text{NPF}_6$.

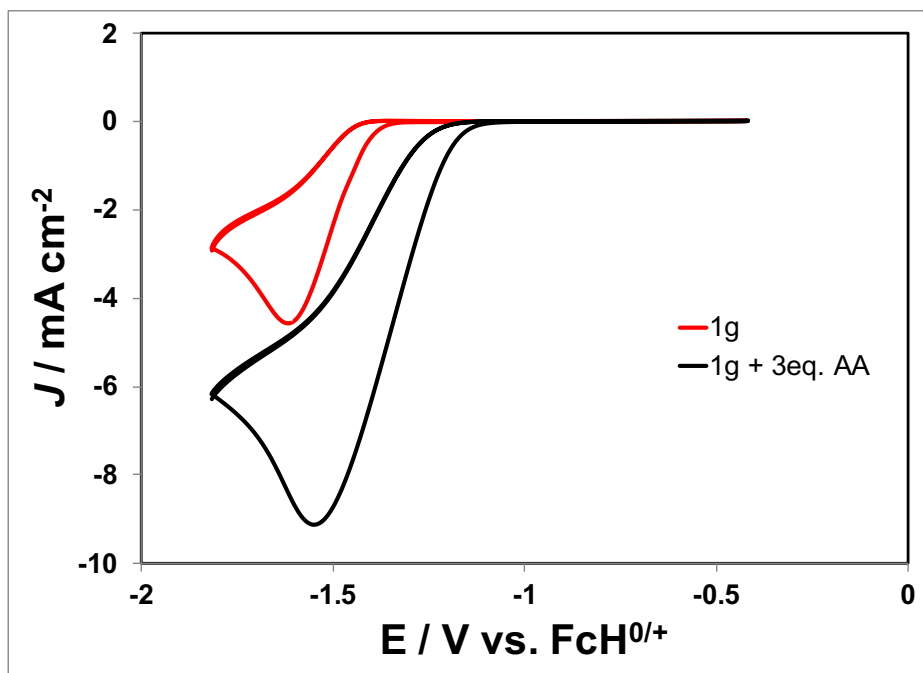


Figure S7. CV of 10 mM **1g** before (red) and after (black) the addition of 3 equivalents of acetic acid, taken at 100 mVs^{-1} in CH_3CN containing 0.1 M $n\text{Bu}_4\text{NPF}_6$.

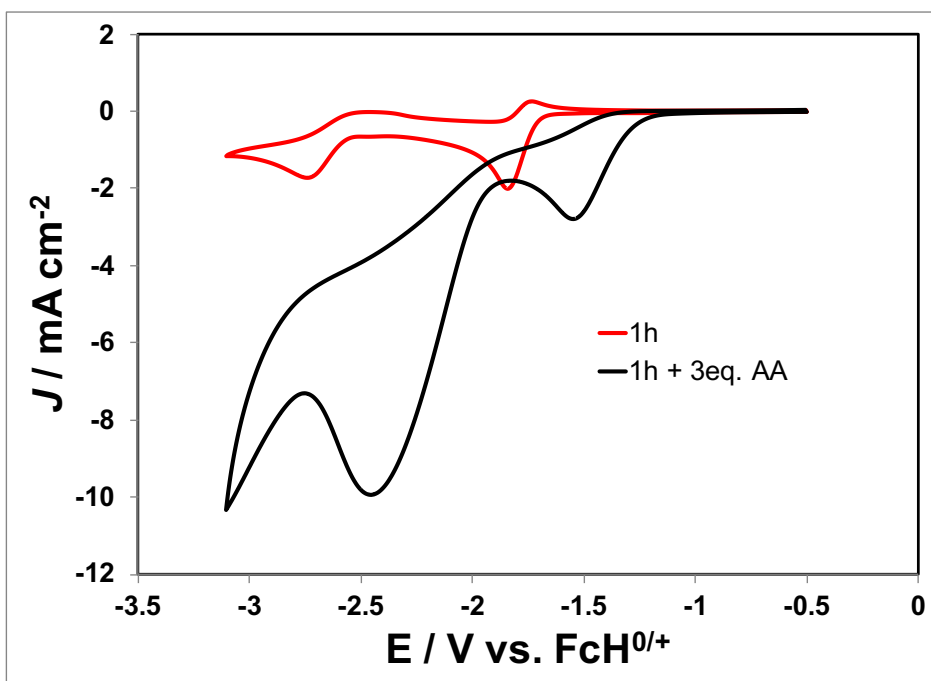


Figure S8. CV of 10 mM **1h** before (red) and after (black) the addition of 3 equivalents of acetic acid, taken at 100 mVs^{-1} in CH_3CN containing 0.1 M $n\text{Bu}_4\text{NPF}_6$.

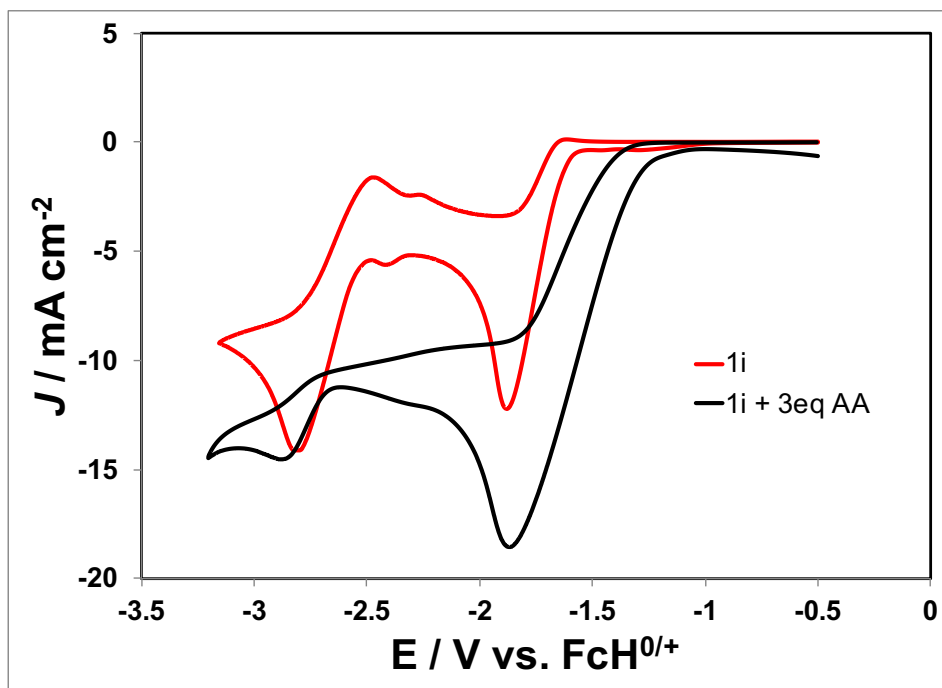


Figure S9. CV of 15 mM **1i** before (red) and after (black) the addition of 3 equivalents of acetic acid, taken at 100 mVs^{-1} in CH_3CN containing 0.1 M $n\text{Bu}_4\text{NPF}_6$.

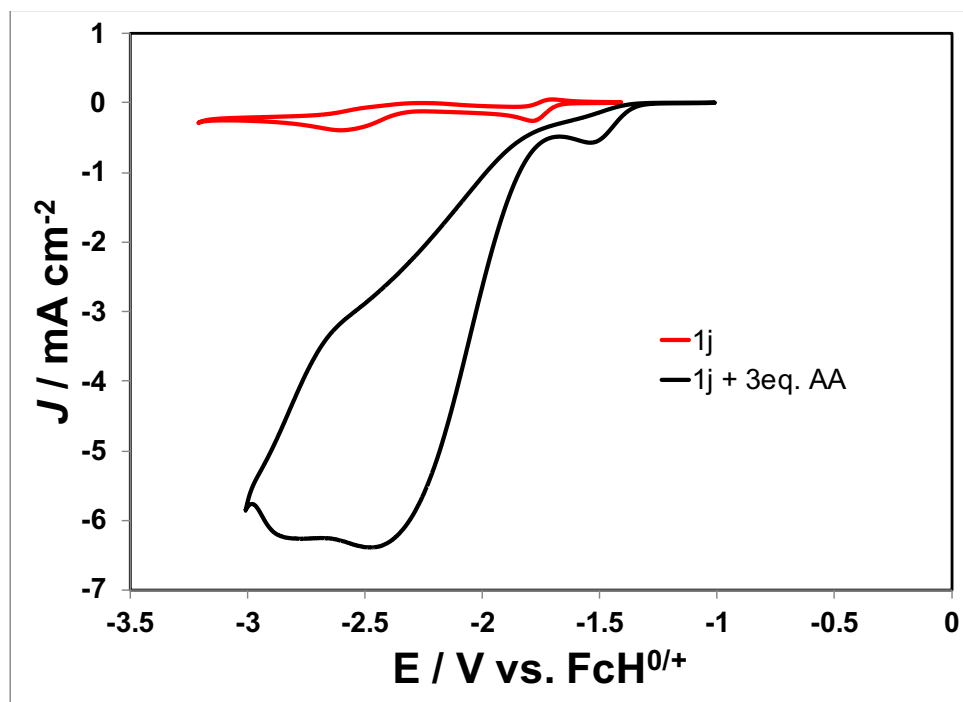


Figure S10. CV of 6 mM **1j** before (red) and after (black) the addition of 3 equivalents of acetic acid, taken at 100 mVs^{-1} in CH_3CN containing 0.1 M $n\text{Bu}_4\text{NPF}_6$.

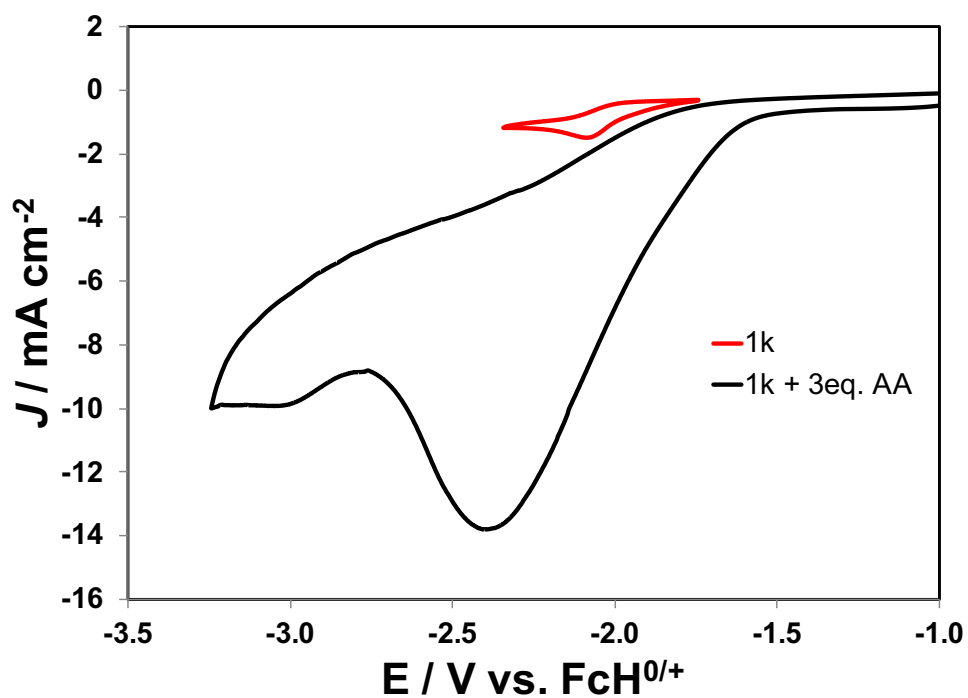


Figure S11. CV of 10 mM **1k** before (red) and after (black) the addition of 3 equivalents of acetic acid, taken at 100 mVs^{-1} in CH_3CN containing $0.1 \text{ M } n\text{Bu}_4\text{NPF}_6$.

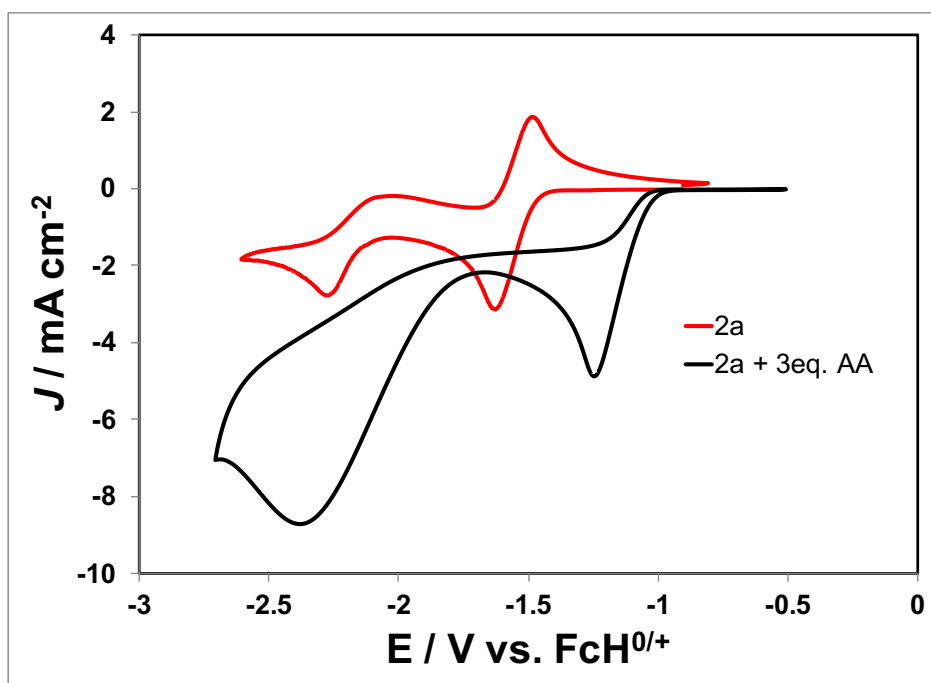


Figure S12. CV of 15 mM **2a** before (red) and after (black) the addition of 3 equivalents of acetic acid, taken at 100 mVs^{-1} in CH_3CN containing $0.1 \text{ M } n\text{Bu}_4\text{NPF}_6$.

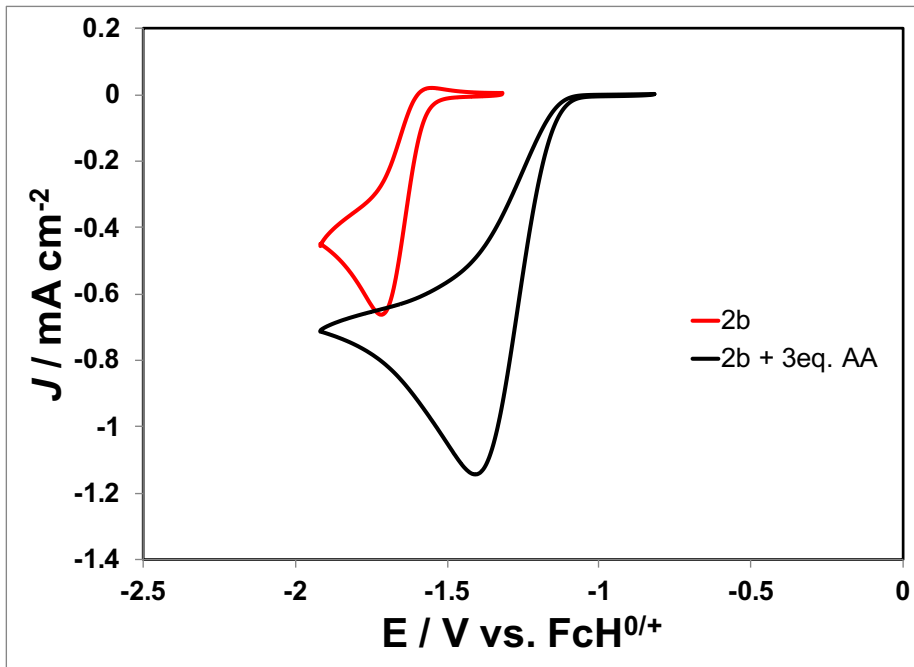


Figure S13. CV of 3 mM **2b** before (red) and after (black) the addition of 3 equivalents of acetic acid, taken at 100 mVs^{-1} in CH_3CN containing 0.1 M $n\text{Bu}_4\text{NPF}_6$.

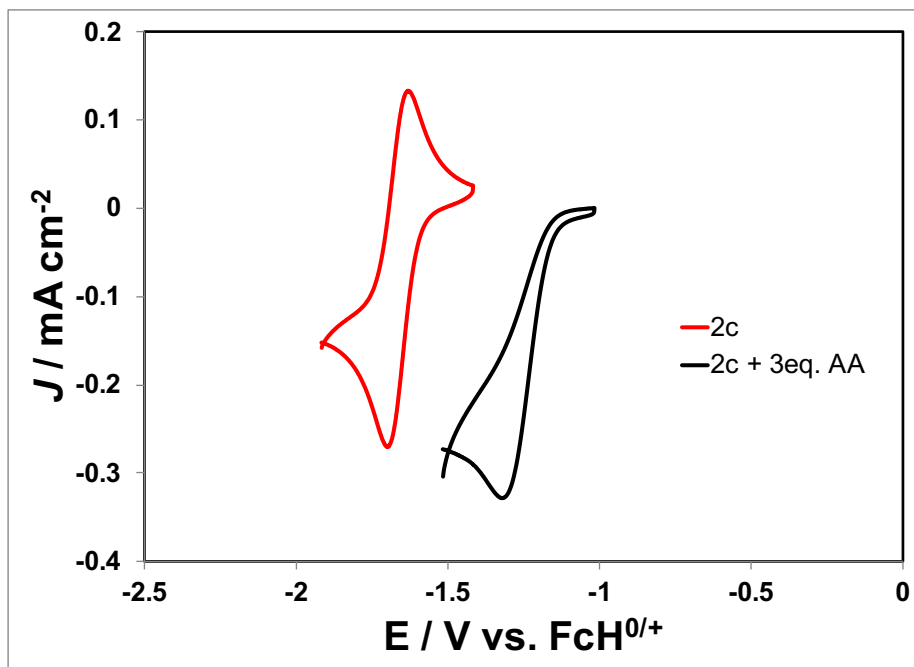


Figure S14. CV of 1 mM **2c** before (red) and after (black) the addition of 3 equivalents of acetic acid, taken at 100 mVs^{-1} in CH_3CN containing 0.1 M $n\text{Bu}_4\text{NPF}_6$.

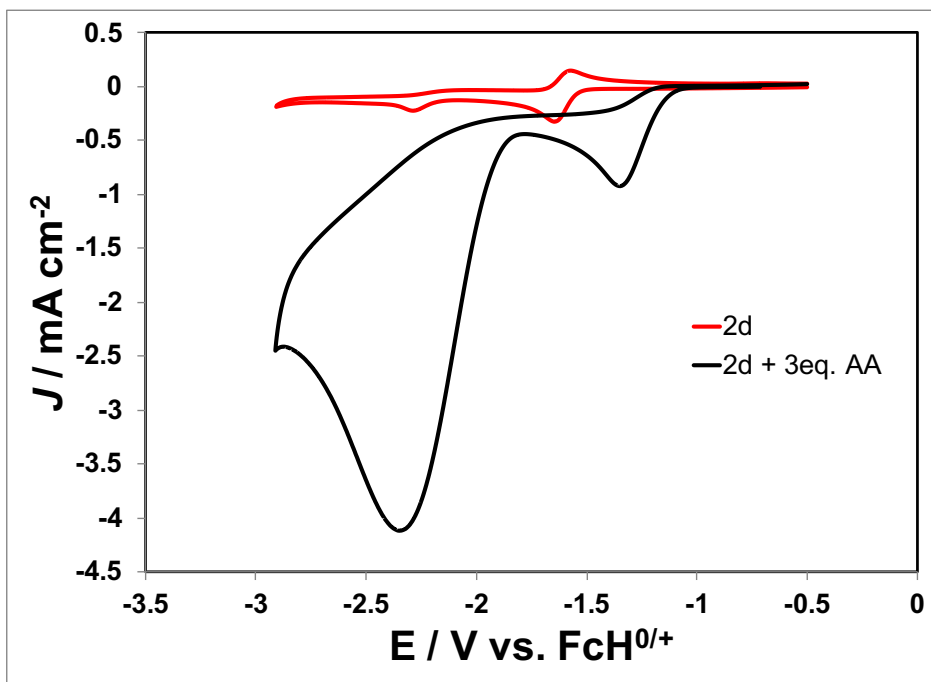


Figure S15. CV of 3 mM **2d** before (red) and after (black) the addition of 3 equivalents of acetic acid, taken at 100 mVs^{-1} in CH_3CN containing 0.1 M $n\text{Bu}_4\text{NPF}_6$.

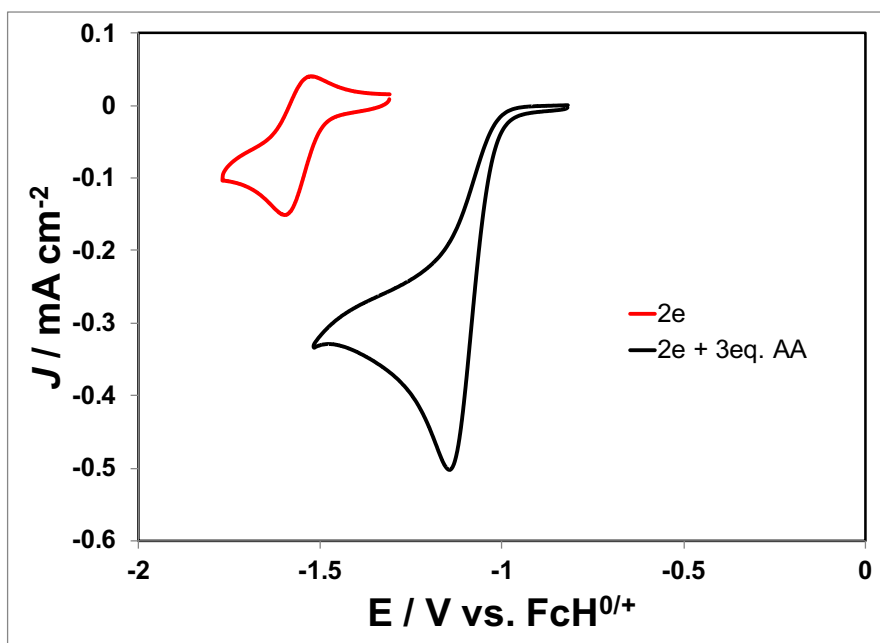


Figure S16. CV of 2 mM **2e** before (red) and after (black) the addition of 3 equivalents of acetic acid, taken at 100 mVs^{-1} in CH_3CN containing 0.1 M $n\text{Bu}_4\text{NPF}_6$.

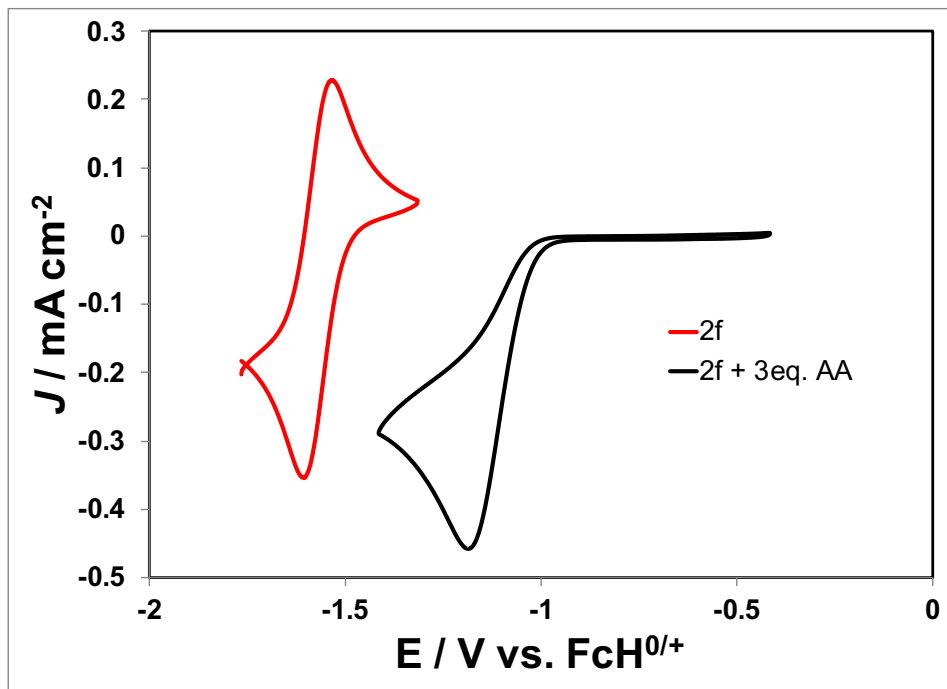


Figure S17. CV of 4 mM **2f** before (red) and after (black) the addition of 3 equivalents of acetic acid, taken at 100 mVs^{-1} in CH_3CN containing 0.1 M $n\text{Bu}_4\text{NPF}_6$.

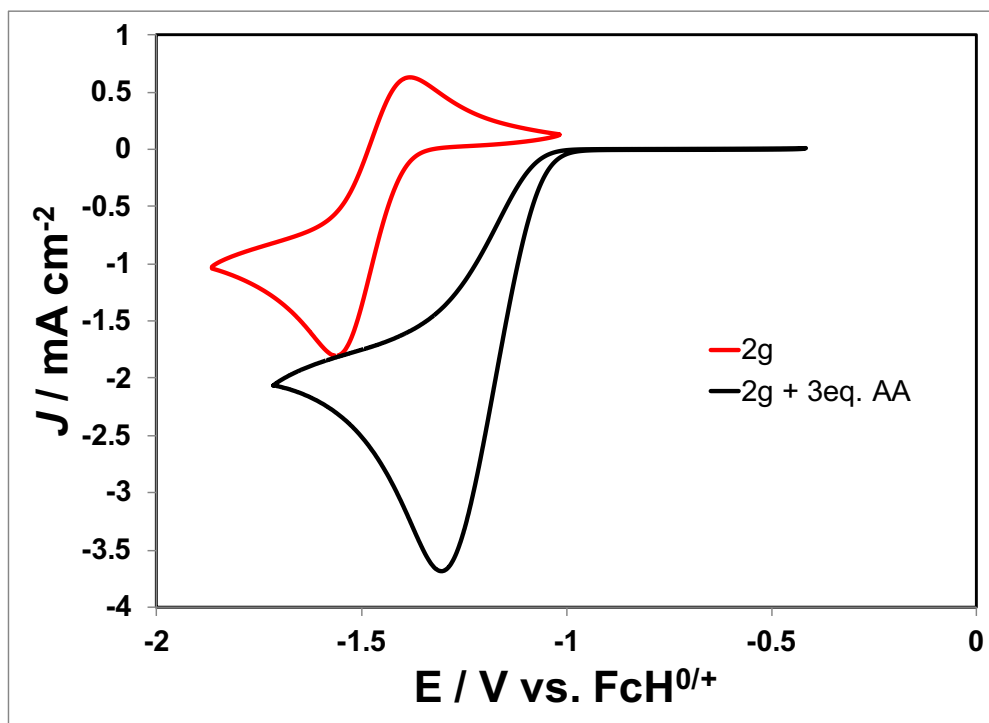


Figure S18. CV of 8 mM **2g** before (red) and after (black) the addition of 3 equivalents of acetic acid, taken at 100 mVs^{-1} in CH_3CN containing 0.1 M $n\text{Bu}_4\text{NPF}_6$.

POTENTIOSTATIC ELECTROLYSIS

Potentiostatic electrolyses were conducted using a reticulated vitreous carbon (RVC) working electrode ($\sim 700 \text{ cm}^2$) placed in a glass cylindrical chamber (85 mL), with Ar constantly bubbled into the solution in the chamber (1 atm) and the solution in the chamber stirred. A 0.60 cm diameter graphite rod counter electrode (submerged length = 5.00 cm; active surface area = 9.42 cm^2) was placed in a fritted tube (10 mL), separating the working and counter electrode chambers in order to minimize product crossover, and a Ag/AgCl quasi-reference electrode placed into the working electrode chamber. A photograph of the assembly is shown below with distances between electrodes in our set-up as follows:

Parameter	Distance
Centre of reference electrode to centre of counter electrode	1.35 cm
Interior edge of reference electrode to interior edge of counter electrode	0.50 cm
Centre of working electrode to centre of counter electrode	1.00 cm
Edge of working electrode to edge of counter electrode	0.10 cm
Centre of working electrode to centre of reference electrode	0.80 cm
Edge of reference electrode to edge of working electrode	0.30 cm

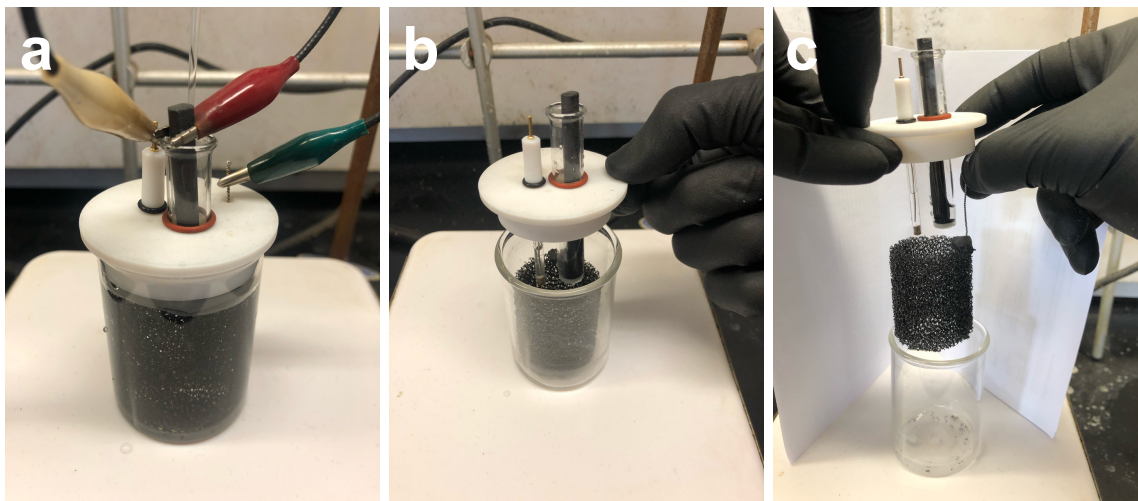


Figure S19. Photographs showing three views of the electrochemical set-up.

The applied potential was kept constant at -0.90 V vs. Ag/AgCl (-1.15 V vs. $\text{FcH}^{0/+}$) for all compounds investigated. Upon completion of electrolysis, the RVC electrode was

cleaned via sonication in 6 M HCl, distilled water, and acetonitrile, and heating to 100 °C before subsequent re-use.

CONTROLLED POTENTIAL ELECTROLYSIS PLOTS

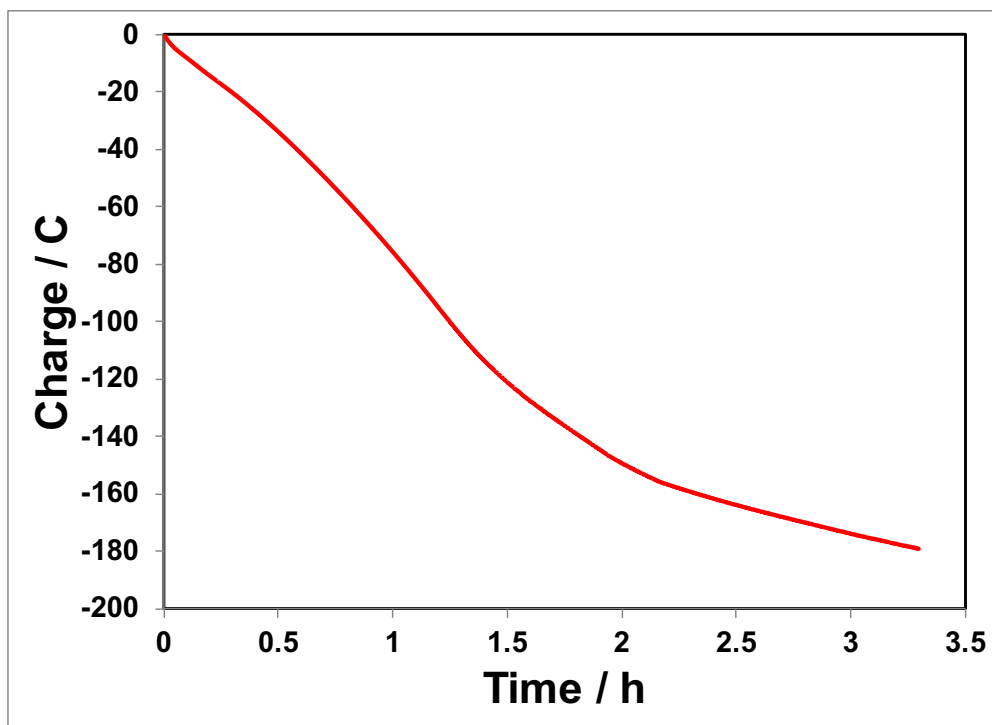


Figure S20. CPE plot for hydrogenation of **1a**.

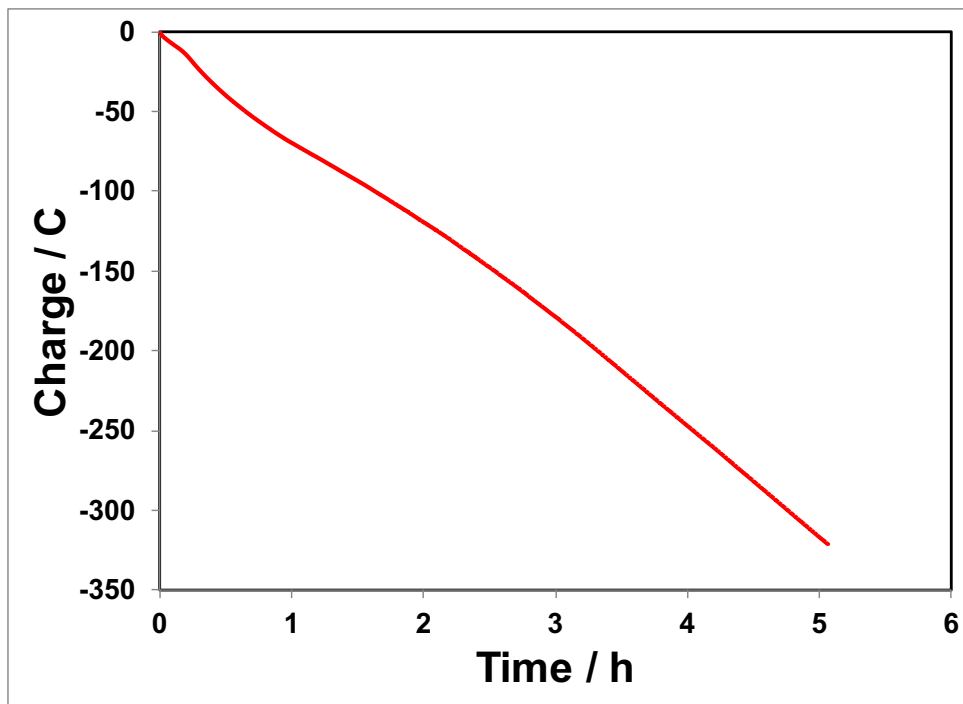


Figure S21. CPE plot for hydrogenation of **1b**.

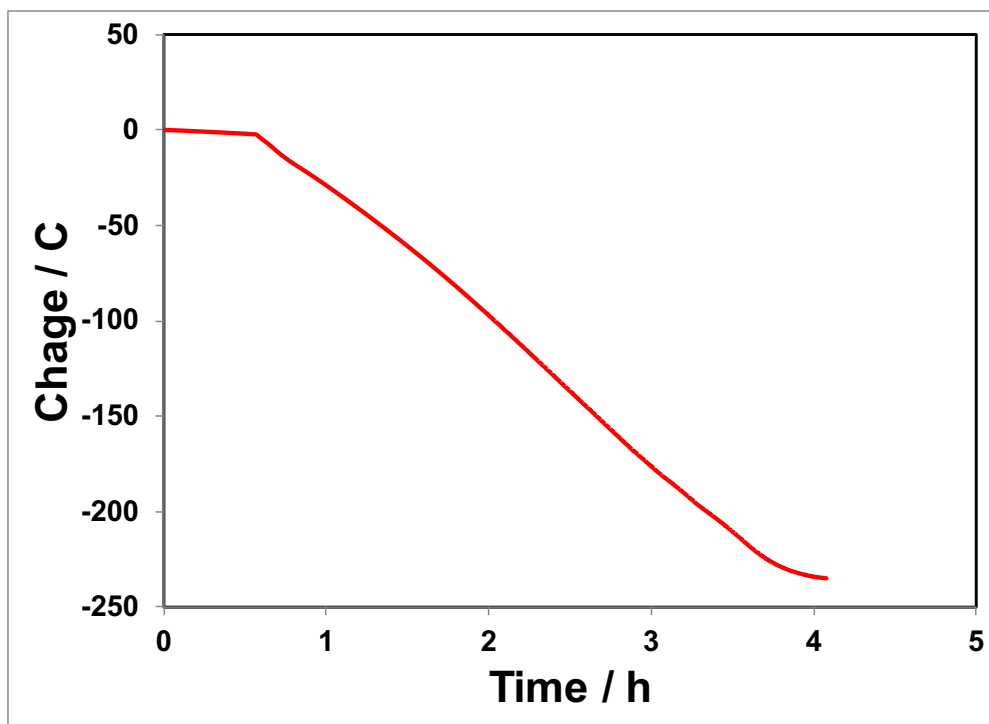


Figure S22. CPE plot for hydrogenation of **1c**.

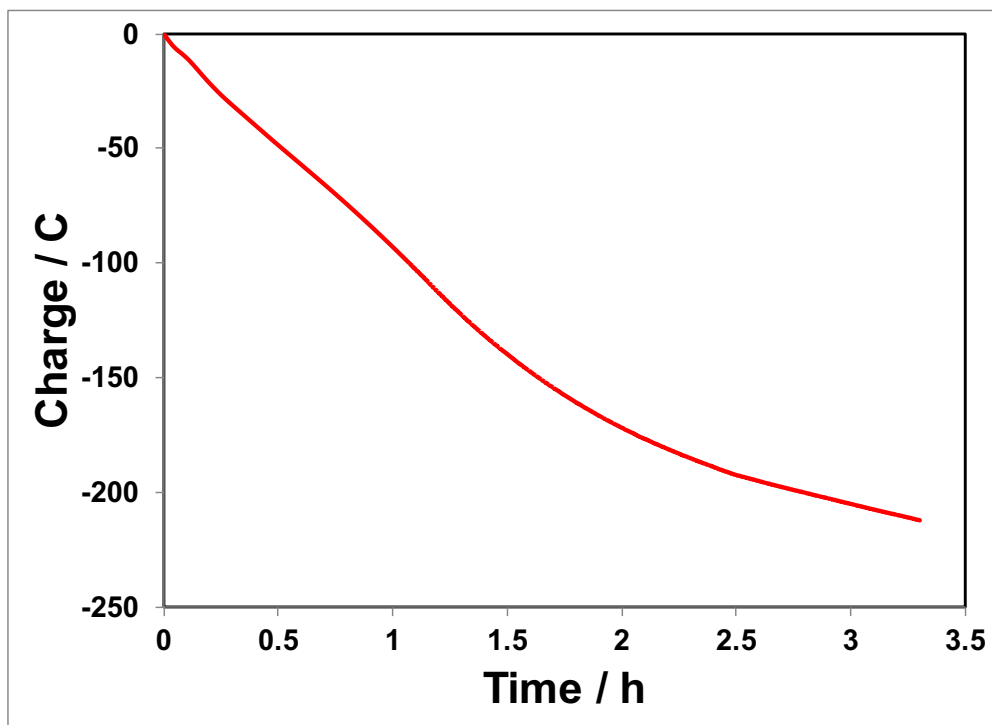


Figure S23. CPE plot for hydrogenation of 1d.

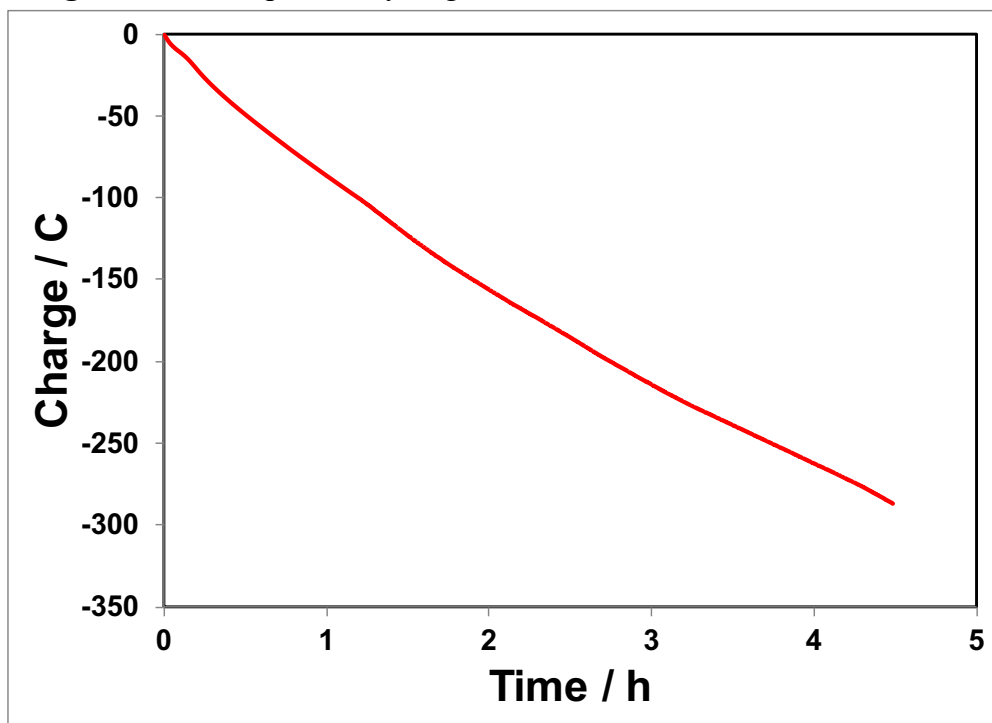


Figure S24. CPE plot for hydrogenation of 1e.

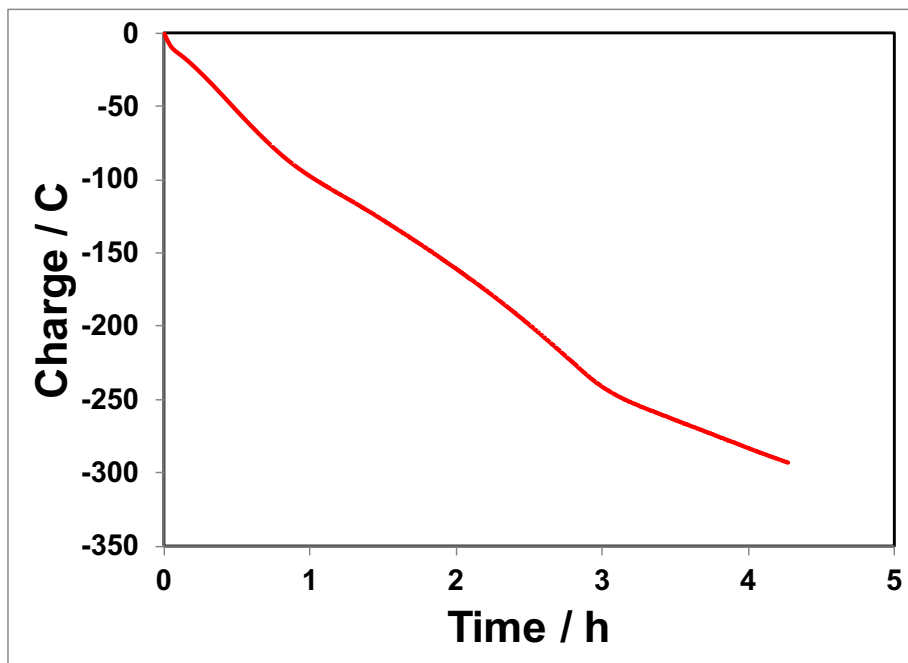


Figure S25. CPE plot for hydrogenation of 1f.

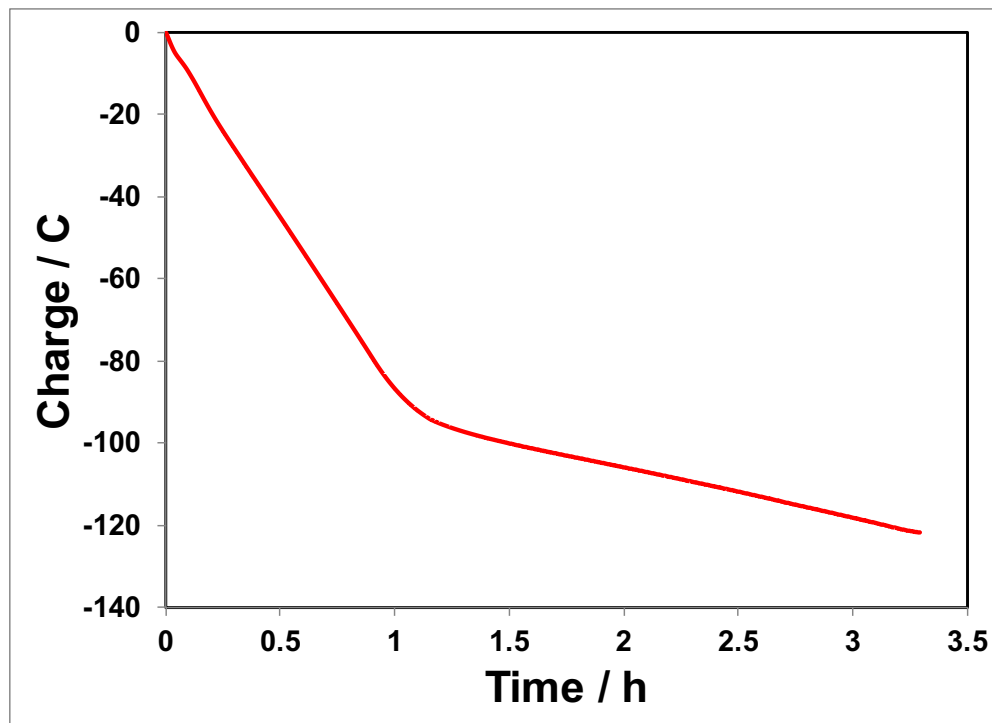


Figure S26. CPE plot for hydrogenation of 1g.

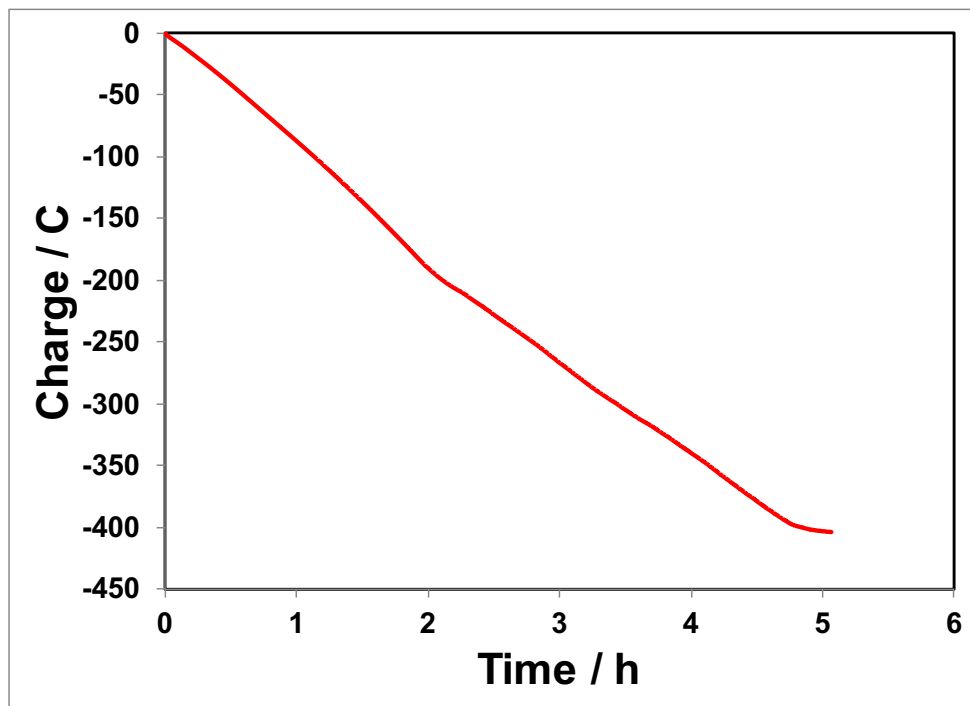


Figure S27. CPE plot for hydrogenation of 1h.

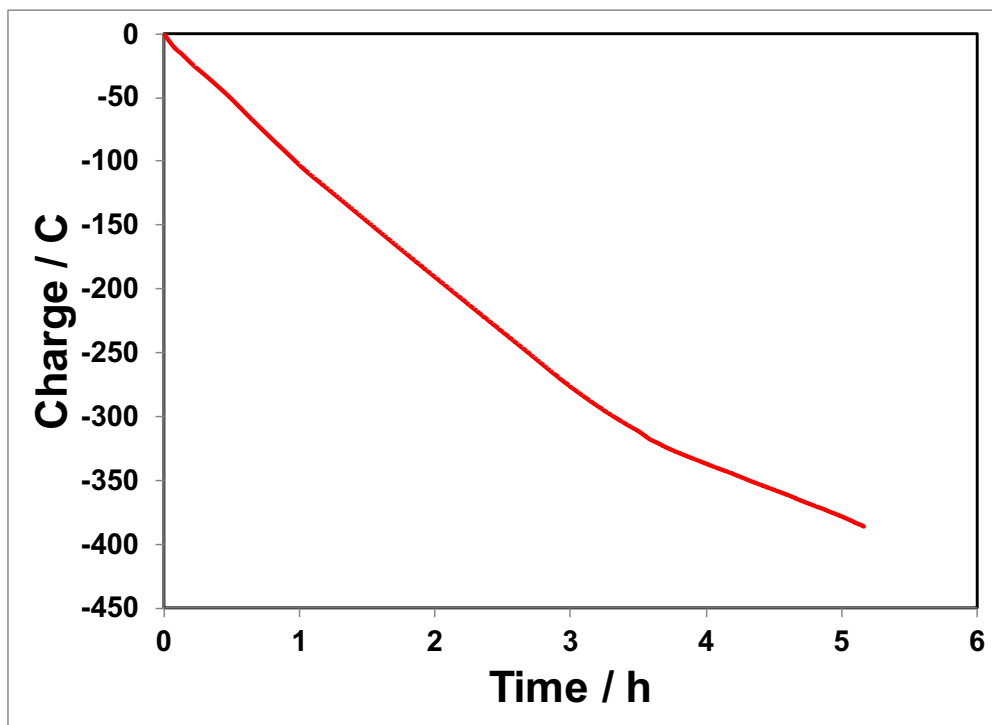


Figure S28. CPE plot for hydrogenation of 1i.

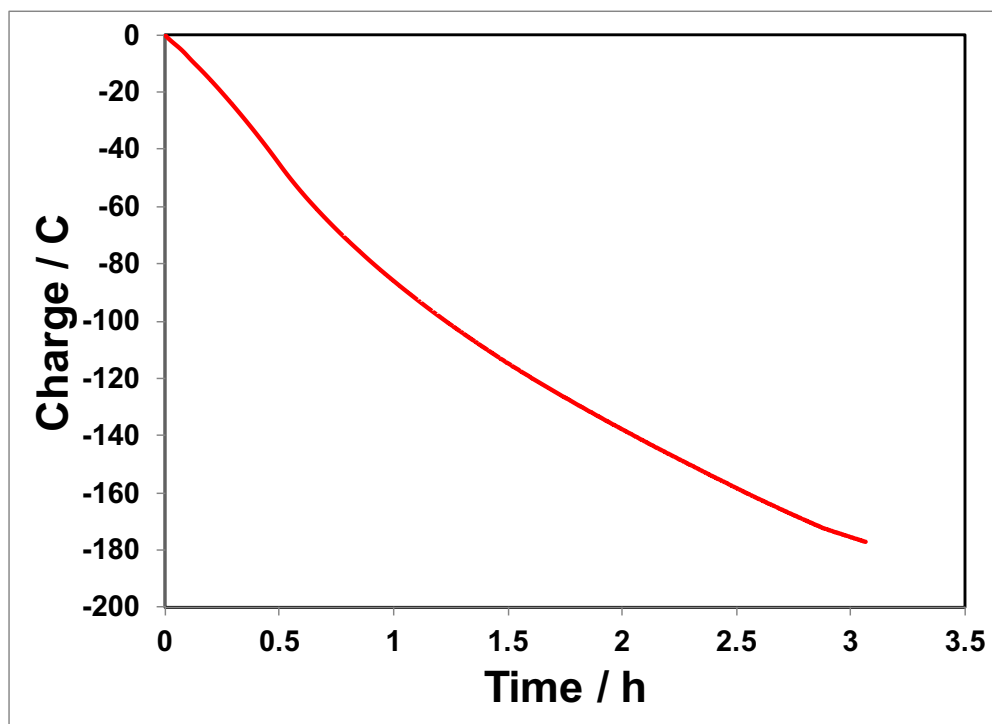


Figure S29. CPE plot for hydrogenation of **1j**.

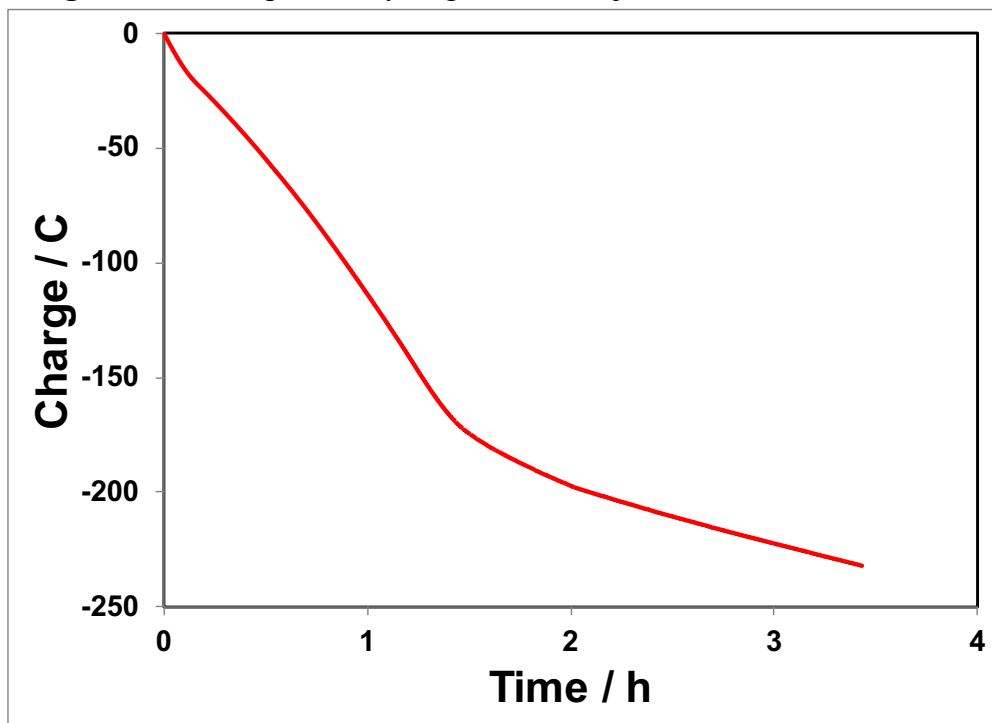


Figure S30. CPE plot for hydrogenation of **2a**.

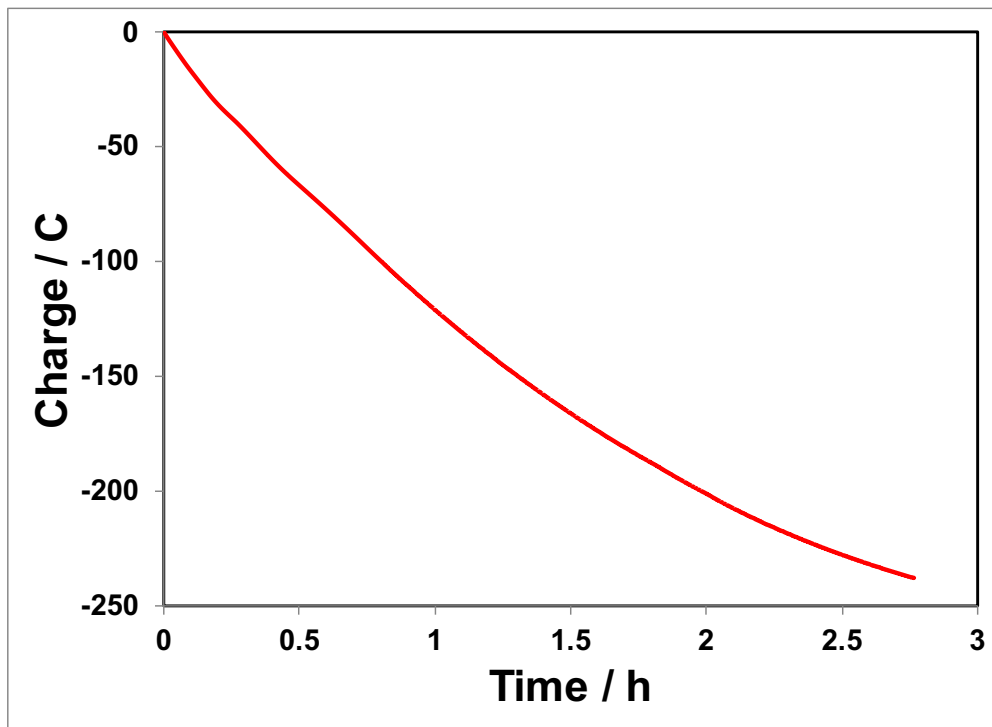


Figure S31. CPE plot for hydrogenation of **2b**.

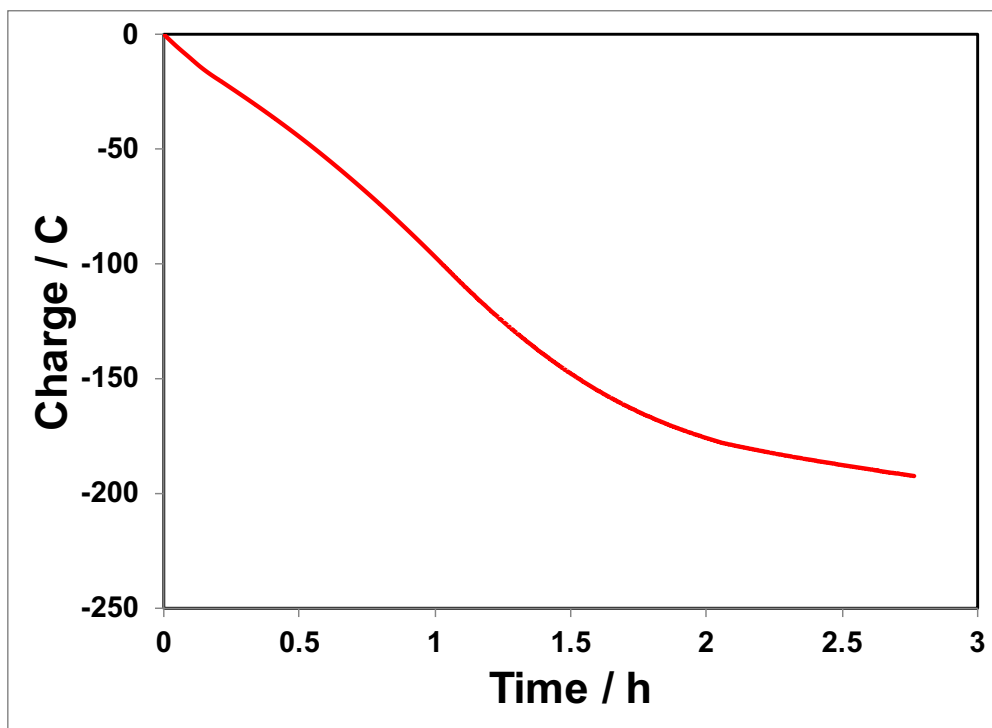


Figure S32. CPE plot for hydrogenation of **2c**.

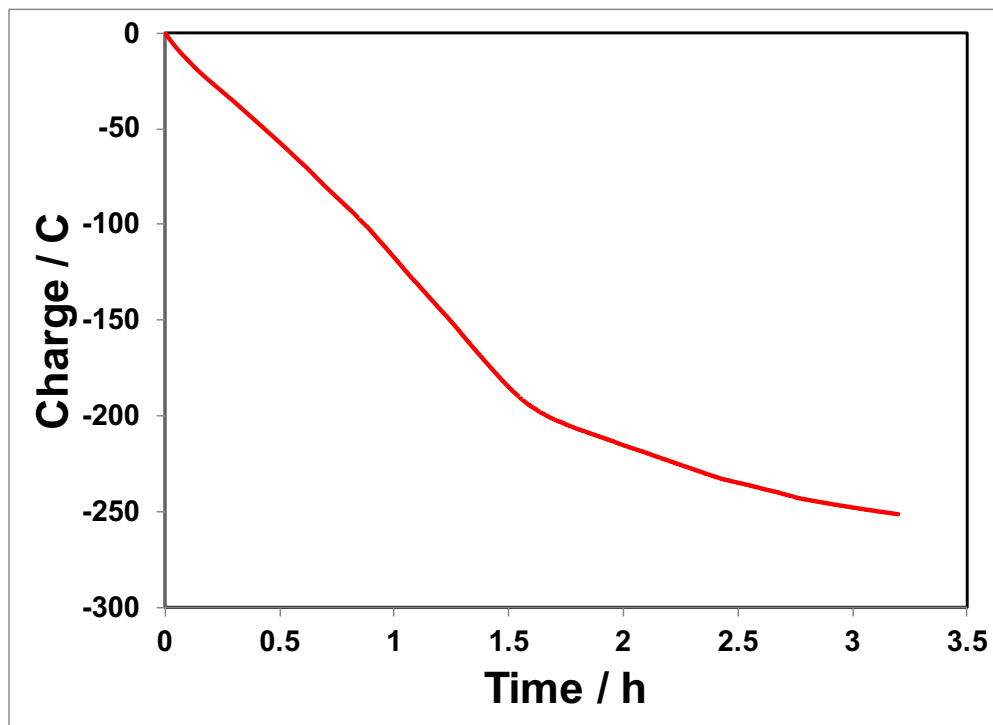


Figure S33. CPE plot for hydrogenation of **2d**.

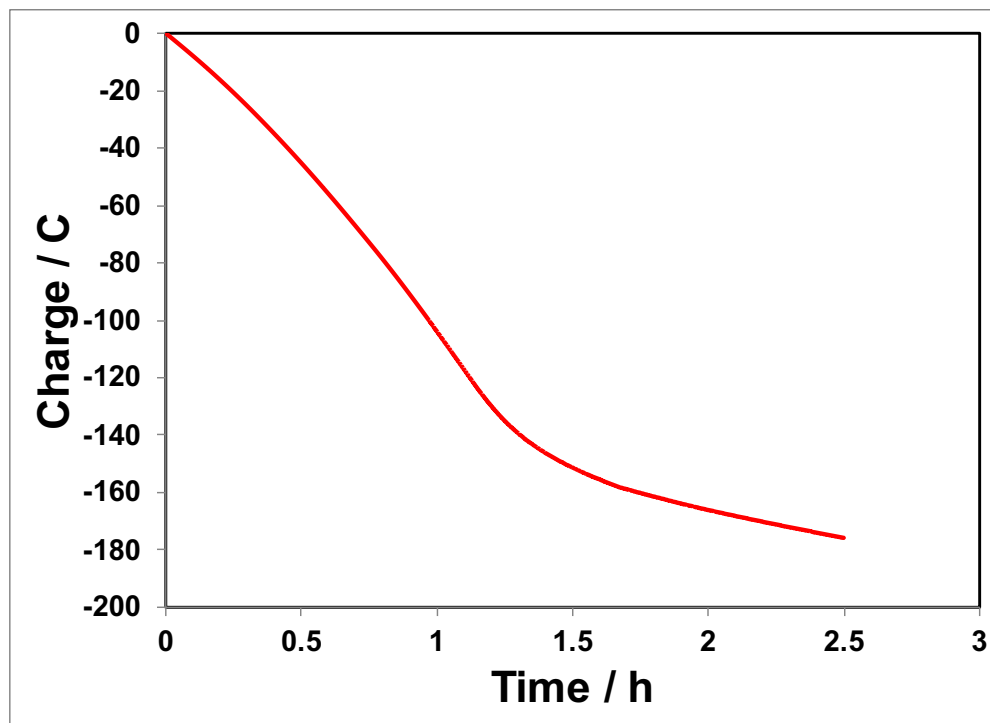


Figure S34. CPE plot for hydrogenation of **2e**.

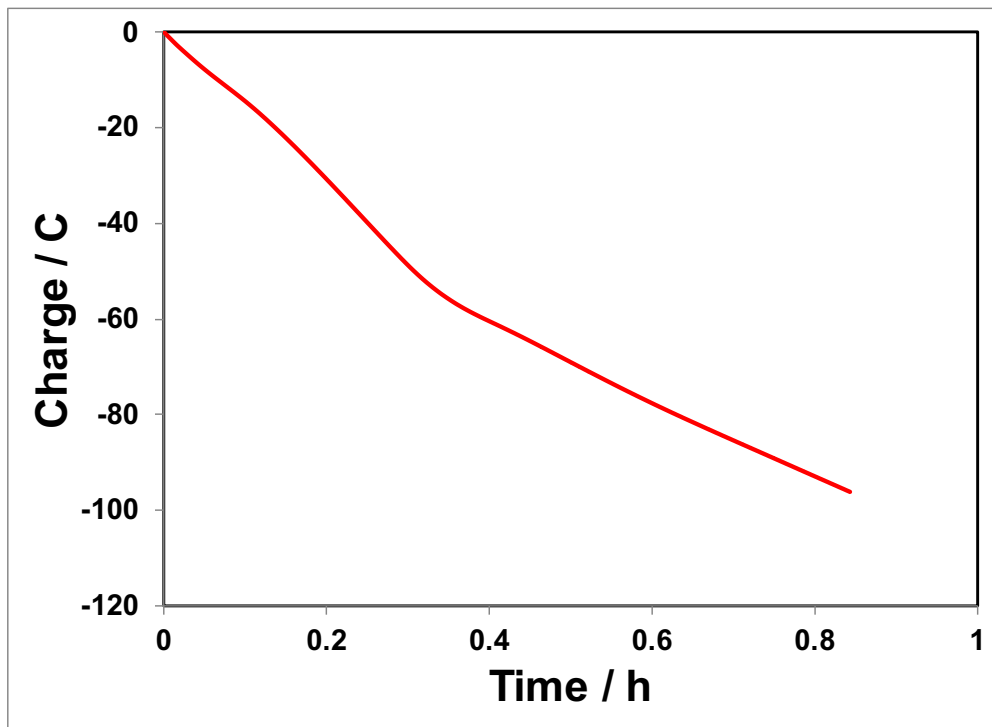


Figure S35. CPE plot for hydrogenation of 2f.

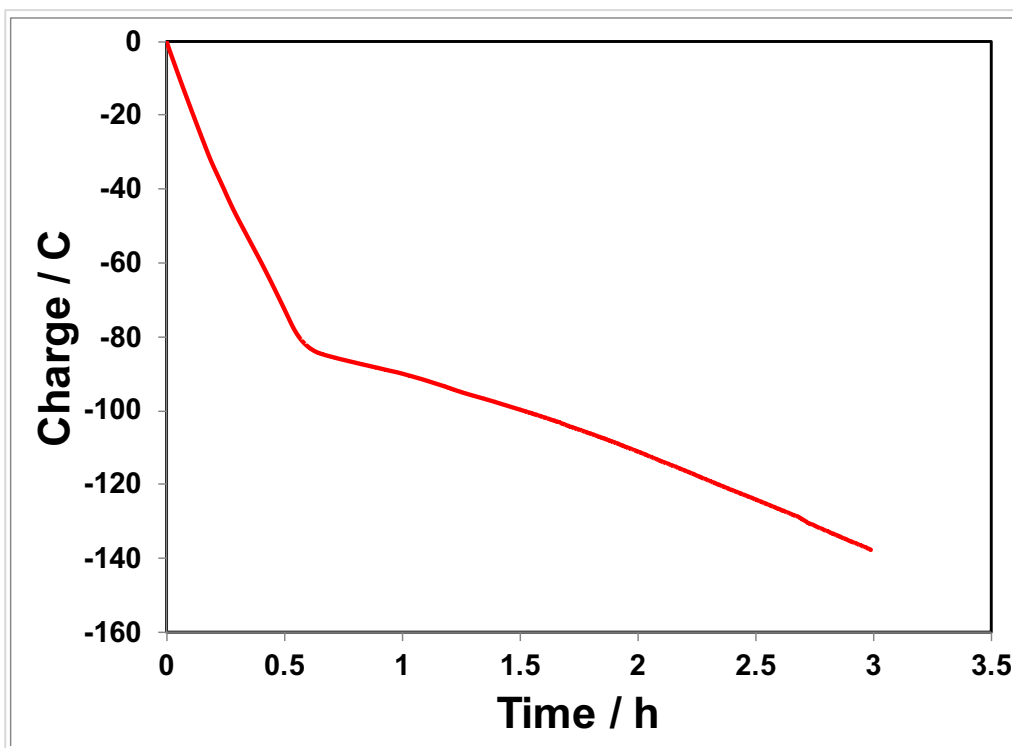


Figure S36. CPE plot for hydrogenation of 2g.

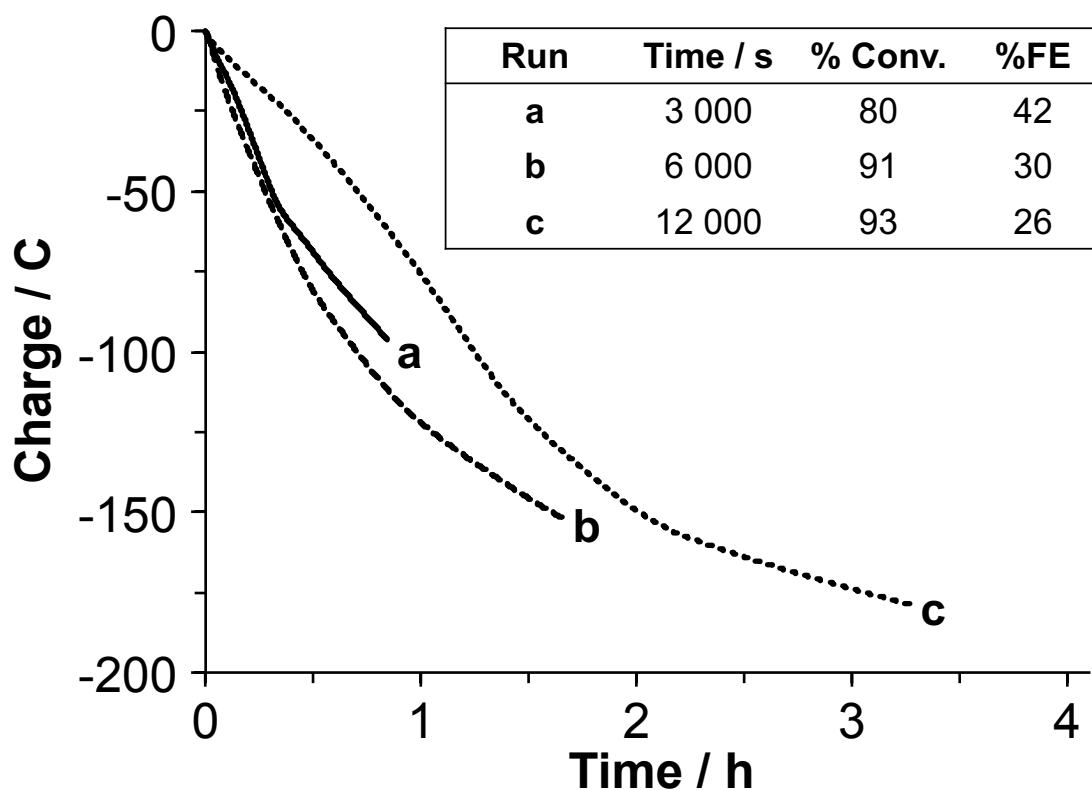


Figure S37. Charge vs. time plots of controlled potential electrolysis of **1a**. Conditions: 3.5 mM **1a**, $E_{\text{app}} = -0.90$ vs Ag/AgCl (-1.23 V vs $\text{FcH}^{0/+}$), 90% v/v $\text{CH}_3\text{CN}/\text{H}_2\text{O}$, 0.1 M LiClO_4 , reticulated vitreous carbon (RVC) working electrode (~ 700 cm^2), graphite rod counter electrode in a fritted tube, Ag/AgCl quasi-reference electrode, constant sparge with Ar (1 atm).

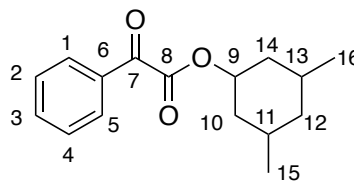
Table S2. Average current consumption during controlled potential electrolysis of **1d** in 90% v/v $\text{CH}_3\text{CN}/\text{H}_2\text{O}$ compared with in neat CH_3CN .

Solvent ^a	Time (s)	Average Current (mA)
90% v/v $\text{CH}_3\text{CN}/\text{H}_2\text{O}$	1800	27.0
	3600	25.8
	7200	23.8
Neat CH_3CN	1800	21.6
	3600	18.3
	7200	16.1

^a Conditions were otherwise as described above.

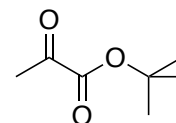
Preparation of Novel Ketoester and Benzoxazinone Substrates

(3,5-Dimethylcyclohexane)benzoylformate (1j): To a solution of phenylglyoxylic acid (1.15 g, 7.66 mmol) in dry CH_2Cl_2 containing one drop of DMF, a CH_2Cl_2 solution of



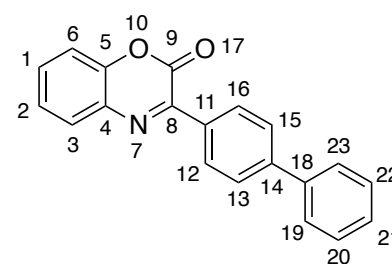
oxalyl chloride (750. μl , 8.80 mmol) was added dropwise over 20 minutes under an Ar atmosphere. The mixture was left to stir over 3 h, following which all solvent was removed under reduced pressure. The residue was then re-dissolved in dry CH_2Cl_2 and a CH_2Cl_2 solution containing 3,5-dimethylcyclohexanol (1.13 g, 8.81 mmol) and dry triethylamine (3.20 ml, 22.9 mmol) was added dropwise over 20 minutes. The resulting mixture was left to stir overnight. Solvent was then removed *via* reduced pressure, and the residue washed with brine and dried under vacuum. The crude mixture was purified using flash chromatography (9:1, hexanes:EtOAc), followed by recrystallization from a solution of diethylether layered with hexanes. Clear, needle-like crystals deposited and were washed with cold hexanes. Yield = 0.755 g (38%). ^1H NMR (300 MHz, CDCl_3 , 22 $^\circ\text{C}$): δ 8.03-7.96 (m, 2H, $C_{1,5}$) 7.70-7.62 (m, 1H, C_3), 7.55-7.48 (m, 2H, $C_{2,4}$), 5.12-4.99 (m, 1H, C_9), 2.16-2.15 (m, 2H, $C_{10,14}$), 1.72-1.55 (m, 3H, $C_{11,12,13}$), 1.17-1.04 (q, $J = 12.0$, 2H, $C_{10,14}$), 1.01-0.93 (d, $J = 6.4$, 6H, $C_{15,16}$), 0.67-0.54 ppm (q, $J = 12.0$, 1H, C_{12}). $^{13}\text{C}\{^1\text{H}\}$ NMR (75 MHz, CDCl_3 , 22 $^\circ\text{C}$): δ 186.9 (C_7), 163.8 (C_8), 134.9 (C_3), 132.7 (C_6), 130.1 ($C_{1,5}$), 129.0 ($C_{2,4}$), 75.8 (C_9), 42.9 (C_{12}), 39.8 (C_{14}), 30.8 ($C_{11,13}$), 22.2 ppm ($C_{15,16}$). HR-MS (ESI-TOF/MS, m/z) calcd. for $\text{C}_{16}\text{H}_{20}\text{O}_3$ $[\text{M}+\text{Na}]^+$, 283.1305; found 283.1299.

tert-Butyl 2-oxopropanoate (1k): This compound has been reported in the literature²; a modified procedure for its synthesis is reported here. A



stirred suspension of sodium pyruvate (1.000 g, 9.091 mmol) in *tert*-butyl alcohol (10 mL) was cooled in an ice bath, and concentrated hydrochloric acid (830 μ L, 10 mmol) added dropwise. The reaction mixture was allowed to warm to room temperature, then heated at reflux for 24 h. After cooling back to room temperature, the solvent was removed under reduced pressure using a rotary evaporator. The residue was then dissolved in dichloromethane (10 mL) and washed three times with brine (10 mL). The organic layer was concentrated under reduced pressure, then passed through a short plug of silica (~ 1cm) using dichloromethane as eluent. Isolated yield = 0.390 g (30%). The ¹H NMR of the product matched that in the literature.² ¹H NMR (300 MHz, CDCl₃, 22 °C): δ 2.40 (s, 3H), 1.53 ppm (s, 9H).

3-(4-Biphenyl)-benzo[*b*][1,4]oxazine-2-one (2e): In a 25 mL Teflon-stoppered flask, (4'-biphenyl)benzoylformate (0.740 g, 2.91 mmol) was added to a solution of 2-aminophenol (0.349 g, 3.20 mmol) in

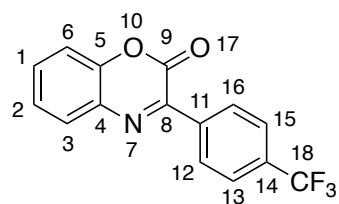


anhydrous EtOH (12 mL) and the mixture heated to reflux in an oil bath set to 110 °C for 24 h. The mixture was then cooled, and the solvent removed under reduced pressure. The crude residue was purified using flash chromatography (silica; 20:1 hexanes:EtOAc). Yield = 0.610 g (70 %). ¹H NMR (300 MHz, CDCl₃, 22 °C): δ 8.46 (d, *J* = 9 Hz, C_{12,16}), 7.88 (dd, *J* = 9 Hz, *J* = 1.8 Hz, 1H, C₃), 7.76-7.72 (m, 2H, C_{13,15}), 7.69-7.66 (m, 2H, C_{1,6}), 7.56-7.46 (m, 3H, C_{2,19,23}), 7.44-7.33 ppm (m, 3H, C_{20,21,22}). ¹³C{¹H} NMR (75 MHz, CDCl₃, 22 °C):

δ 152.51 (C_9), 150.46 (C_8), 146.57 (C_4), 144.23 (C_5), 140.27 (C_{11}), 133.14 (C_{14}), 131.87 ($C_{19,23}$), 131.23 ($C_{20,22}$), 130.09 ($C_{12,16}$), 129.57 (C_3), 129.05 (C_{18}), 128.14 (C_6), 127.35 (C_{21}), 127.19 ($C_{13,15}$), 125.75 (C_2), 116.32 ppm (C_1). HR-MS (ESI-TOF/MS, m/z) calcd. for $C_{20}H_{13}NO_2$ [$M+nH$] $^+$, 300.1019; found 300.1019.

3-(4-Trifluoromethyl)-benzo[*b*][1,4]oxazine-2-one (2g): In

a 25 mL Teflon-stoppered flask, (4'-trifluoromethyl)benzoylformate (0.280 g, 1.20 mmol) was



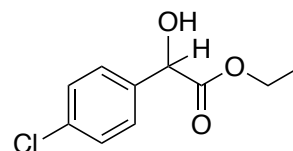
added to a solution of 2-aminophenol (0.144 g, 1.32 mmol) in anhydrous EtOH (12 mL) and the reaction mixture was heated to reflux in an oil bath set to 110 °C for 24 h. The mixture was then cooled, and the solvent removed under reduced pressure. The crude residue was purified using flash chromatography (silica; 20:1 hexanes:EtOAc). Yield = 0.210 g (60 %). 1H NMR (300 MHz, $CDCl_3$, 22 °C): δ 8.48 (d, J = 9 Hz, 2H, $C_{12,16}$), 7.88 (dd, J = 9 Hz, J = 1.7 Hz, 1H, C_3), 7.75 Hz (d, J = 9 Hz, 2H, $C_{13,15}$), 7.60-54 (m, 1H, C_6), 7.45-7.40 (m, 1H, C_2), 7.37-7.34 ppm (m, 1H, C_1). ^{13}C { 1H } NMR (75 MHz, $CDCl_3$, 22 °C): δ 152.20 (C_9), 149.50 (C_8), 146.67 (C_4), 137.34 (C_{14}), 133.11 (C_5), 132.68 (C_{11}), 132.09 (C_6), 131.59 ($C_{13,15}$), 129.92 ($C_{12,16}$), 129.87 (C_3), 125.97 (C_2), 125.41 (q, C_{18}), 116.43 ppm (C_1). ^{19}F NMR (282 MHz, $CDCl_3$, 22 °C): δ -62.94 ppm (s). HR-MS (ESI-TOF/MS, m/z) calcd. for $C_{15}H_8F_3NO_2$ [$M+nH$] $^+$, 292.0580; found 292.0581.

General Procedure for Electrochemical Hydrogenation and Product Isolation

A solution of LiClO₄ electrolyte, substrate and acetic acid using the amounts noted below was prepared in 20 mL of 10% (v/v) H₂O/CH₃CN and added to an electrochemical cell equipped with an RVC working electrode, graphite counter electrode, and Ag/AgCl reference electrode. An additional volume of the solvent mixture was added to bring the total volume of the solution to 85 mL. The solution was sparged with argon gas for 5 minutes with stirring, then subjected to a controlled potential ($E_{app} = -0.9$ V vs. Ag/AgCl) until the current passed had slowed significantly (see Figures S1-S17). Once stopped, the organic solvent was then removed *in vacuo* and the remaining slurry extracted with CH₂Cl₂ (3 x 15 mL) and washed with brine (3 x 10 mL). The organic phase was separated, filtered and the solvent removed to give the isolated product, which was then analyzed as described above.

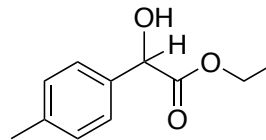
Hydrogenated Product Characterization

Ethyl 2-(4-chlorophenyl)-2-hydroxyacetate (1a-H₂): The general procedure was followed using LiClO₄ (1.30 g, 12.2 mmol), ethyl 4-chlorobenzoylformate (0.075 g, 0.19 mmol), and



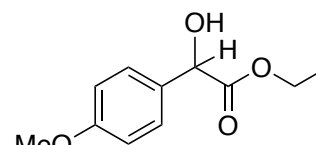
acetic acid (0.155 mL, 2.55 mmol); $E_{app} = -0.9$ V vs. Ag/AgCl, 3.3 h. Colorless solid. Yield = 56 mg (69 % yield). Spectroscopic data of the hydrogenated product was matched to literature.⁵ ¹H NMR (300 MHz, CDCl₃, 22 °C): δ 7.39-7.29 (m, 4H; Ar-H), 5.13 (s, 1H, CH-OH), 4.30-4.11 (m, 2H, CH₂CH₃), 3.69 (s, 1H, CH-OH), 1.21 ppm (t, $J = 7.1$, 3H, CH₂CH₃). ¹³C {¹H} NMR (75 MHz, CDCl₃, 22 °C): δ 173.4 (C=O), 136.92 (Ar-CH-OH), 134.29 (Ar-Cl), 128.8 (Ar-H), 128.0 (Ar-H), 72.3 (C-OH), 62.6 (CH₂CH₃), 14.1 ppm (CH₂CH₃).

Ethyl 2-hydroxy-2-(*para*-tolyl)acetate (1b-H₂): The general procedure was followed using LiClO₄ (1.20 g, 11.3 mmol), ethyl 4-methylbenzoylformate (0.075 g, 0.390 mmol), and acetic acid



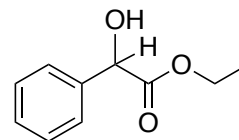
(0.160 mL, 2.63 mmol); $E_{app} = -0.9$ V vs. Ag/AgCl, 4.2 h. Yellow oil. Yield = 73 mg (89 % yield). Spectroscopic data of the hydrogenated product was matched to literature.⁵ ¹H NMR (300 MHz, CDCl₃, 22 °C): δ 7.34-7.27 (d, $J = 8.1$, 2H; Ar CH), 7.20-7.14 (d, $J = 8.1$, 2H; Ar-H), 5.12 (s, 1H, CH-OH), 4.35-4.05 (m, 2H, CH₂CH₃), 3.48 (s, 1H, CH-OH), 2.34 (s, 3H, Ar-CH₃), 1.22 ppm (t, $J = 7.2$, 3H, CH₂CH₃). ¹³C{¹H} NMR (75 MHz, CDCl₃, 22 °C): δ 173.9 (C=O), 138.2 (Ar CH), 135.6 (Ar CH), 128.6 (Ar CH), 128.5 (Ar-CH), 126.6 (Ar-CH), 73.0 (C-OH), 62.3 (CH₂CH₃), 14.1 ppm (CH₂CH₃).

Ethyl 2-hydroxy-2-(4-methoxyphenyl)acetate (1c-H₂): The general procedure was followed using LiClO₄ (1.21 g, 11.4 mmol), ethyl 4-methoxybenzoylformate (0.107 g, 0.513 mmol),



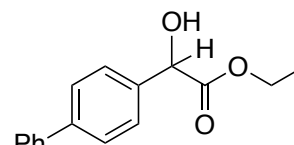
and acetic acid (0.085 mL, 1.4 mmol); $E_{app} = -0.9$ V vs. Ag/AgCl, 4.1 h. Colorless semi-solid. Yield = 81 mg (72 % yield). Spectroscopic data of the hydrogenated product was matched to literature.⁵ ¹H NMR (300 MHz, CDCl₃, 22 °C): δ 7.36-7.28 (d, $J = 8.8$, 2H; Ar-H), 6.91-6.84 (d, $J = 8.8$, 2H; Ar-H), 5.10 (s, 1H, CH-OH), 4.29-4.10 (m, 2H, CH₂CH₃), 3.78 (s, 3H, Ar-O-CH₃), 3.55 (s, 1H, CH-OH), 1.21 ppm (t, $J = 7.2$, 3H, CH₂CH₃). ¹³C{¹H} NMR (75 MHz, CDCl₃, 22 °C): δ 173.9 (C=O), 159.7 (Ar), 130.8 (Ar), 127.9 (Ar-H), 114.0 (Ar-H), 72.6 (C-OH), 62.1 (CH₂CH₃), 55.32 (Ar-O-CH₃), 14.1 ppm (CH₂CH₃).

Ethyl 2-hydroxy-2-phenylacetate (1d-H₂): The general procedure was followed using LiClO₄ (1.20 g, 11.3 mmol), ethyl-benzoylformate (0.094 g, 0.527 mmol), and acetic acid (0.094 mL, 1.6 mmol); $E_{app} = -$



0.9 V vs. Ag/AgCl, 3.3 h. Light yellow oil. Yield = 65 mg (68% yield). Spectroscopic data of the hydrogenated product was matched to literature.⁵ ¹H NMR (300 MHz, CDCl₃, 22 °C): δ 7.45-7.40 (m, 2H; Ar CH), 7.40-7.30 (m, 3H; Ar CH) 5.16 (s, 1H, CH-OH), 4.29-4.14 (m, 2H, CH₂CH₃), 3.61 (s, 1H, CH-OH), 1.22 ppm (t, $J = 7.2$, 3H, CH₂CH₃). ¹³C{¹H} NMR (75 MHz, CDCl₃, 22 °C): δ 173.8 (C=O), 138.6 (Ar CH), 128.6 (Ar CH), 128.5 (Ar-CH), 126.6 (Ar-CH), 73.0 (C-OH), 62.3 (CH₂CH₃), 14.1 ppm (CH₂CH₃).

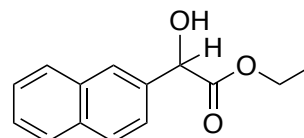
Ethyl 2-hydroxy-2(4-biphenyl)acetate (1e-H₂): The general procedure was followed using LiClO₄ (1.20 g, 11.3 mmol), ethyl-4-phenylbenzoylformate (0.108 g, 0.42 mmol), and acetic



acid (71 μL, 1.0 mmol); $E_{app} = -0.9$ V vs. Ag/AgCl, 4.5 h. Colorless solid. Yield = 85 mg (73 % yield). Spectroscopic data of the hydrogenated product was matched to literature.⁶ ¹H NMR (300 MHz, CDCl₃, 22 °C): δ 7.64-7.58 (m, 5H, Ar-H), 7.55-7.36 (m, 5H, Ar-H), 5.23 (s, 1H, CH-OH), 4.35-4.18 (m, 2H, CH₂CH₃), 3.63 (s, 1H, CH-OH), 1.27 ppm (t, $J = 7.1$, 3H, CH₂CH₃). ¹³C{¹H} NMR (75 MHz, CDCl₃, 22 °C): δ 173.7 (C=O), 141.4 (Ar-Ar), 140.7 (Ar-Ar), 137.5 (Ar-CH-OH), 128.9 (Ar-H), 127.5 (Ar-H), 127.4 (Ar-H), 127.2 (Ar-H), 127.1 (Ar-H), 72.8 (C-OH), 62.4 (CH₂CH₃), 14.2 ppm (CH₂CH₃).

Ethyl 2-hydroxy-2(naphthalen-2-yl)acetate (1f-H₂): The

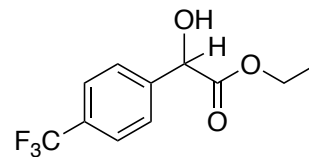
general procedure was followed using LiClO₄ (1.20 g, 11.3 mmol), ethyl-3,4-naphthylbenzoylformate (0.063 g, 0.29



mmol), and acetic acid (61 μ l, 0.87 mmol); $E_{app} = -0.9$ V vs. Ag/AgCl, 4.3 h. Colorless solid. Yield = 43 mg (96 % conversion, 68 % mass recovery). Spectroscopic data of the hydrogenated product was matched to literature.⁷ ¹H NMR (300 MHz, CDCl₃, 22 °C): δ 7.92 (s, 1H, Ar-CH), 7.87-7.82 (m, 3H, Ar-CH), 7.55-7.46 (m, 3H, Ar-CH), 5.34 (s, 1H, CH-OH), 4.35-4.10 (m, 2H, CH₂CH₃), 3.68 (s, 1H, CH-OH), 1.22 ppm (t, $J = 7.1$, 3H, CH₂CH₃). ¹³C {¹H} NMR (75 MHz, CDCl₃, 22 °C): δ 173.77 (C=O), 135.92, 133.39, 133.30, 128.50, 128.23, 127.79, 126.40, 125.98, 124.26, 73.17 (C-OH), 62.40 (CH₂CH₃), 14.122 ppm (CH₂CH₃).

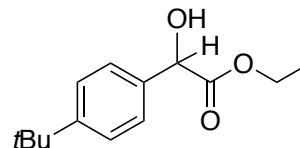
Ethyl 2-hydroxy-2(4-(trifluoromethyl)phenyl)acetate (1g-

H₂): The general procedure was followed using LiClO₄ (1.20 g, 11.3 mmol), ethyl-4-(trifluoromethyl)benzoylformate (0.0610 g,



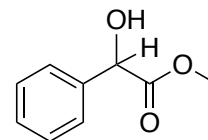
0.248 mmol), and acetic acid (150 μ l, 2.62 mmol); $E_{app} = -0.9$ V vs. Ag/AgCl, 3.3 h. Colorless solid. Yield = 39 mg (60 % yield). Spectroscopic data of the hydrogenated product was matched to literature.⁵ ¹H NMR (300 MHz, CDCl₃, 22 °C): δ 7.65-7.52 (m, 4H, Ar-H), 5.23 (s, 1H, CH-OH), 4.34-4.12 (m, 2H, CH₂CH₃), 3.90 (s, 1H, CH-OH), 1.24 ppm (t, $J = 7.2$, 3H, CH₂CH₃). ¹³C {¹H} NMR (75 MHz, CDCl₃, 22 °C): δ 173.18 (C=O), 142.24, 130.68 (q, $J = 32.0$), 126.98, 125.61 (q, $J = 3.9$), 124.13 (q, $J = 270.0$ Hz), 72.39 (C-OH), 62.87, 14.12 ppm.

Ethyl 2-(4-(*tert*-butyl)phenyl)-2-hydroxyacetate (1h-H₂): The general procedure was followed using LiClO₄ (1.20 g, 11.3 mmol), ethyl-4-*tert*-butyl-benzoylformate (0.102 g, 0.435 mmol), and



acetic acid (74 μ l, 1.3 mmol); $E_{app} = -0.9$ V vs. Ag/AgCl, 5.1 h. Clear oil. Yield = 74 mg (72 % yield). Spectroscopic data of the hydrogenated product was matched to literature.⁵ ¹H NMR (300 MHz, CDCl₃, 22 °C): δ 7.41-7.31 (m, 4H; Ar-CH) 5.15 (s, 1H, CH-OH), 4.32-4.10 (m, 2H, CH₂CH₃), 3.62 (s, 1H, CH-OH), 1.32 (s, 9H, (C(CH₃))), 1.24 ppm (t, $J = 7.1$, 3H, CH₂CH₃). ¹³C{¹H} NMR (75 MHz, CDCl₃, 22 °C): δ 173.9 (C=O), 151.4 ppm (Ar-CH-OH), 135.5(Ar-(C(CH₃)₃)), 126.3 (Ar-H), 125.6 (Ar-H), 72.8 (C-OH), 62.3 (CH₂CH₃), 34.7 (C(CH₃)), 31.4 (C(CH₃)), 14.2 ppm (CH₂CH₃).

Methyl (2-hydroxy-2-phenyl)acetate (1i-H₂): The general procedure was followed using LiClO₄ (1.25 g, 11.8 mmol), methyl-benzoylformate (0.104 g, 0.634 mmol), and acetic acid (0.105 mL, 1.79 mmol); $E_{app} = -$

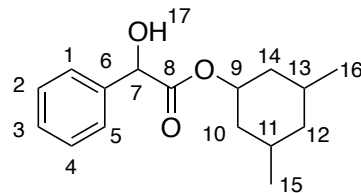


0.9 V vs. Ag/AgCl, 5.2 h. Colorless semi-solid. Yield = 56 mg (45% yield). Spectroscopic data of the hydrogenated product was matched to literature.⁸ ¹H NMR (300 MHz, CDCl₃, 22 °C): δ 7.45-7.31 (m, 5H; Ar-H) 5.18 (s, 1H, CH-OH), 3.75 (s, 3H, O-CH₃), 3.56 ppm (s, 1H, CH-OH), ¹³C{¹H} NMR (75 MHz, CDCl₃, 22 °C): δ 174.5 (C=O), 138.3 (Ar CH), 128.7 (Ar CH), 128.6 (Ar-CH), 126.7 (Ar-CH), 73.0 (C-OH), 53.2 ppm (O-CH₃).

(3,5-Dimethylcyclohexane)(2-hydroxy)(2-phenyl)acetate

(1j-H₂): The general procedure was followed using LiClO₄

(1.301 g, 12.22 mmol), (3,5-



dimethylcyclohexane)benzoylformate (0.1221 g, 0.467 mmol), and acetic acid (155 μ l,

2.55 mmol); $E_{app} = -0.9$ V vs. Ag/AgCl, 3.1 h. Yellow oil. Yield = 122 mg (61% conversion

by ¹H NMR, 60.5% yield). ¹H NMR (300 MHz, CDCl₃, 22 °C): δ 7.46-7.30 (m, 5H; C₁₋₅)

5.15-5.10 ($J = 6.0$, d, 1H, C₇), 4.85-4.73 (m, 1H, C₉), 3.55 ($J = 6.0$, d, 1H, O₁₇), 2.05-1.94

(m, 1H, C₁₄), 1.80-1.69 (m, 1H, C₁₀), 1.64-1.41 (m, 3H, C_{11,12,13}), 1.00-0.75 (m, 8H,

C_{10,14,15,16}), 0.59-0.44 ppm (q, $J = 12.0$, 1H, C₁₂). ¹³C{¹H} NMR (75 MHz, CDCl₃, 22 °C):

δ 173.4 (C₈), 138.7 (C₆), 128.6 (C_{1,5}), 128.3 (C₃), 126.5 (C_{2,4}), 75.3 (C₉), 73.0 (C₇), 42.9

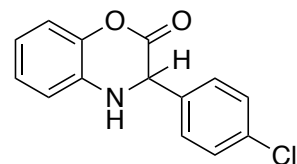
(C₁₂), 39.8 (C₁₄), 39.4 (C₁₀), 30.7 (C₁₁), 30.6 (C₁₃), 22.2 (C₁₆), 22.1 ppm (C₁₅). HR-MS (ESI-

TOF/MS, m/z) calcd. for C₁₆H₂₂O₃ [M+Na]⁺, 285.1461; found 285.1459.

3-(4-Chlorophenyl)-3,4-dihydrobenzo[*b*][1,4]oxazine-2-one

(2a-H₂): The general procedure was followed using LiClO₄ (1.301

g, 12.22 mmol), 3-(4-chlorophenyl)-2*H*-benzo[*b*][1,4]oxazine-2-



one (0.0985 g, 0.379 mmol), acetic acid (150 μ l, 2.62 mmol); $E_{app} = -0.9$ V vs. Ag/AgCl,

3.4 h. Off-white solid (0.126 g, 90% yield). Spectroscopic data of the hydrogenated product

was matched to literature.⁹ ¹H NMR (300 MHz, CDCl₃, 22 °C): δ 7.38-7.31 (m, 4H, Ar-

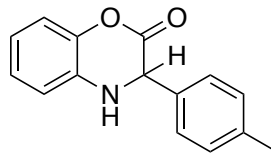
CH), 7.08-7.01 (m, 2H, Ar *H*), 6.93-6.80 (m, 2H, Ar *H*), 5.01 (s, 1H, NHCH), 4.33 ppm (s,

1H, NHCH). ¹³C{¹H} NMR (75 MHz, CDCl₃, 22 °C): δ 165.10 (C=O), 140.87, 135.01,

134.75, 132.22, 129.22, 129.00, 125.41, 120.70, 117.06, 115.11, 58.72 ppm (NHCH).

3-Para-tolyl-3,4-dihydrobenzo[*b*][1,4]oxazin-2-one (2b-H₂): The

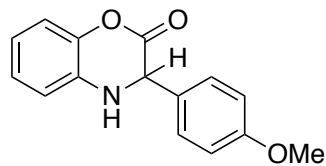
general procedure was followed using LiClO₄ (1.320 g, 12.41 mmol), 3-*para*-tolyl-2*H*-benzo[*b*][1,4]oxazin-2-one (0.120 g, 0.506



mmol), acetic acid (150 μl, 2.62 mmol); $E_{app} = -0.9$ V vs. Ag/AgCl, 5.1 h. Off-white solid (0.120 g, 96% yield). Spectroscopic data of the hydrogenated product was matched to literature.⁹ ¹H NMR (300 MHz, CDCl₃, 22 °C): δ 7.30-7.24 (m, 2H, Ar-CH) 7.19-7.14 (m, 2H, Ar-H), 7.09-6.99 (m, 2H, Ar-H), 6.90-6.77 (m, 2H, Ar-H), 4.96 (s, 1H, NHCH), 4.39 (s, 1H, NHCH), 2.34 ppm (s, 3H, CH₃). ¹³C{¹H} NMR (75 MHz, CDCl₃, 22 °C): δ 165.65 (C=O), 140.87, 138.83, 133.39, 132.58, 129.63, 127.36, 125.18, 120.18, 116.83, 114.97, 58.94 (NHCH), 21.18 ppm (Ph-CH₃).

3-(4-Methoxyphenyl)-3,4-dihydrobenzo[*b*][1,4]oxazine-2-

one (2c-H₂): The general procedure was followed using LiClO₄ (1.310 g, 12.31 mmol), 3-(4-methoxyphenyl)-2*H*-



benzo[*b*][1,4]oxazine-2-one (0.1000 g, 0.395 mmol), acetic acid (160 μl, 2.79 mmol); $E_{app} = -0.9$ V vs. Ag/AgCl, 2.7 h. Off-white solid (0.099 g, 97% yield). Spectroscopic data of the hydrogenated product was matched to literature.⁹ ¹H NMR (300 MHz, CDCl₃, 22 °C): δ 7.34-7.30 (d, $J = 8.3$, 2H, Ar-*H*), 7.07-6.99 (m, 4H, Ar-*H*), 6.92-6.78 (m, 4H, Ar-*H*), 5.00 (s, 1H, NHCH), 4.20 (s, 1H, NHCH), 3.80 ppm (s, 3H, O-CH₃). ¹³C{¹H} NMR (75 MHz, CDCl₃, 22 °C): δ 165.66 (C=O), 160.19, 141.11, 132.68, 128.93, 128.50, 125.26, 120.51, 117.11, 114.97, 114.51, 58.96 (NHCH), 55.47 ppm.

3-Phenyl-3,4-dihydrobenzo[*b*][1,4]oxazin-2-one (2d-H₂): The

general procedure was followed using LiClO₄ (1.285 g, 12.07 mmol),

3-phenyl-2*H*-benzo[*b*][1,4]oxazin-2-one (0.120 g, 0.538 mmol),

acetic acid (150 μl, 2.62 mmol); $E_{app} = -0.9$ V vs. Ag/AgCl, 3.2 h. Off-white solid (0.121 g,

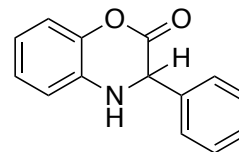
98% yield). Spectroscopic data of the hydrogenated product was matched to literature.⁹ ¹H

NMR (300 MHz, CDCl₃, 22 °C): δ 7.34-7.42 (m, 5H, Ar-CH) 7.00-7.07 (m, 2H, Ar *H*),

6.80-6.87 (m, 2H, Ar *H*), 5.01 (s, 1H, NHCH), 4.38 ppm (s, 1H, NHCH). ¹³C{¹H} NMR

(75 MHz, CDCl₃, 22 °C): δ 165.52 (C=O), 140.96, 136.4, 132.5, 129.1, 129.0, 127.6, 125.3,

120.4, 117.0, 115.0, 59.3 ppm (NHCH).



3-(4-Biphenyl)-3,4-dihydrobenzo[*b*][1,4]oxazine-2-one

(2e-H₂): The general procedure was followed using

LiClO₄ (1.310 g, 12.31 mmol), 3-(4-biphenyl)-2*H*-

benzo[*b*][1,4]oxazine-2-one (0.110 g, 0.367 mmol), acetic

acid (160 μl, 2.97 mmol); $E_{app} = -0.9$ V vs. Ag/AgCl, 2.5 h. Yellow solid (0.105 g, 93.0%

yield). ¹H NMR (300 MHz, CDCl₃, 22 °C): δ 7.63-7.53 (m, 4H, C_{12,13,15,16}), 7.52-7.40 (m,

4H, C_{19,20,22,23}), 7.39-7.42 (m, 1H, C₂₁), 7.10-7.01 (m, 2H, C_{2,3}), 6.94-6.80 (m, 2H, C_{1,6}),

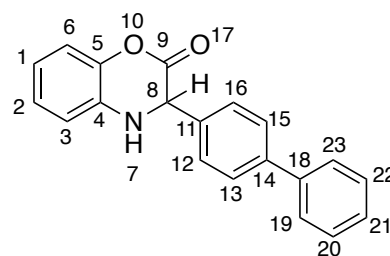
5.12 (s, 1H, C₈), 4.27 ppm (s, 1H, N₇). ¹³C{¹H} NMR (75 MHz, CDCl₃, 22 °C): δ 165.33

(C₉), 142.15 (C₁₁), 141.09 (C₁₄), 140.46 (C₁₈), 135.36, 132.50 (C₂₁), 128.99 (C_{12,16}), 128.10

(C_{13,15}), 127.88 (C_{19,23}), 127.77, 127.27 (C_{20,22}), 125.36 (C₂), 120.65 (C₆), 117.20 (C₃),

115.04 (C₁), 59.24 ppm (N₇). HR-MS (ESI-TOF/MS, m/z) calcd. for C₁₅H₂₀NO₂ [M+Na]⁺,

324.0995; found 324.0995.



3-(Naphthalen-2-yl)-3,4-dihydrobenzo[*b*][1,4]oxazine-2-one



(**2f-H₂**): The general procedure was followed using LiClO₄

(1.285 g, 12.43 mmol), 3-(2-naphthyl)-2H-benzo[*b*][1,4]oxazine-

2-one (0.100 g, 0.363 mmol), acetic acid (150 μ l, 2.62 mmol); E_{app} = -0.9 V vs. Ag/AgCl,

0.8 h. Off-white solid (0.096 g, 93 % yield). Spectroscopic data of the hydrogenated

product was matched to literature.¹⁰ ¹H NMR (300 MHz, CDCl₃, 22 °C): δ 7.54-7.46 (m,

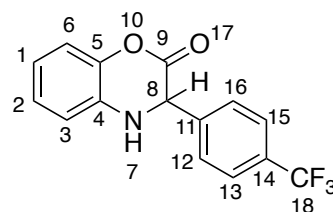
3H, Ar-CH) 7.09-7.00 (m, 2H, Ar *H*), 6.92-6.80 (m, 2H, Ar *H*), 5.18 (s, 1H, NHCH), 4.35

ppm (s, 1H, NHCH). ¹³C{¹H} NMR (75 MHz, CDCl₃, 22 °C): δ 165.34 (C=O), 140.30,

133.71, 133.49, 133.16, 132.48, 129.07, 128.19, 127.85, 127.03, 126.79, 126.67, 125.33,

124.93, 120.53, 117.09, 115.04, 59.51 ppm (NHCH).

3-(4-Trifluoromethyl)-3,4-dihydro-2H-benzo[1,4]oxazine



(**2g-H₂**): The general procedure was followed using LiClO₄

(1.285 g, 12.43 mmol), 3-(4-(trifluoromethyl)phenyl)-2H-

benzo[*b*][1,4]oxazin-2-one (0.0985 g, 0.336 mmol), acetic acid

(150 μ l, 2.62 mmol); E_{app} = -0.9 V vs. Ag/AgCl, 3.0 h. Off-white solid (0.0779. g, 86.4%

yield). ¹H NMR (300 MHz, CDCl₃, 22 °C): δ 7.66-7.53 (m, 4H, C_{12,13,15,16}), 7.09-7.01 (m,

2H, C_{2,3}), 6.93-6.83 (m, 2H, C_{1,6}), 5.13 (s, 1H, C₈), 4.34 ppm (s, 1H, N₇). ¹³C{¹H} NMR

(75 MHz, CDCl₃, 22 °C): δ 164.71(C₉), 140.92 (C₄), 140.14 (C₃), 132.01 (C₁₁), 131.30

(C₁₄), 128.14 (C_{12,16}), 126.05 (J = 3.82, C_{13,15}), 125.54 (C₂), 123.91 (J = 272.2, C₁₈), 120.96

(C₆), 117.20 (C₃), 115.20 (C₁), 58.99 ppm (C₈). HR-MS (ESI, m/z) calcd. for C₁₆H₂₂O₃

[M+H]⁺, 294.0736; found 294.0672.

^1H NMR/ ^{13}C NMR SPECTRA

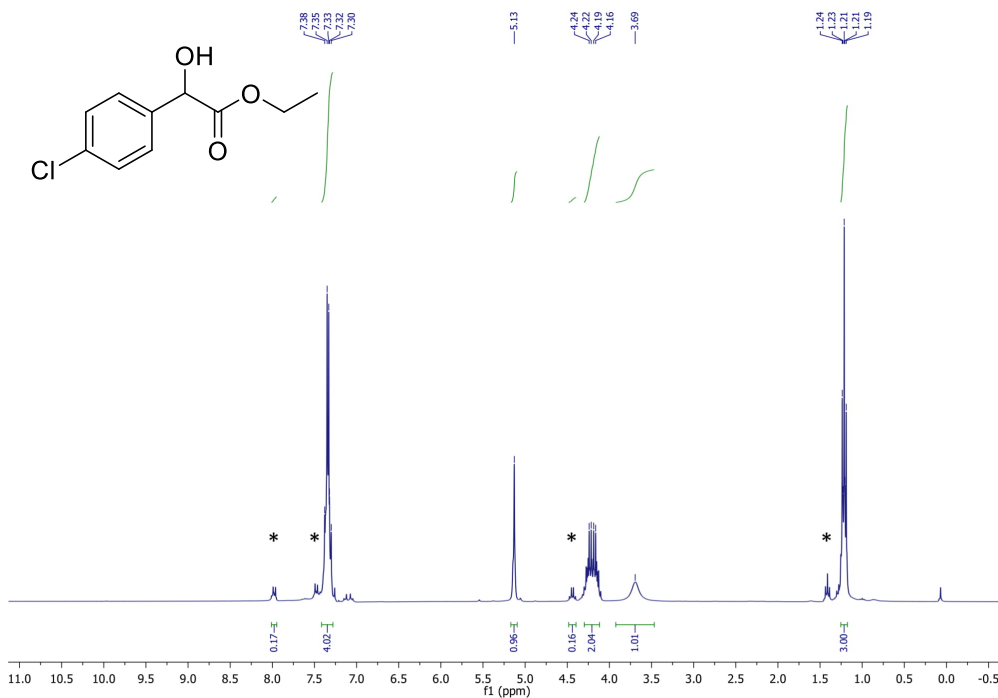


Figure S38. ^1H NMR (300 MHz, 22 °C, CDCl_3) of **1a-H₂**. Unreacted starting material **1a** is denoted with an asterisk (*).

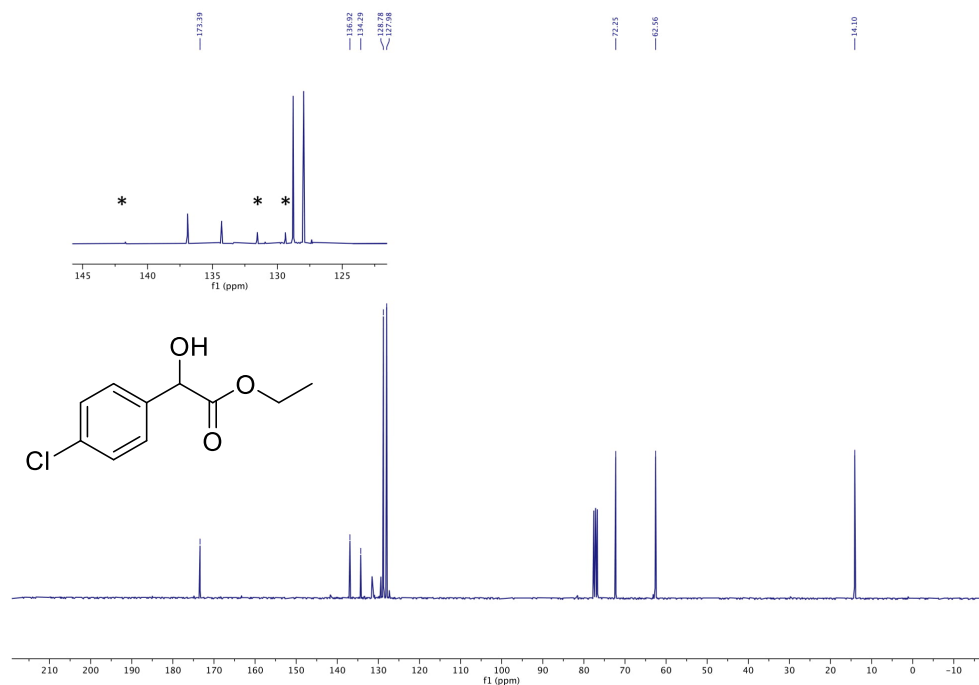


Figure S39. $^{13}\text{C}\{^1\text{H}\}$ NMR (75 MHz, 22 °C, CDCl_3) of **1a-H₂**. Unreacted starting material **1a** is denoted with an asterisk (*).

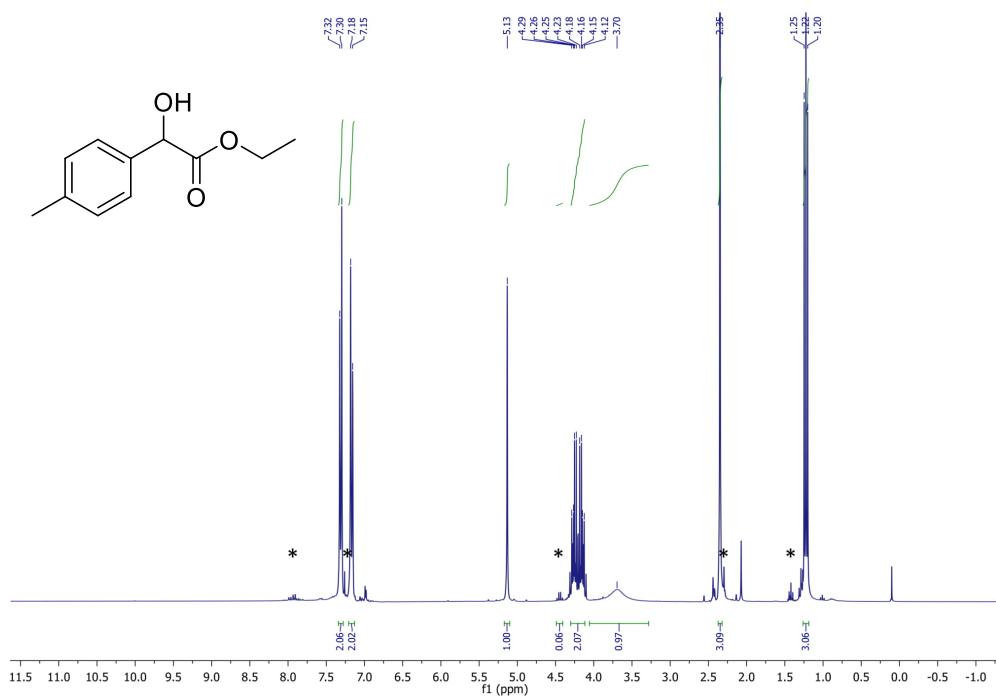


Figure S40. ¹H NMR (300 MHz, 22 °C, CDCl₃) of **1b-H₂**. Unreacted starting material **1b** is denoted with an asterisk (*).

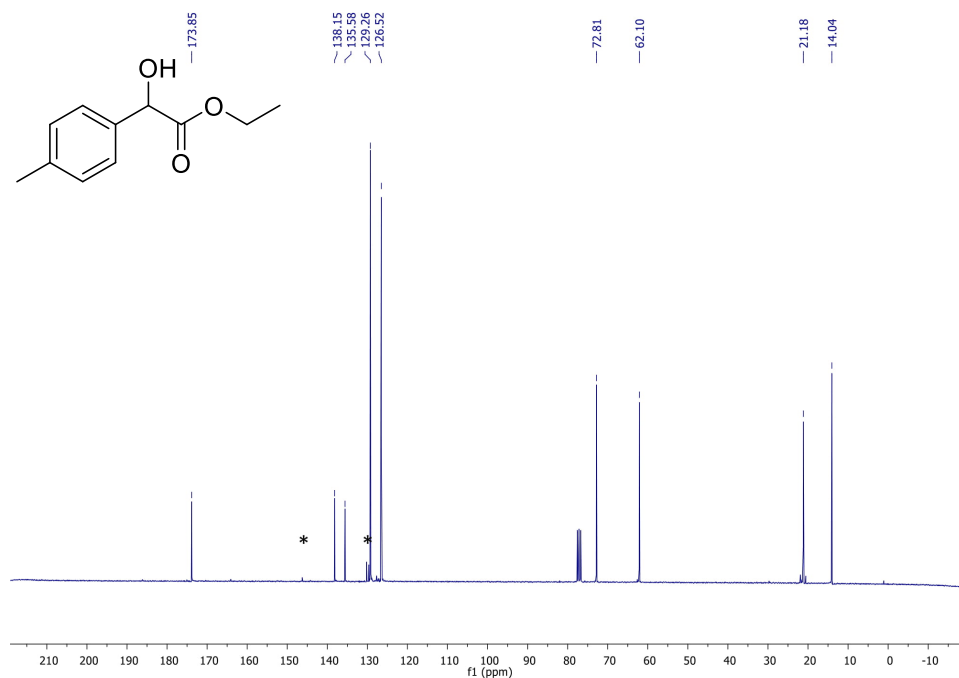


Figure S41. ¹³C {¹H} NMR (75 MHz, 22 °C, CDCl₃) of **1b-H₂**. Unreacted starting material **1b** is denoted with an asterisk (*).

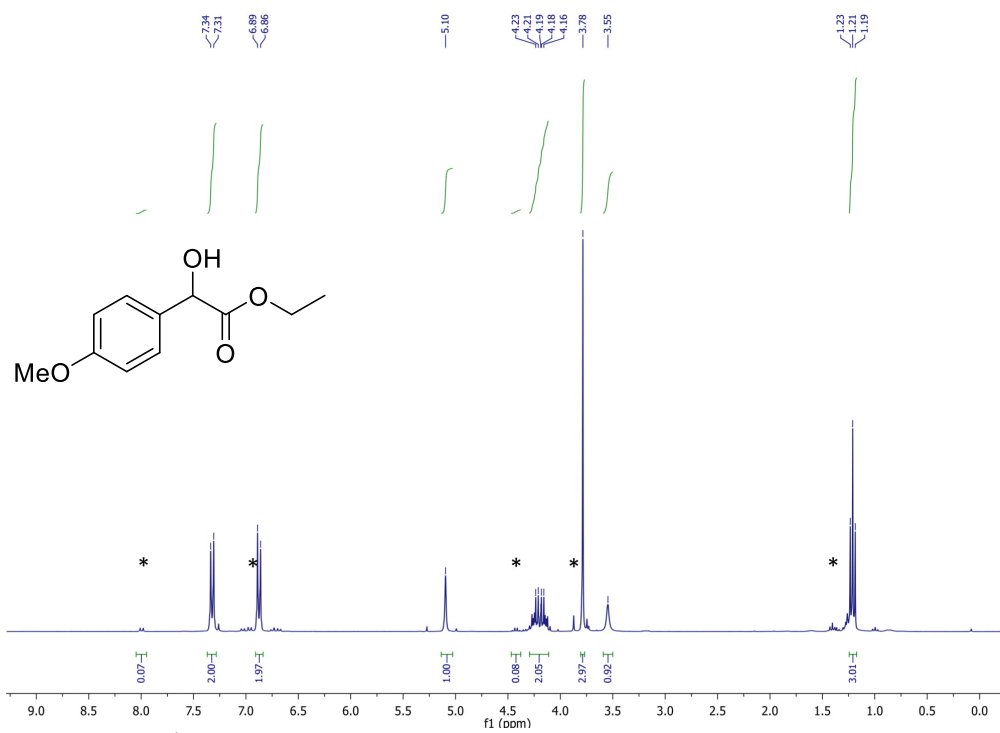


Figure S42. ¹H NMR (300 MHz, 22 °C, CDCl₃) of **1c-H₂**. Unreacted starting material **1c** is denoted with an asterisk (*).

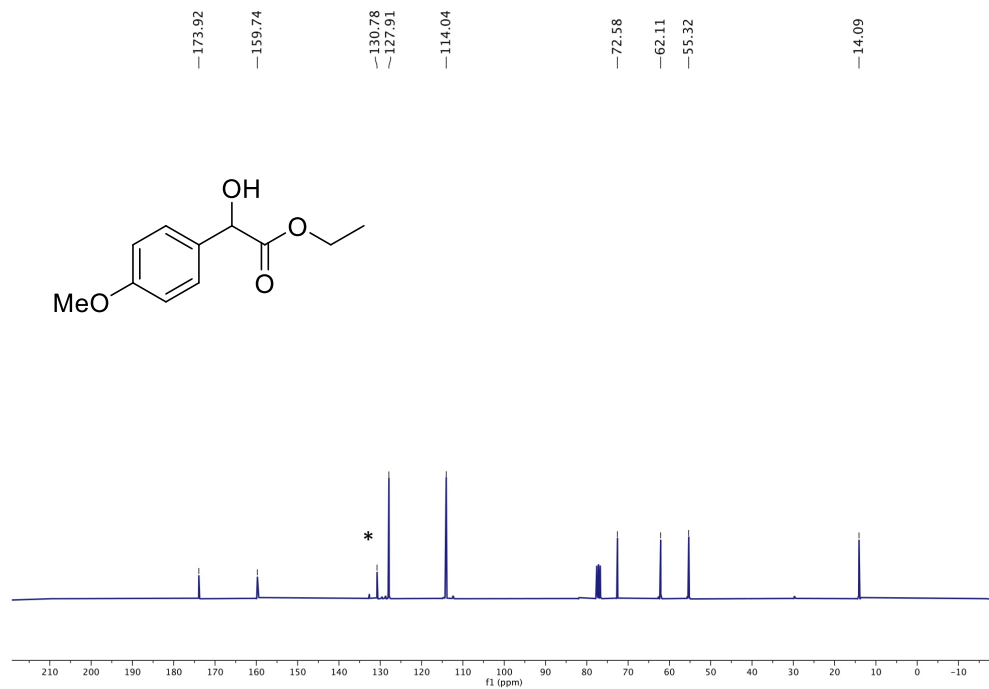


Figure S43. ¹³C{¹H} NMR (75 MHz, 22 °C, CDCl₃) of **1c-H₂**. Unreacted starting material **1c** is denoted with an asterisk (*).

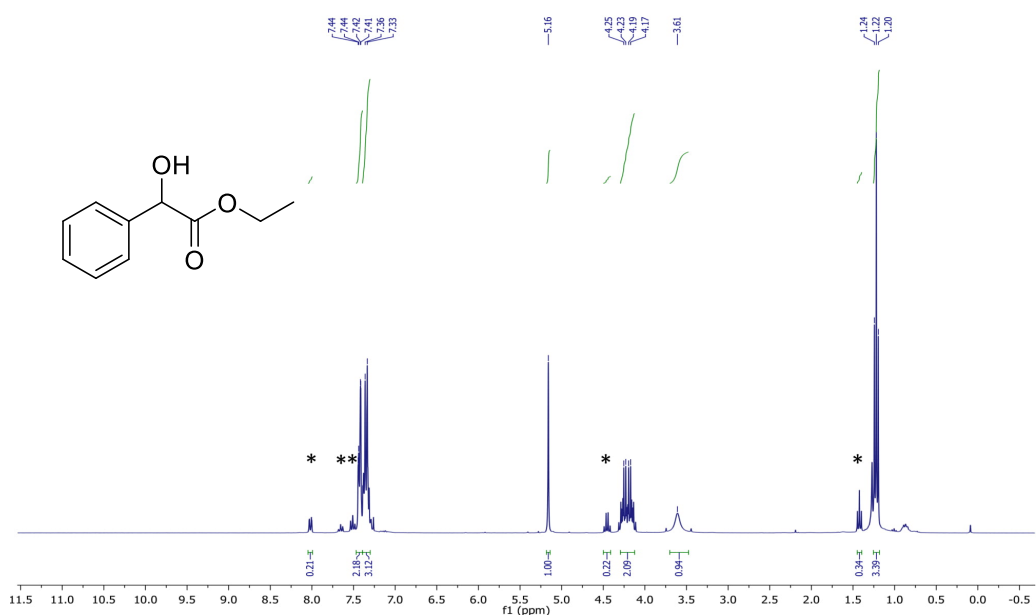


Figure S44. ^1H NMR (300 MHz, 22 °C, CDCl_3) of **1d-H₂**. Unreacted starting material **1d** is denoted with an asterisk (*).

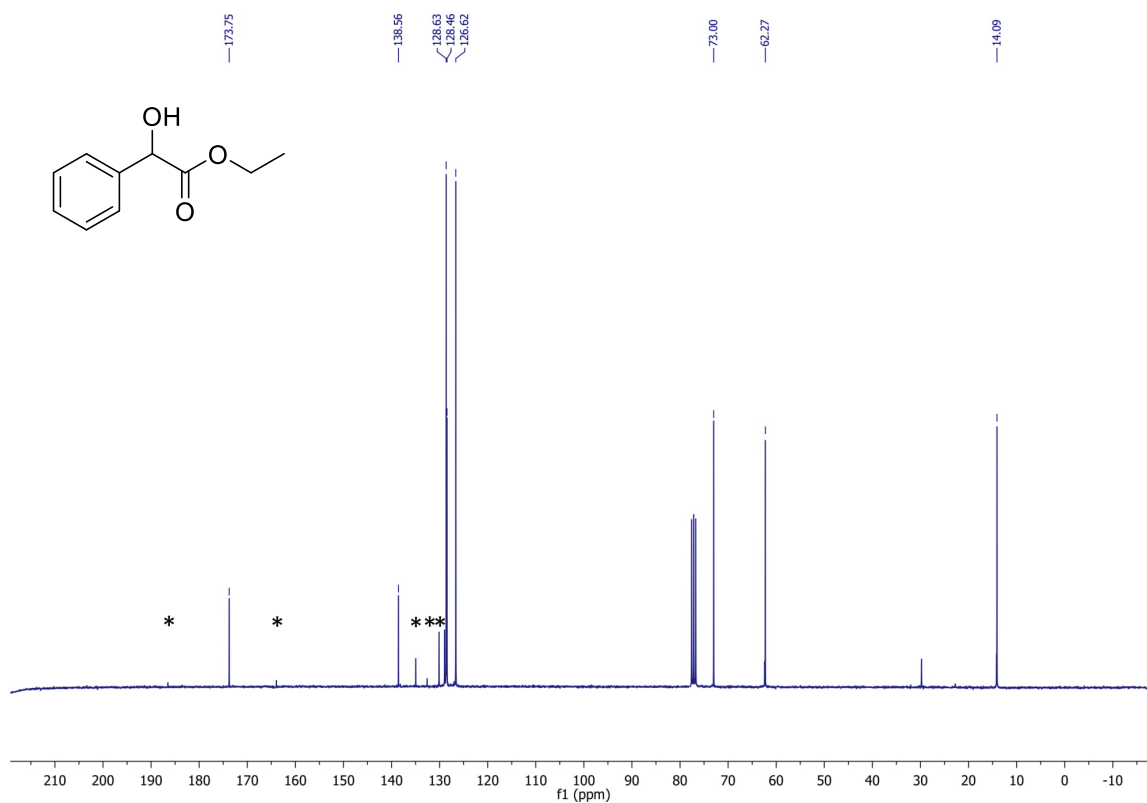


Figure S45. $^{13}\text{C}\{^1\text{H}\}$ NMR (75 MHz, 22 °C, CDCl_3) of **1d-H₂**. Unreacted starting material **1d** is denoted with an asterisk (*).

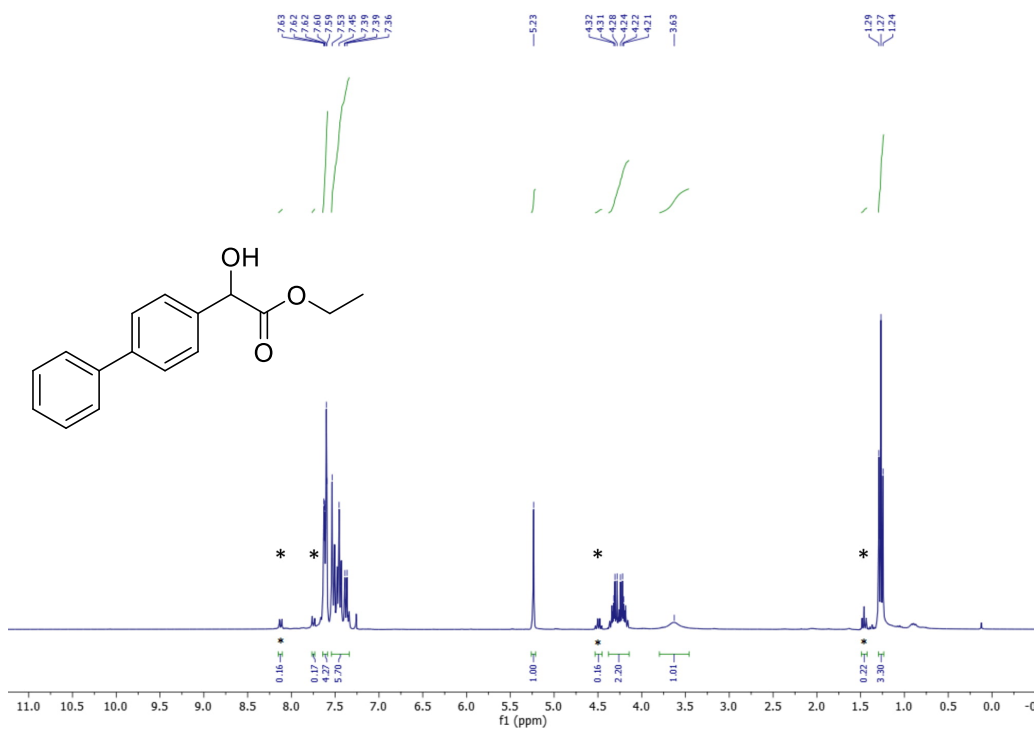


Figure S46. ¹H NMR (300 MHz, 22 °C, CDCl₃) of **1e-H₂**. Unreacted starting material **1e** is denoted with an asterisk (*).

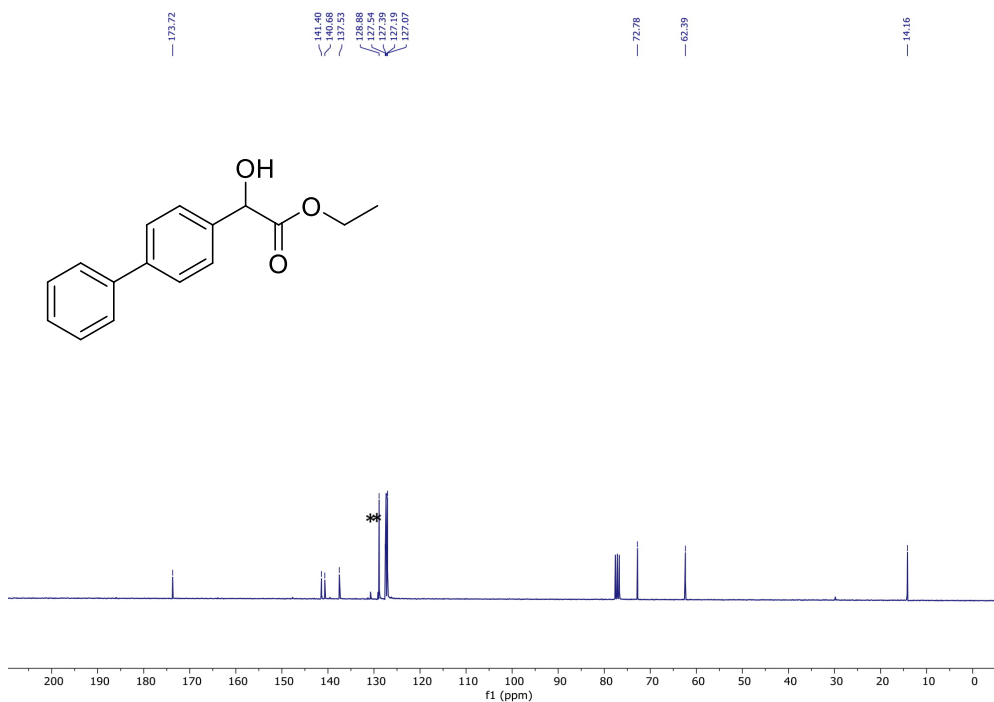
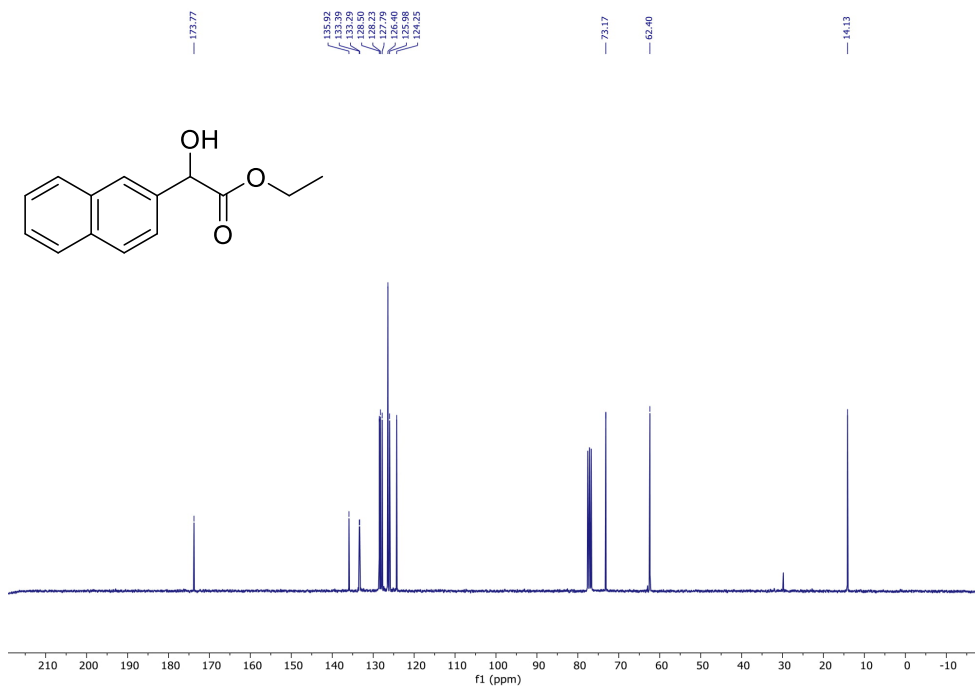
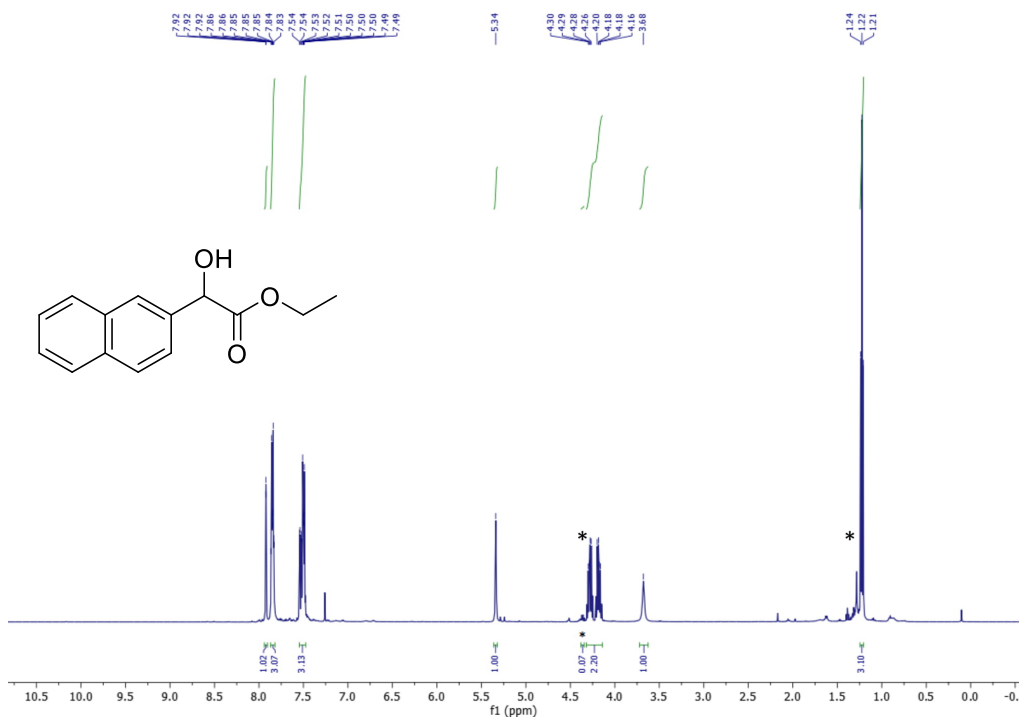


Figure S47. ¹³C {¹H} NMR (75 MHz, 22 °C, CDCl₃) of **1e-H₂**. Unreacted starting material **1e** is denoted with an asterisk (*).



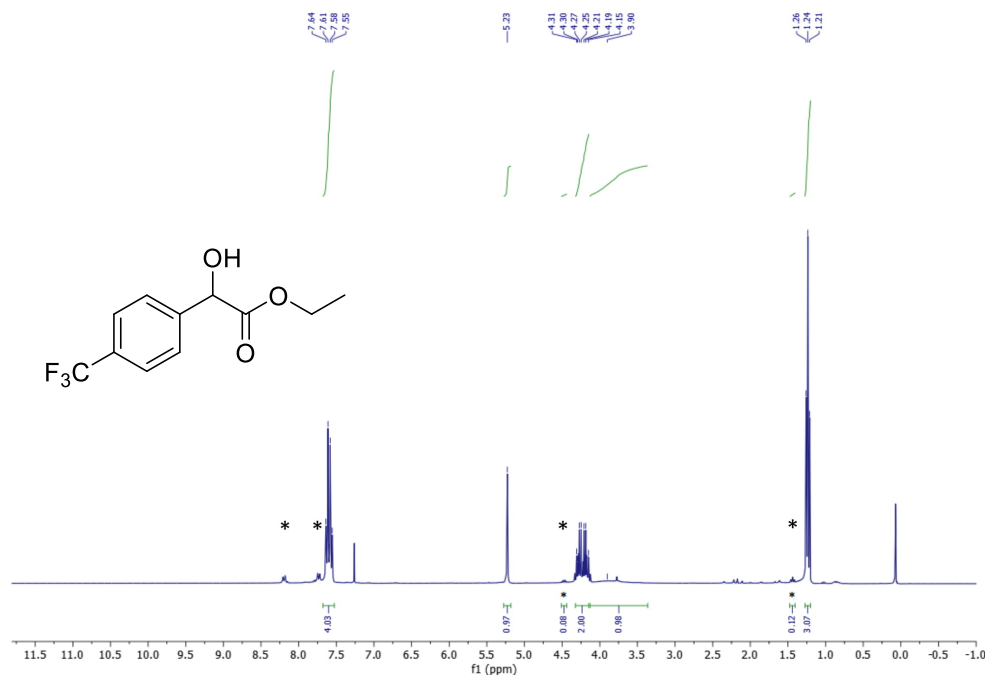


Figure S50. ¹H NMR (300 MHz, 22 °C, CDCl₃) of **1g-H₂**. Unreacted starting material **1g** is denoted with an asterisk (*).

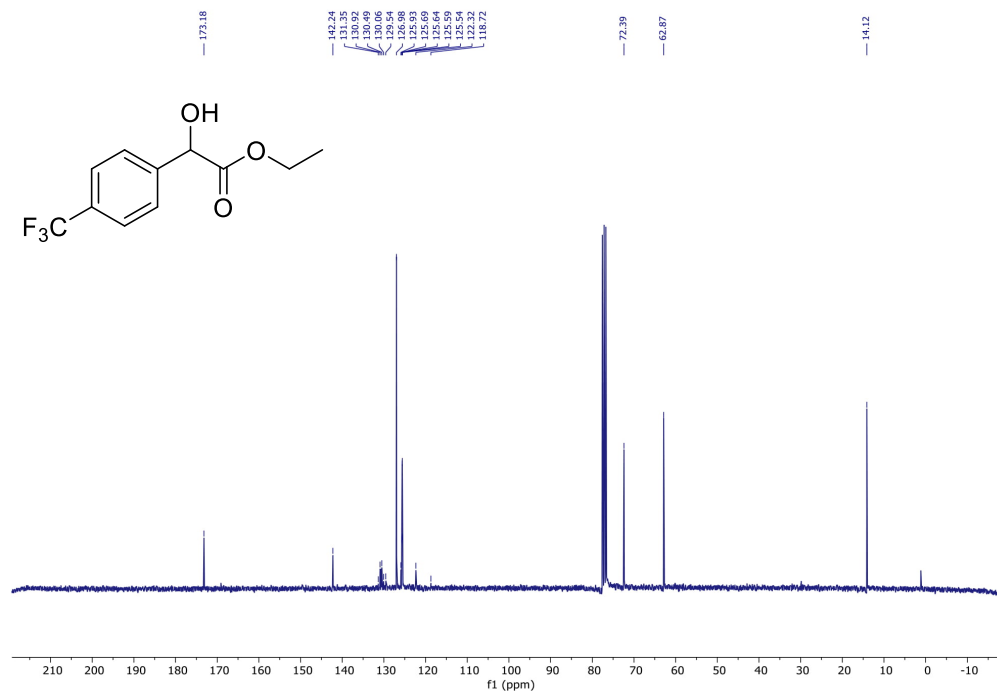


Figure S51. ¹³C{¹H} NMR (75 MHz, 22 °C, CDCl₃) of **1g-H₂**. Unreacted starting material **1g** is denoted with an asterisk (*).

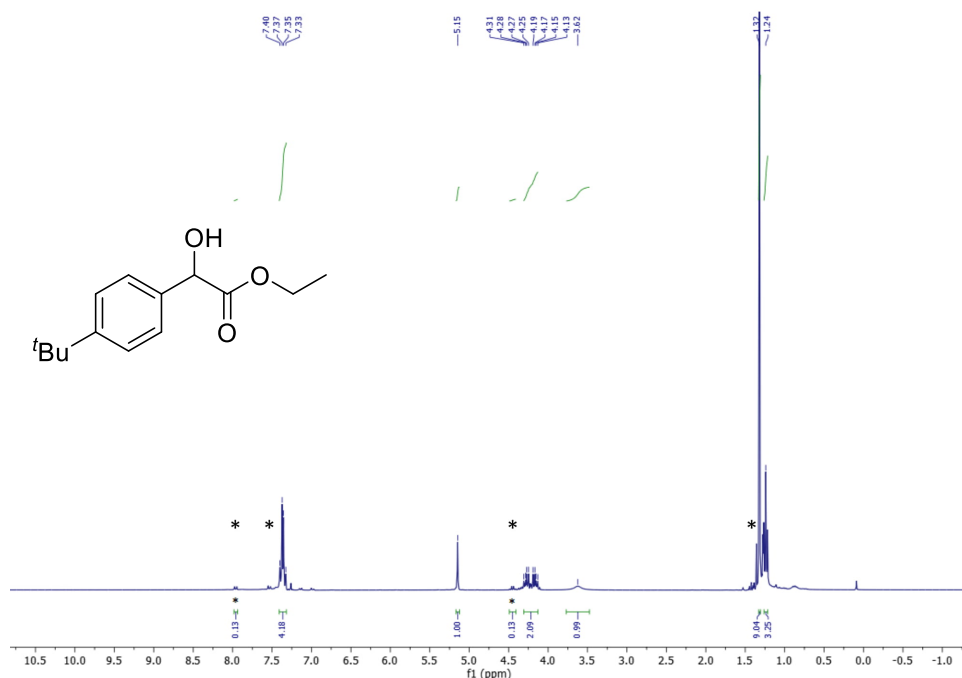


Figure S52. ¹H NMR (300 MHz, 22 °C, CDCl₃) of **1h-H₂**. Unreacted starting material **1h** is denoted with an asterisk (*).

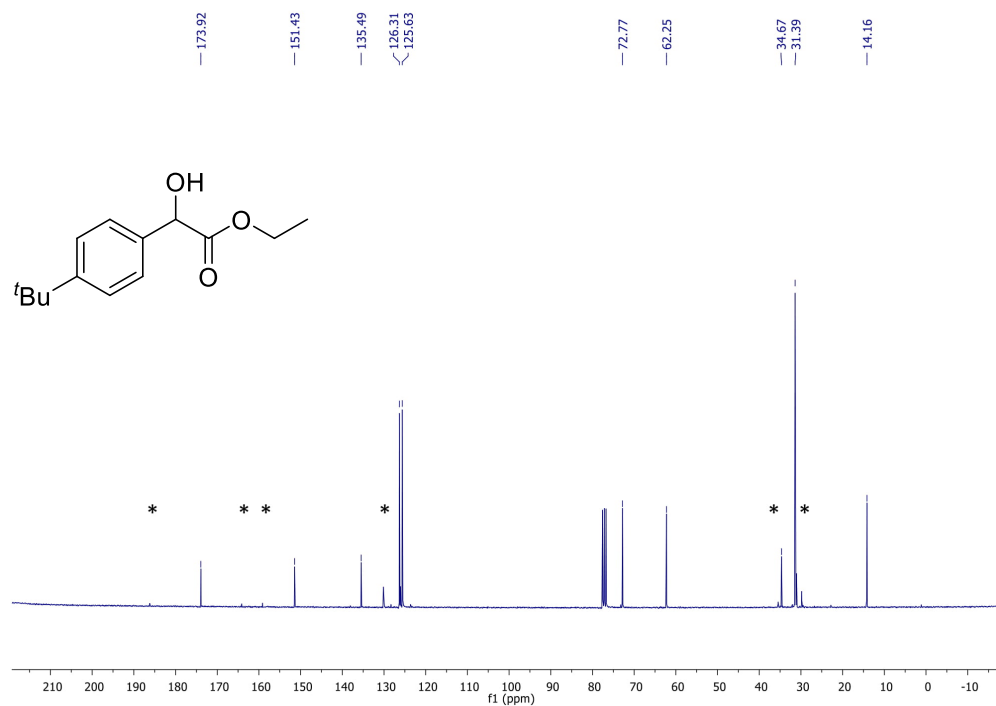


Figure S53. ¹³C NMR (75 MHz, 22 °C, CDCl₃) of **1h-H₂**. Unreacted starting material **1h** is denoted with an asterisk (*).

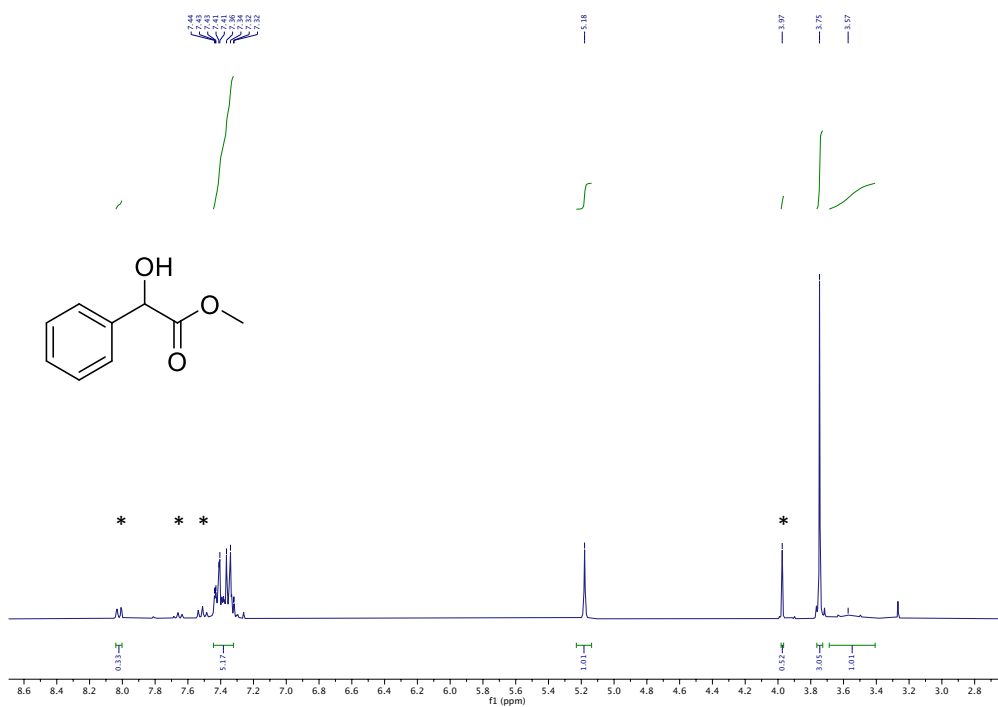


Figure S54. ¹H NMR (300 MHz, 22 °C, CDCl₃) of **1i-H₂**. Unreacted starting material **1i** is denoted with an asterisk (*).

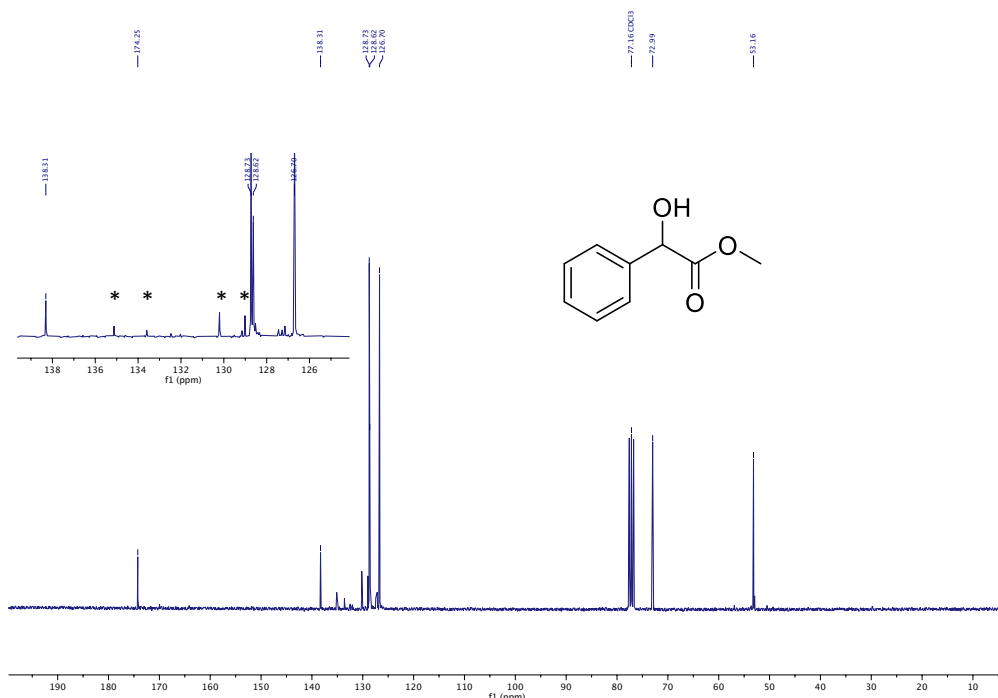


Figure S55. ¹³C{¹H} NMR (75 MHz, 22 °C, CDCl₃) of **1i-H₂**. Unreacted starting material **1i** is denoted with an asterisk (*).

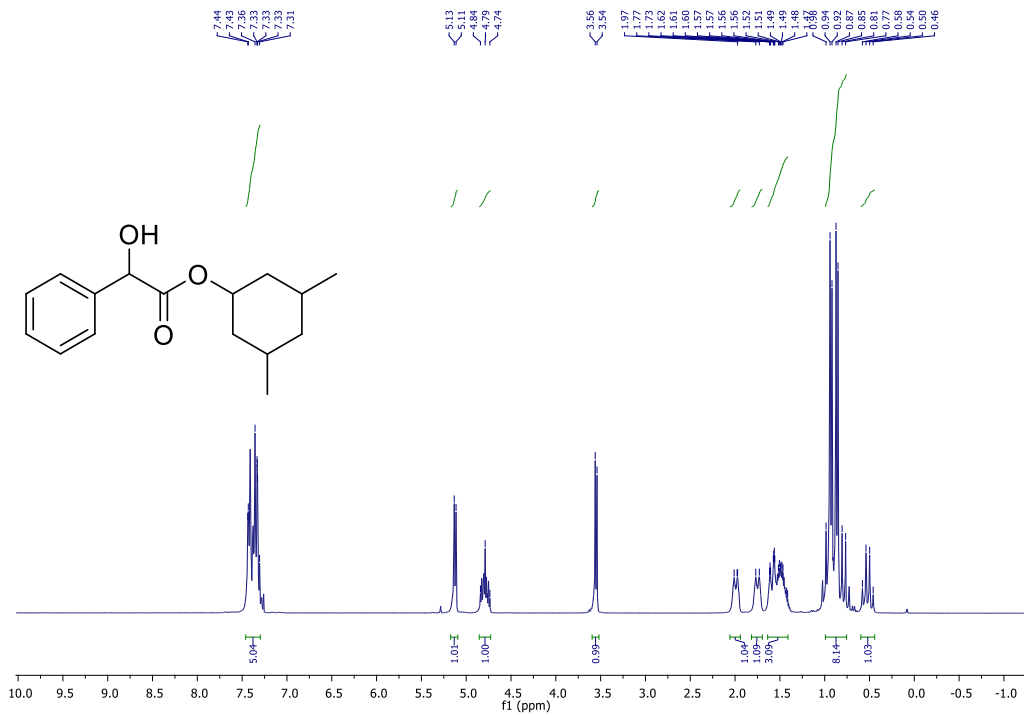


Figure S56. ¹H NMR (300 MHz, 22 °C, CDCl₃) of 1j-H₂.

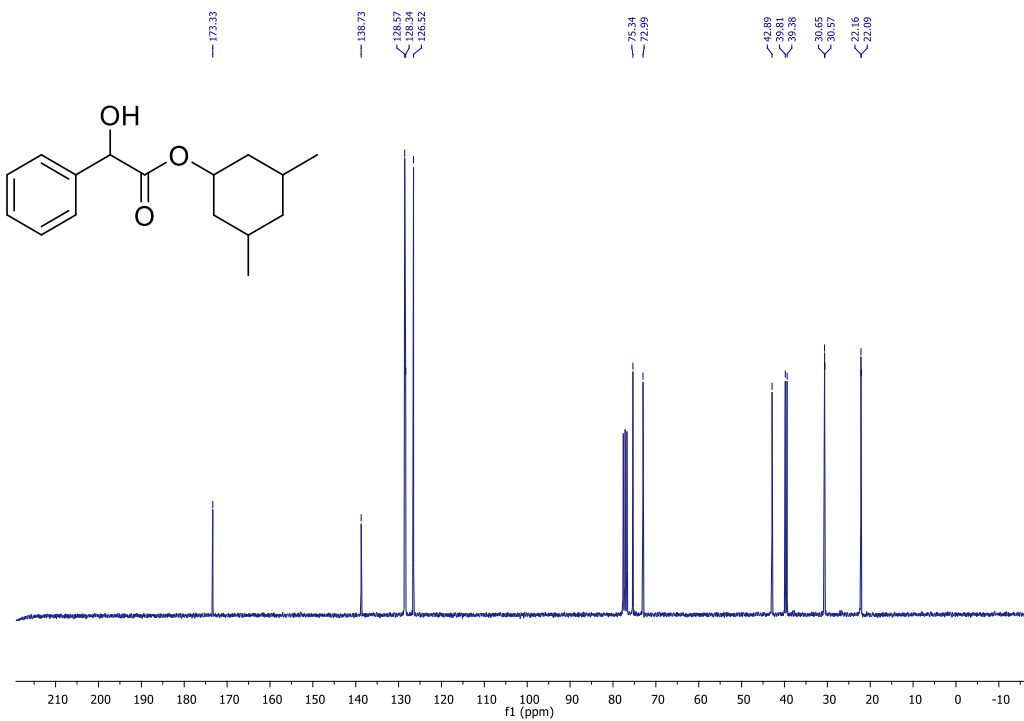


Figure S57. ¹³C {¹H} NMR (75 MHz, 22 °C, CDCl₃) of 1j-H₂.

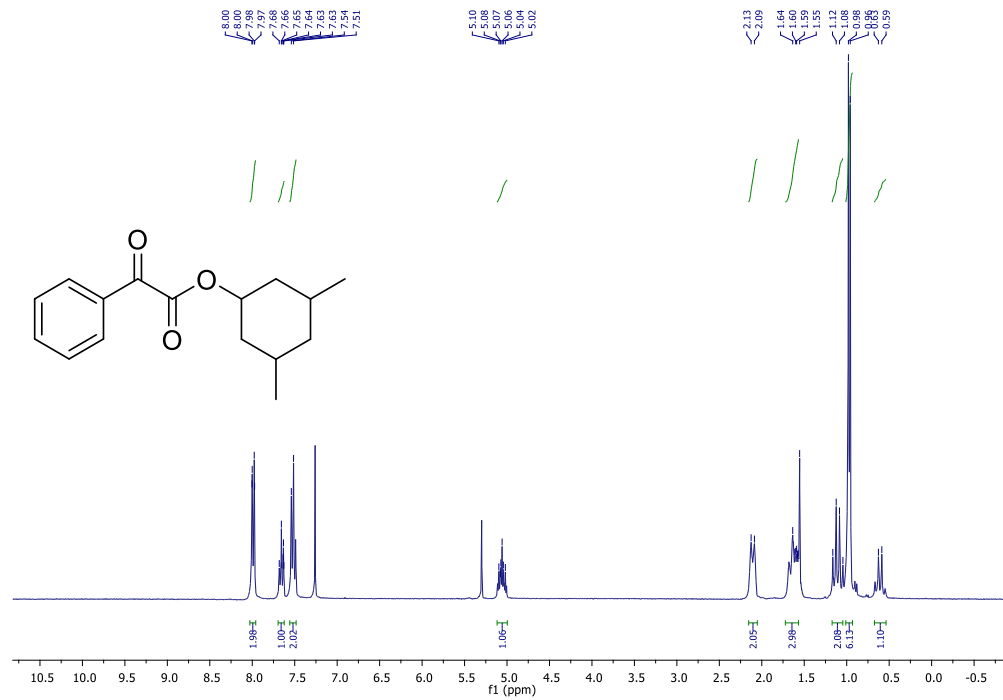


Figure S58. ¹H NMR (300 MHz, 22 °C, CDCl₃) of **1j**.

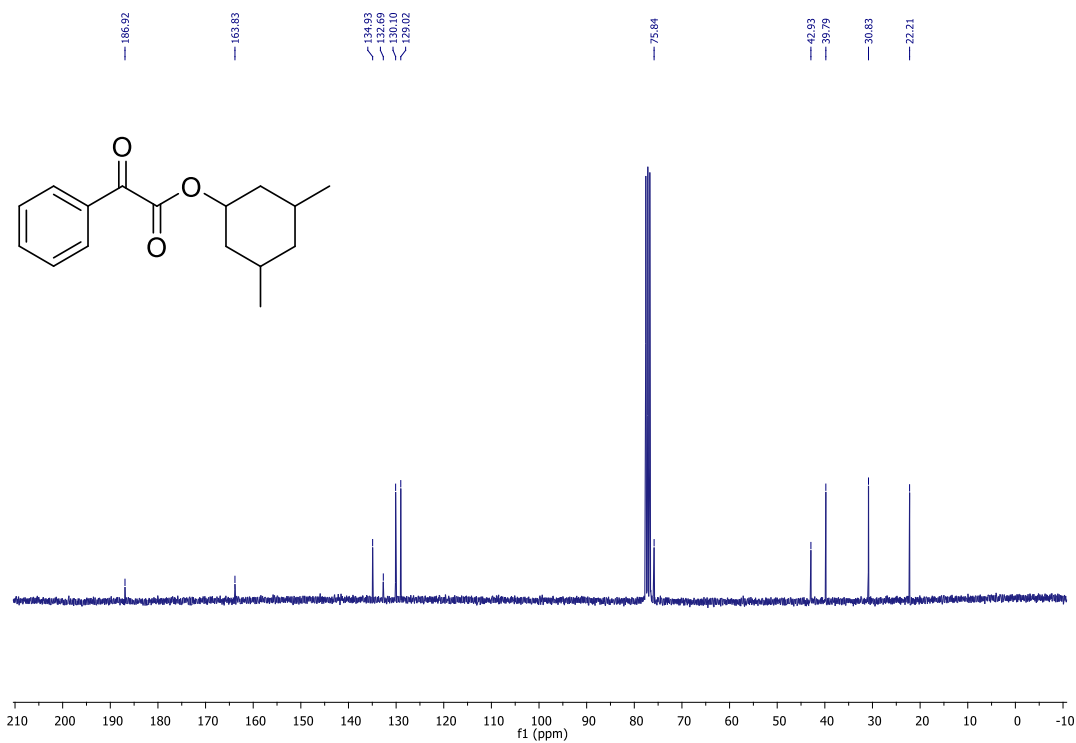


Figure S59. ¹³C{¹H} NMR (75 MHz, 22 °C, CDCl₃) of **1j**.

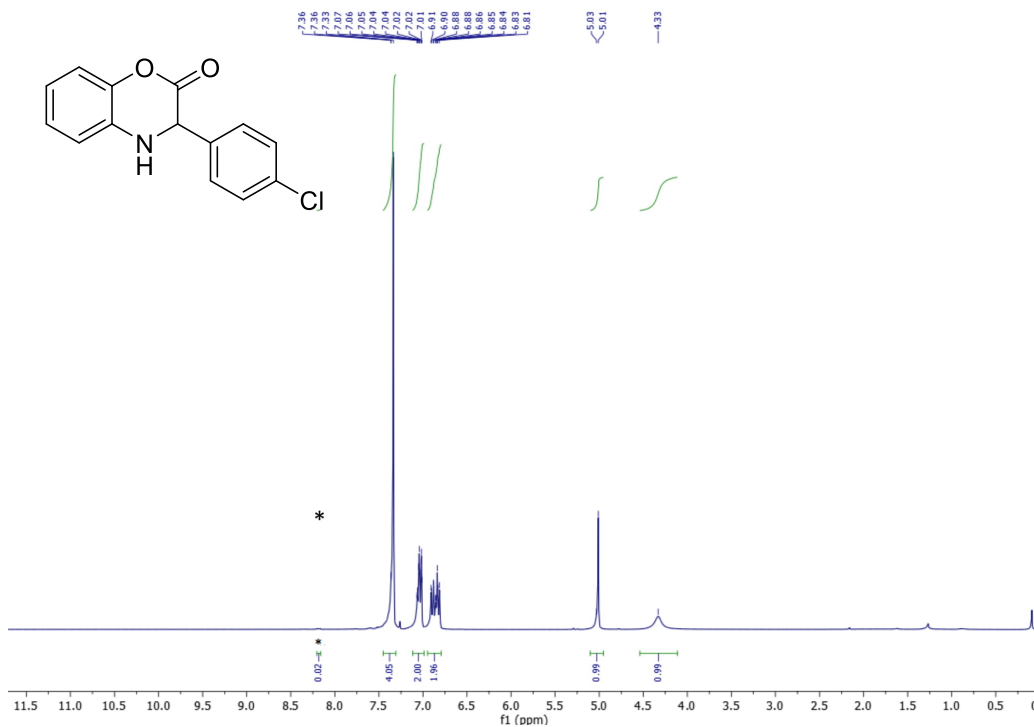


Figure S60. ¹H NMR (300 MHz, 22 °C, CDCl₃) of **2a-H₂**. Unreacted starting material **2a** is denoted with an asterisk (*).

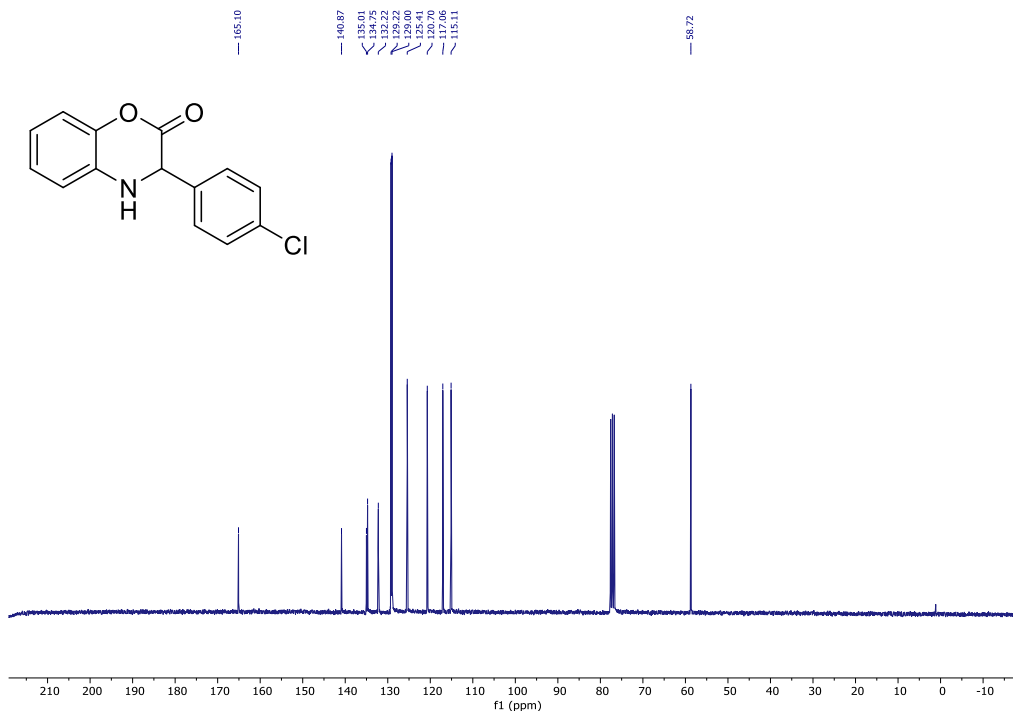


Figure S61. ¹³C{¹H} NMR (75 MHz, 22 °C, CDCl₃) of **2a-H₂**.

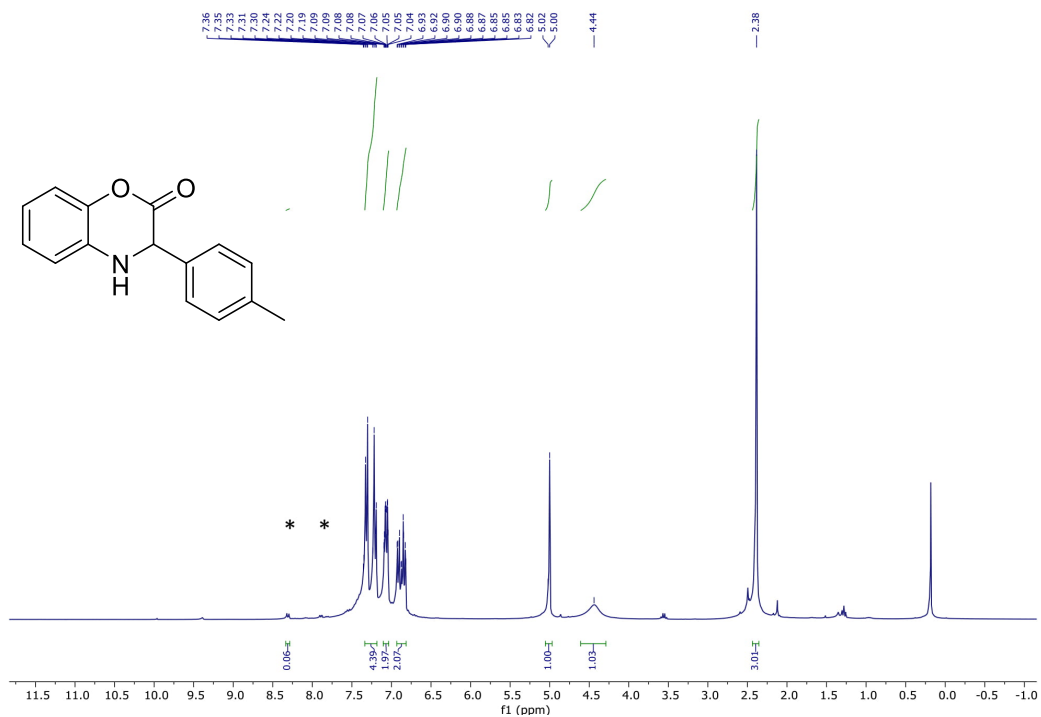


Figure S62. ¹H NMR (500 MHz, 22 °C, CDCl₃) of **2b-H₂**. Unreacted starting material **2b** is denoted with an asterisk (*).



Figure S63. ¹³C{¹H} NMR (126 MHz, 22 °C, CDCl₃) of **2b-H₂**.

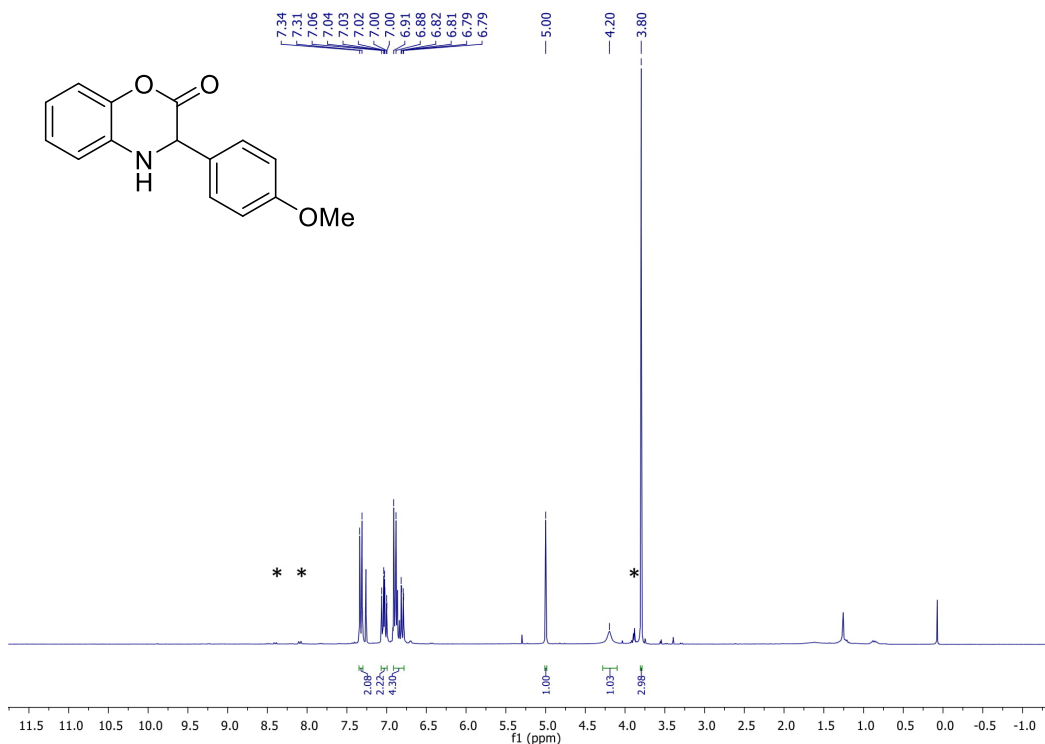


Figure S64. ¹H NMR (300 MHz, 22 °C, CDCl₃) of **2c-H₂**. Unreacted starting material **2c** is denoted with an asterisk (*).

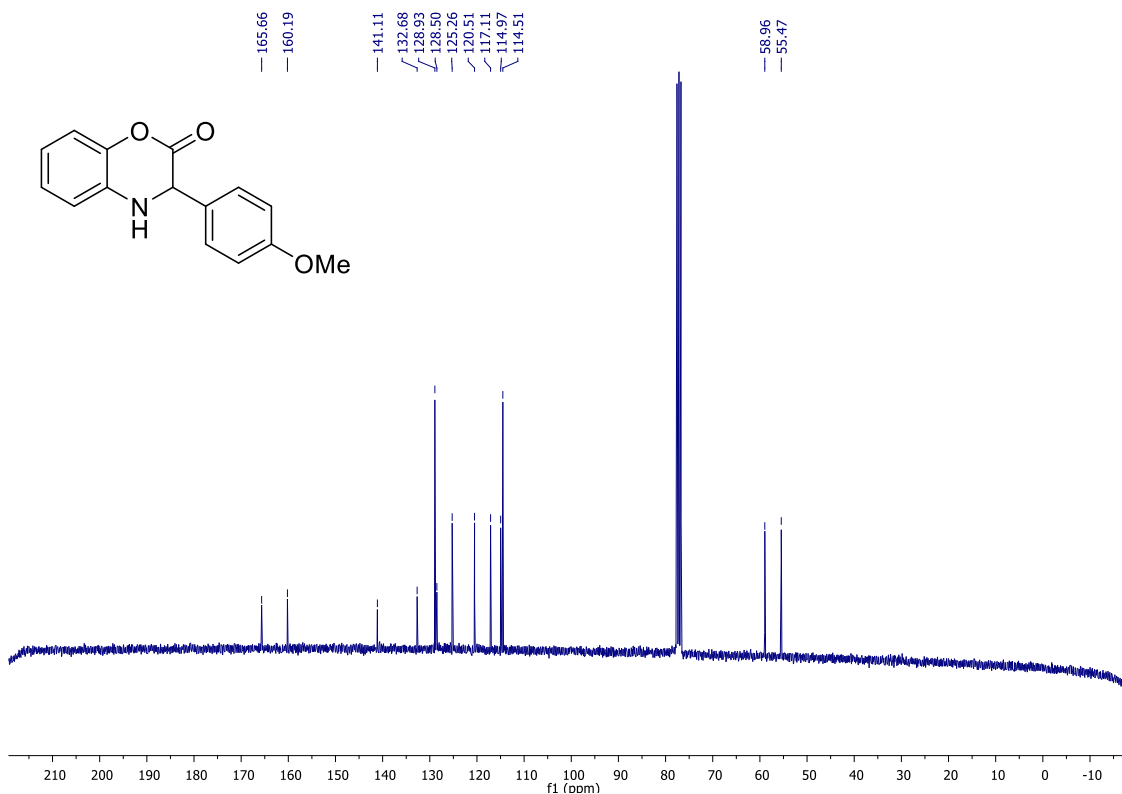


Figure S65. ¹³C{¹H} NMR (75 MHz, 22 °C, CDCl₃) of **2c-H₂**.

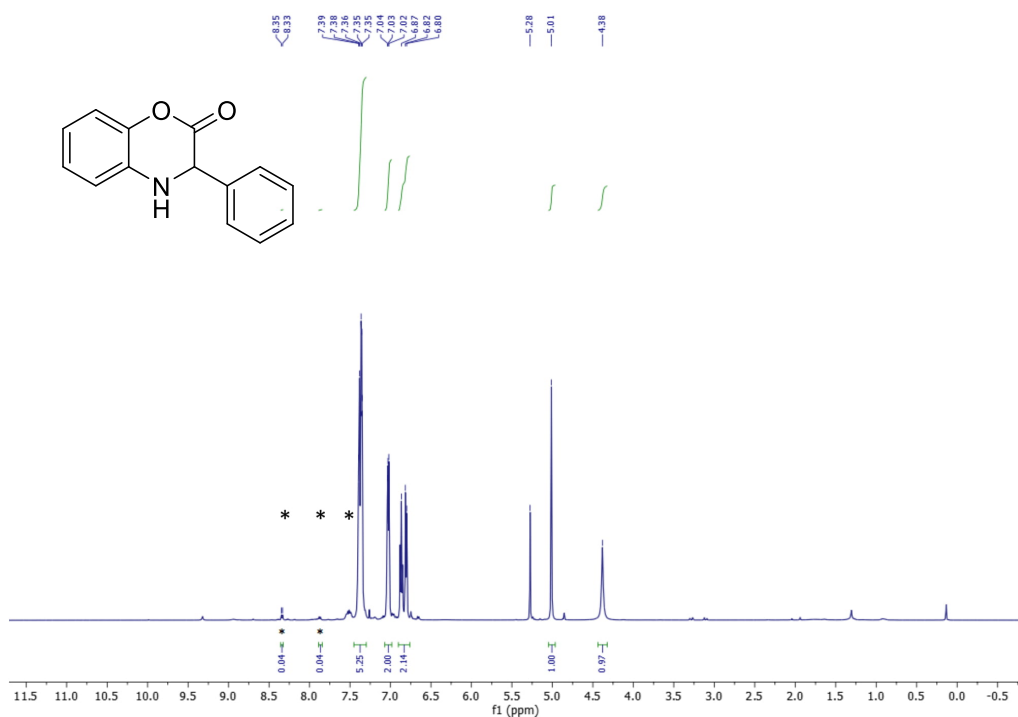


Figure S66. ¹H NMR (500 MHz, 22 °C, CDCl₃) of **2d-H₂**. Unreacted starting material **2d** is denoted with an asterisk (*).

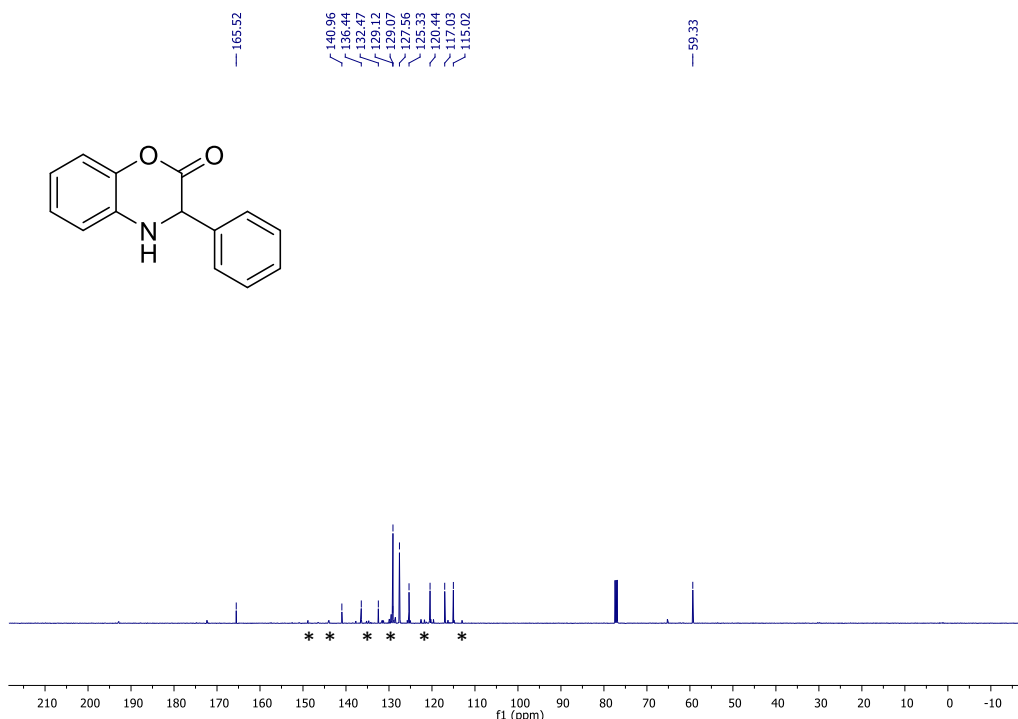


Figure S67. ¹³C {¹H} NMR (126 MHz, 22 °C, CDCl₃) of **2d-H₂**. Unreacted starting material **2d** is denoted with an asterisk (*).

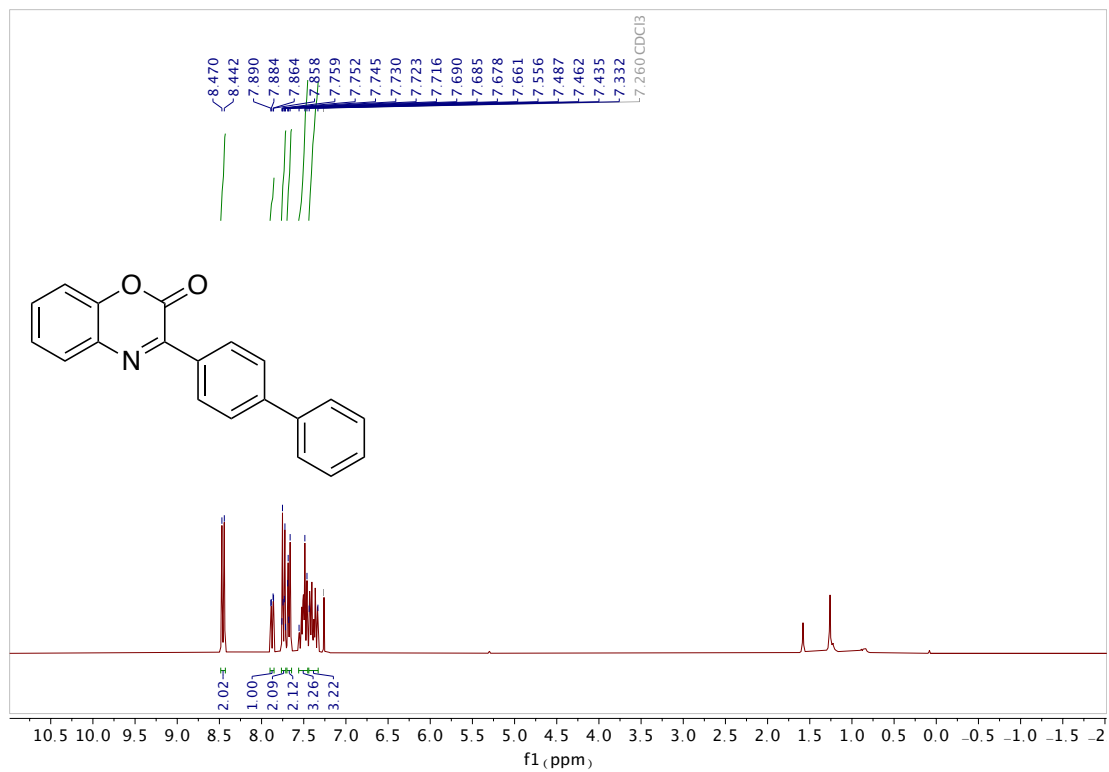


Figure S68. ¹H NMR (300 MHz, 22 °C, CDCl₃) of **2e**.

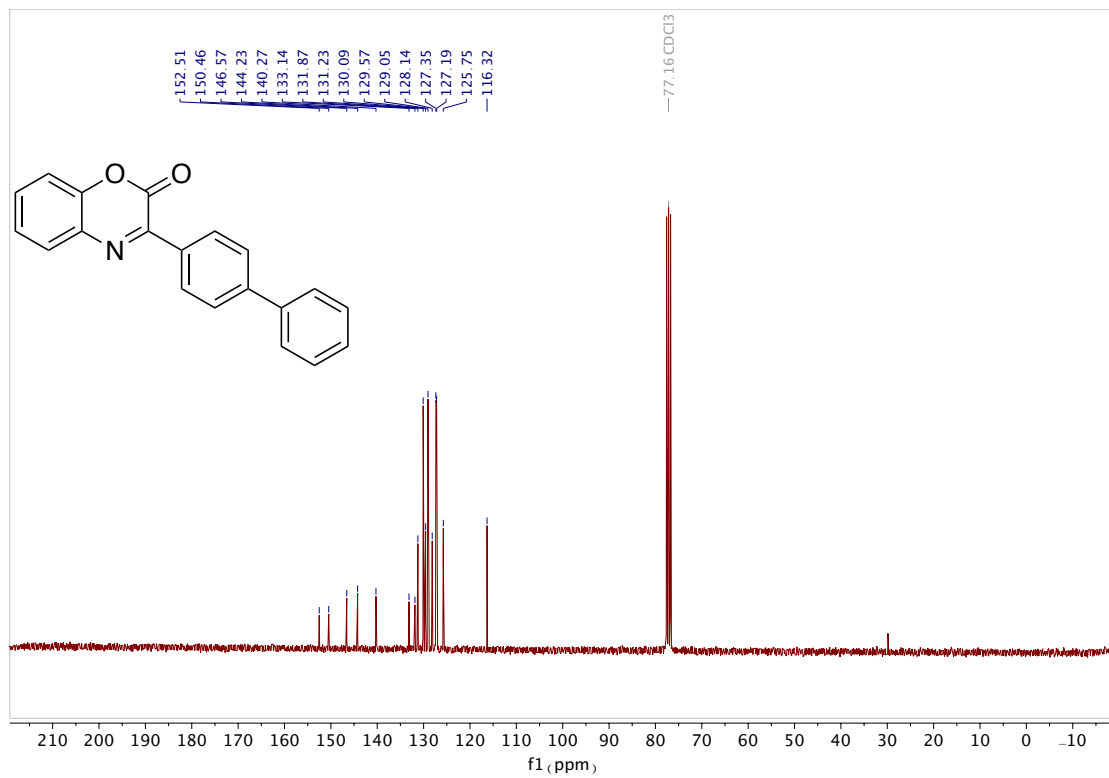


Figure S69. ¹³C{¹H} NMR (75 MHz, 22 °C, CDCl₃) of **2e**.

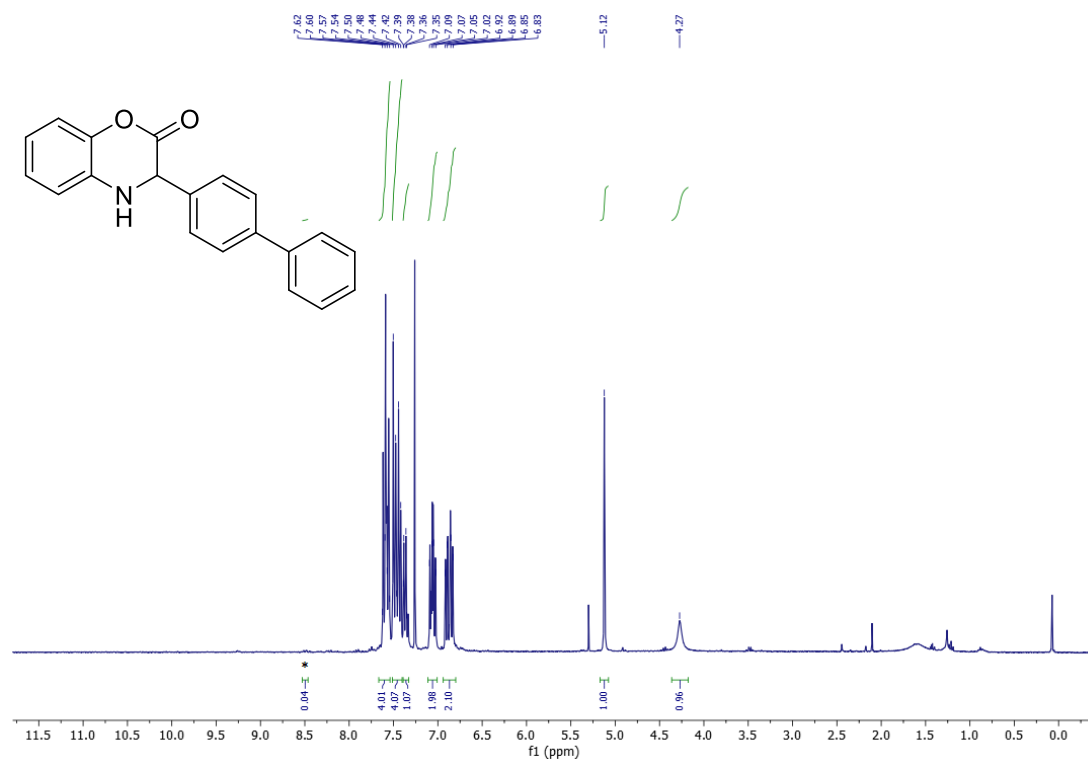


Figure S70. ¹H NMR (300 MHz, 22 °C, CDCl₃) of **2e-H₂**.

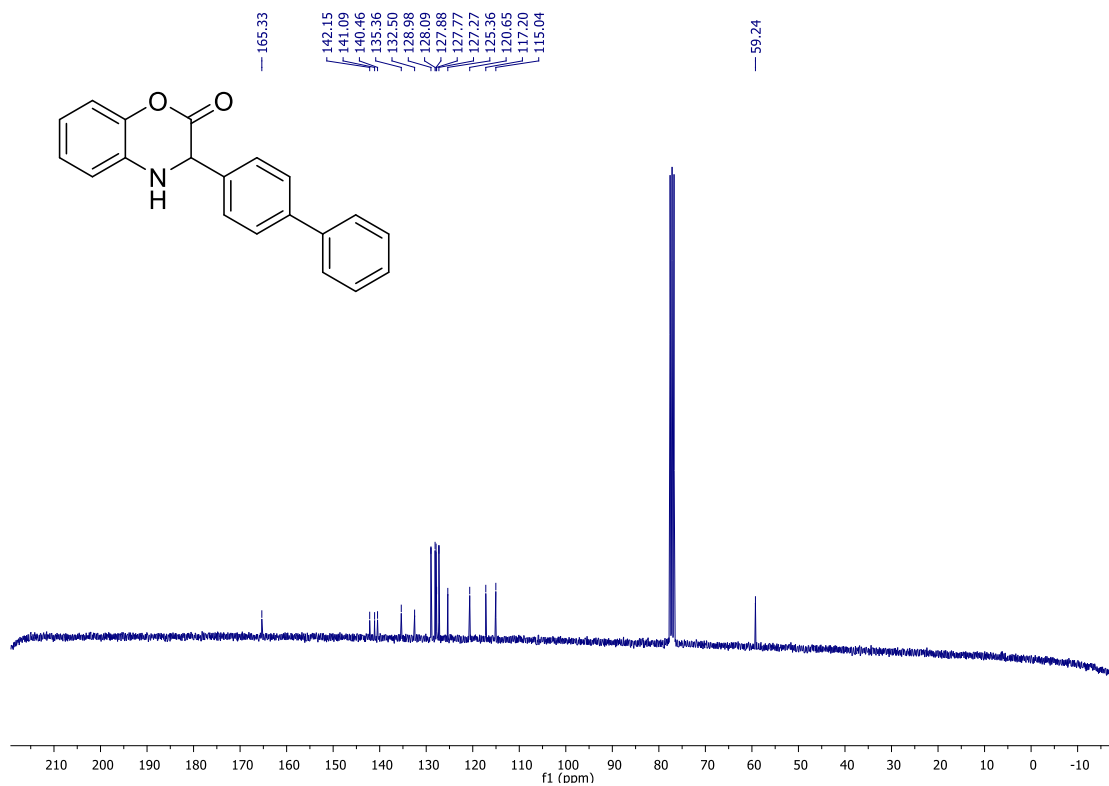


Figure S71. ¹³C {¹H} NMR (75 MHz, 22 °C, CDCl₃) of **2e-H₂**.

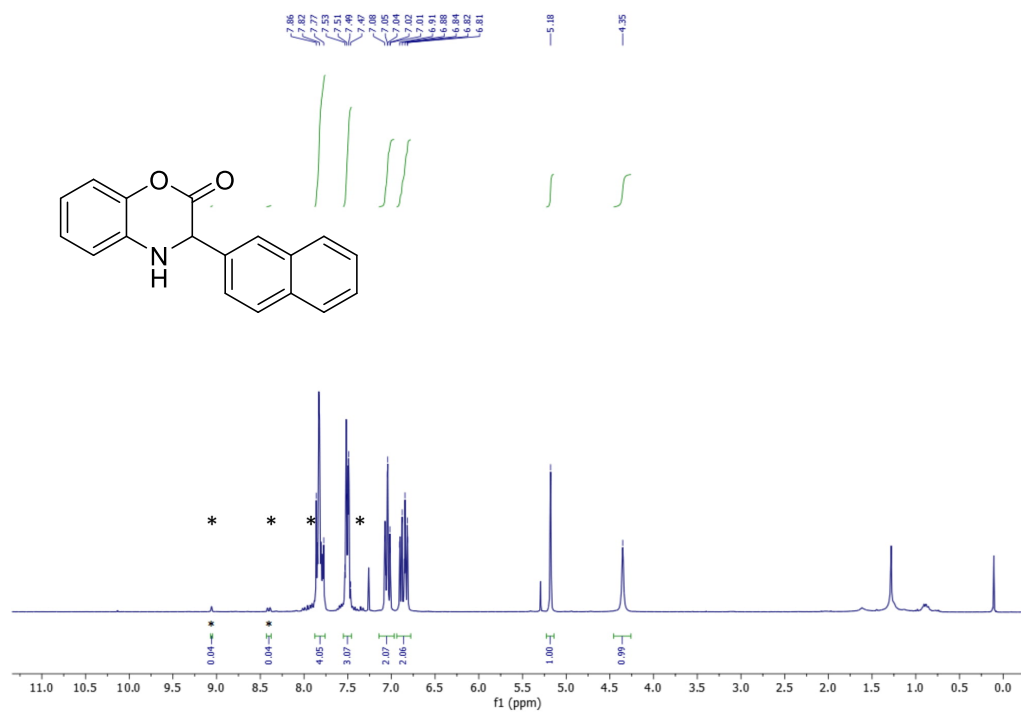


Figure S72. ^1H NMR (300 MHz, 22 °C, CDCl_3) of **2f-H₂**. Unreacted starting material **2f** is denoted with an asterisk (*).

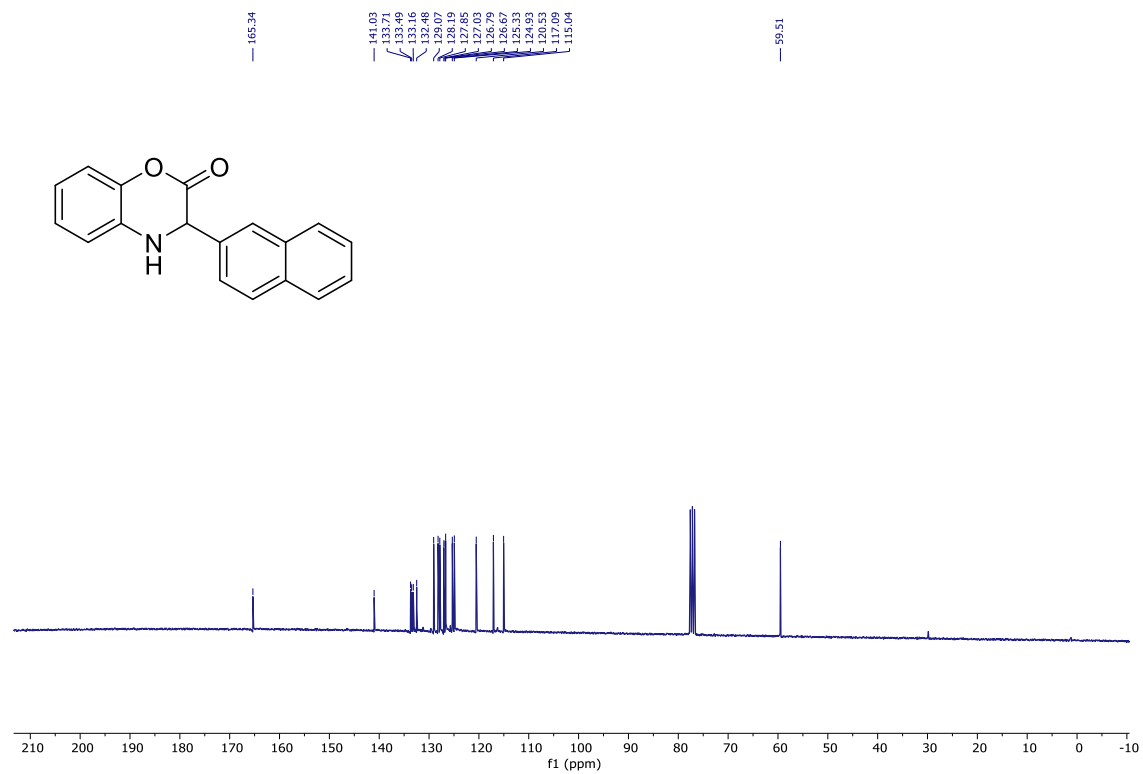


Figure S73. $^{13}\text{C}\{^1\text{H}\}$ NMR (75 MHz, 22 °C, CDCl_3) of **2f-H₂**.

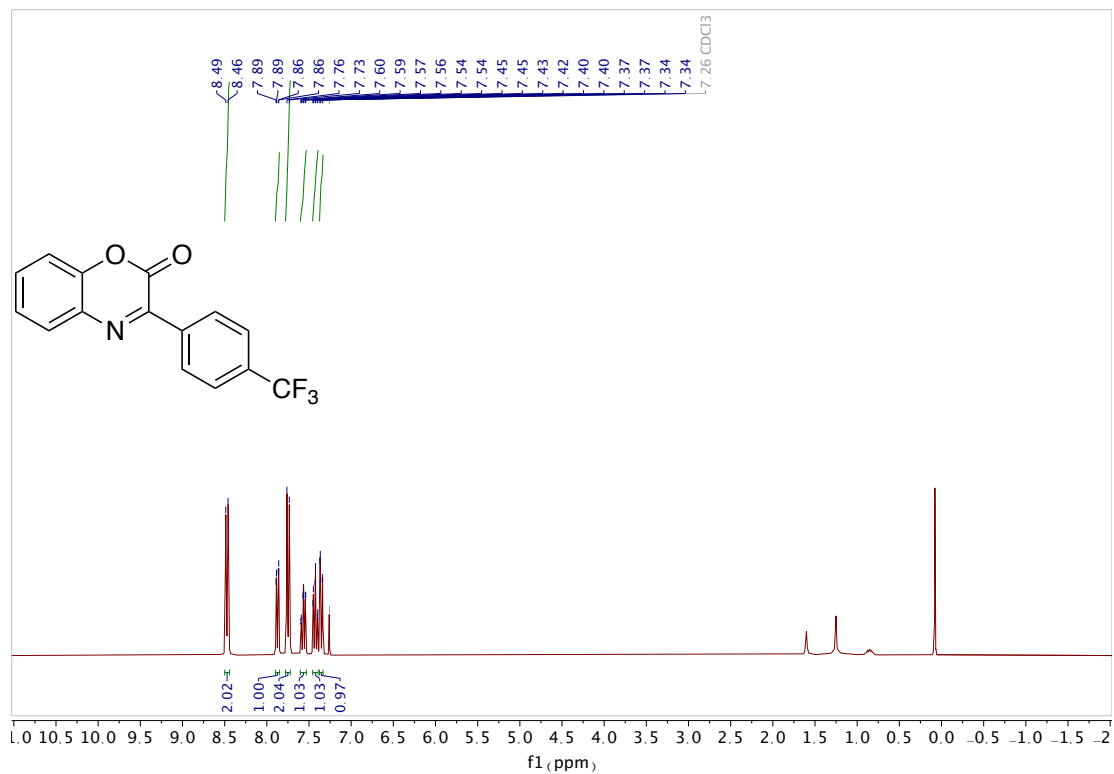


Figure S74. $^1\text{H NMR}$ (300 MHz, 22 °C, CDCl_3) of **2g**.

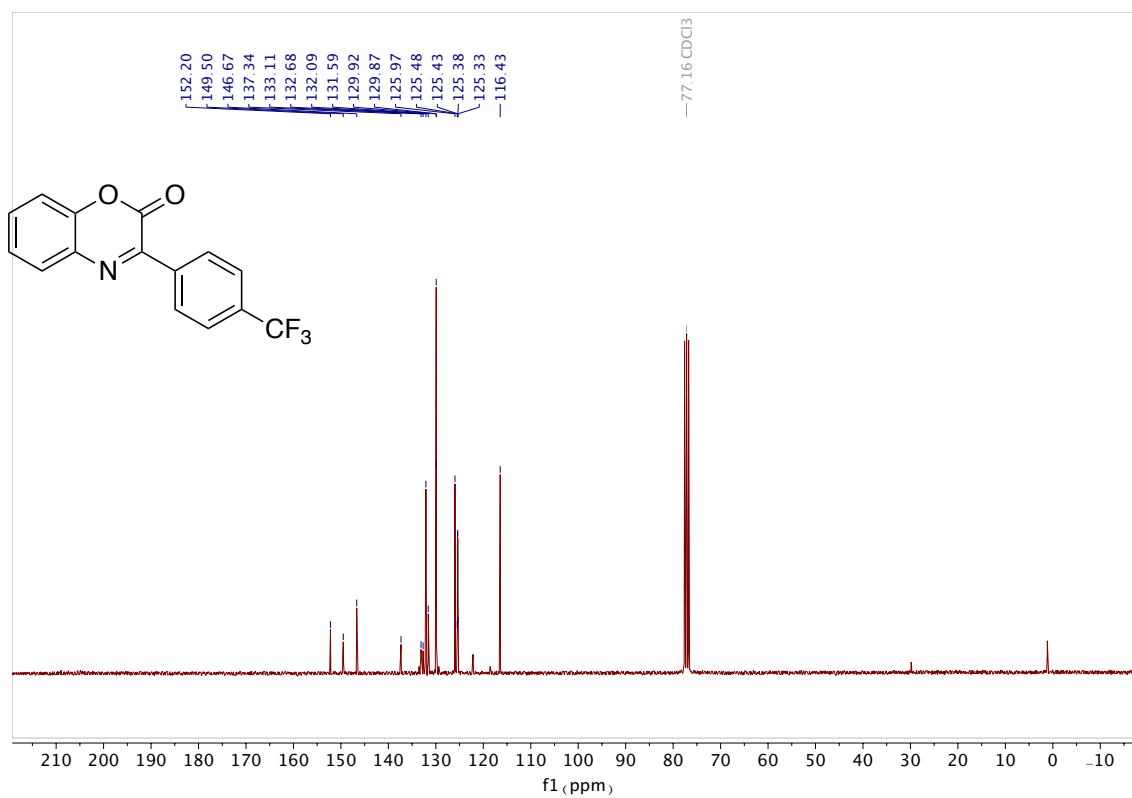


Figure S75. $^{13}\text{C}\{^1\text{H}\}$ NMR (75 MHz, 22 °C, CDCl_3) of **2g**.

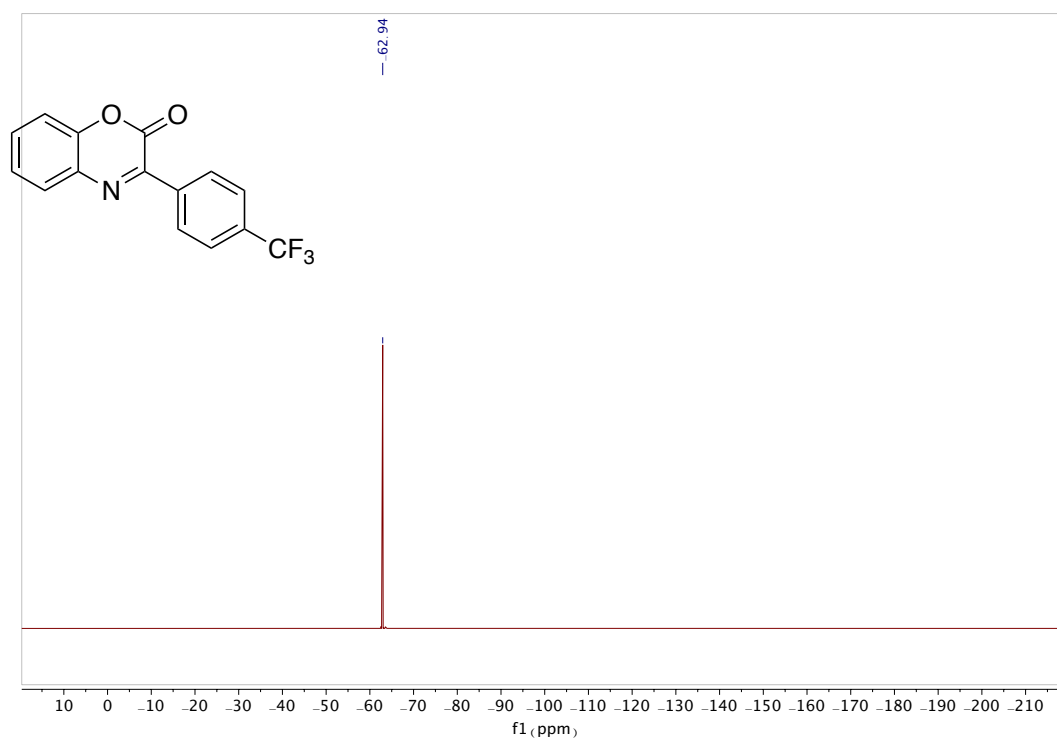


Figure S76. ^{19}F NMR (282 MHz, 22 °C, CDCl_3) of **2g**.

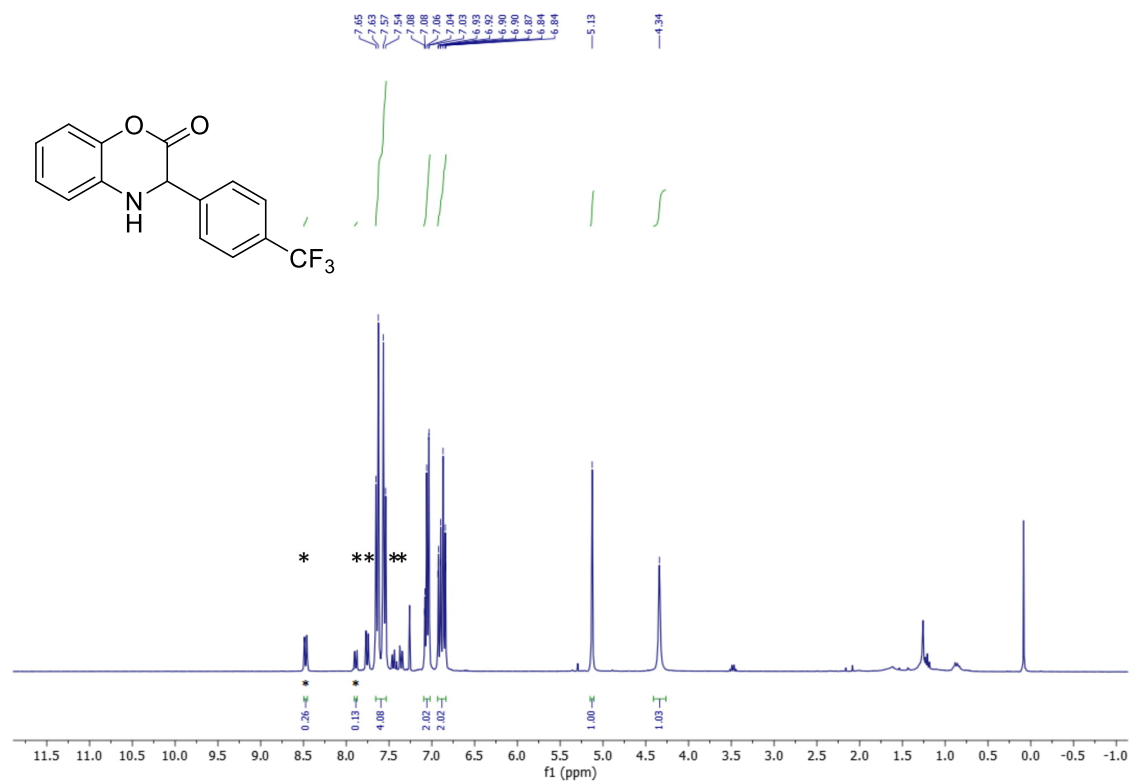


Figure S77. ^1H NMR (300 MHz, 22 °C, CDCl_3) of **2g-H₂**. Unreacted starting material **2g** is denoted with an asterisk (*)

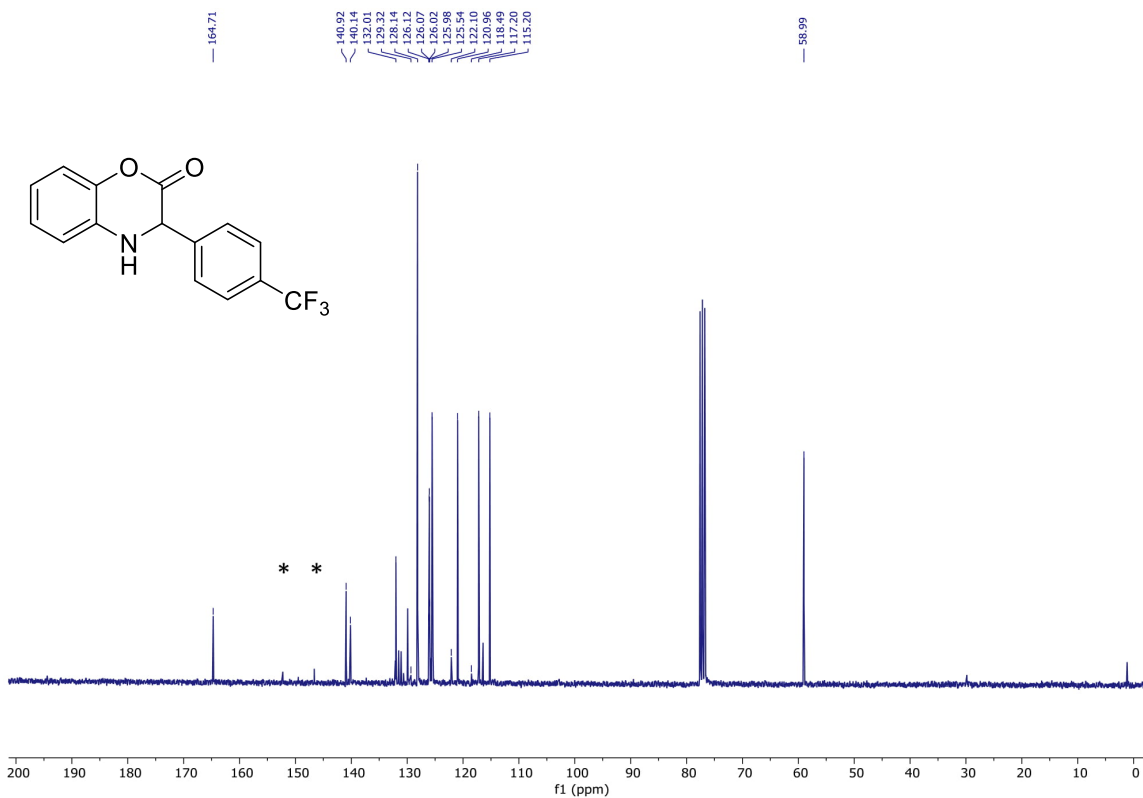


Figure S78. ¹³C{¹H} NMR (75 MHz, 22 °C, CDCl₃) of **2g-H₂**. Unreacted starting material **2g** is denoted with an asterisk (*).

ADDITIONAL EXPERIMENTS

Electrolysis Using a Pt Mesh Working Electrode

Using a Pt working electrode, but otherwise following the general procedure, a bulk electrolysis was performed using LiClO₄ (1.285 g, 12.07 mmol), 3-phenyl-2*H*-benzo[*b*][1,4]oxazin-2-one (**2d**; 0.120 g, 0.538 mmol), acetic acid (150 μl, 2.62 mmol); $E_{app} = -0.9$ V vs. Ag/AgCl, 3.2 h. No hydrogenated product was observed. Charge passed = 323 C.

Similarly, using a Pt working electrode, but otherwise following the general procedure a bulk electrolysis was performed using LiClO₄ (1.285 g, 12.07 mmol), ethylbenzoylformate (**1d**; 0.095 g, 0.533 mmol), acetic acid (150 μl, 2.62 mmol); $E_{app} = -0.9$ V vs. Ag/AgCl, 3.3 h. No hydrogenated product was observed. Charge passed = 316 C.

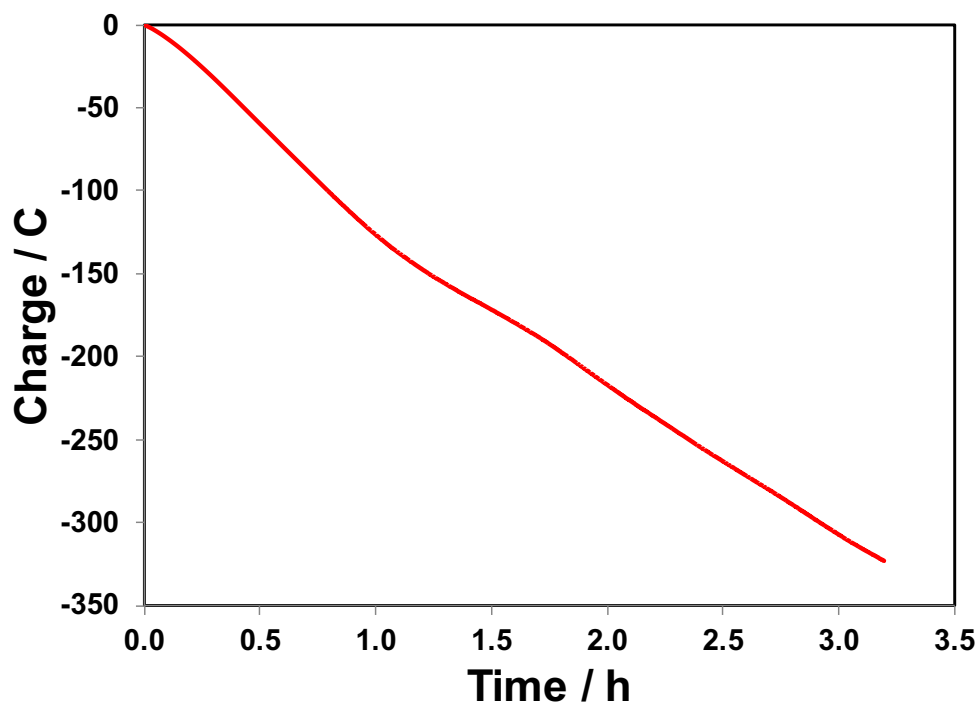


Figure S79. CPE plot of **2d** using the standard electrochemical hydrogenation conditions and a Pt mesh working electrode.

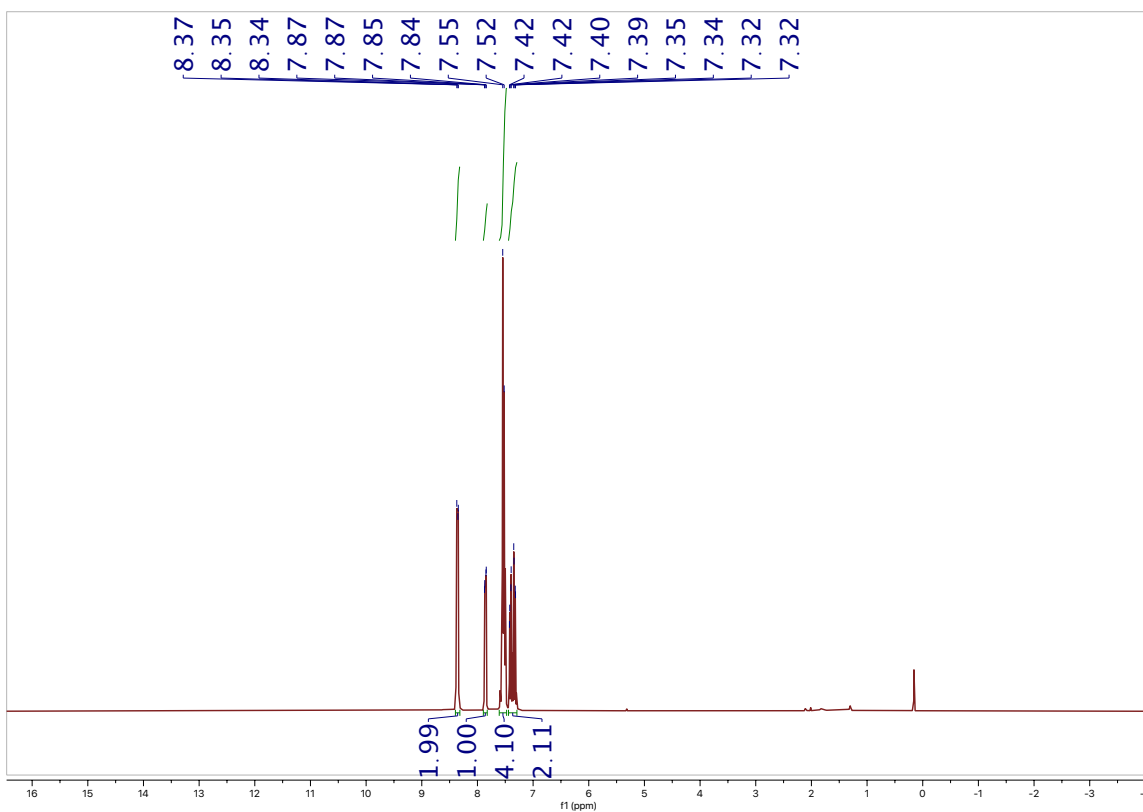


Figure S80. ^1H NMR (300 MHz, 22 °C, CDCl_3) of **2d** using a Pt mesh working electrode. No conversion to product is observed.

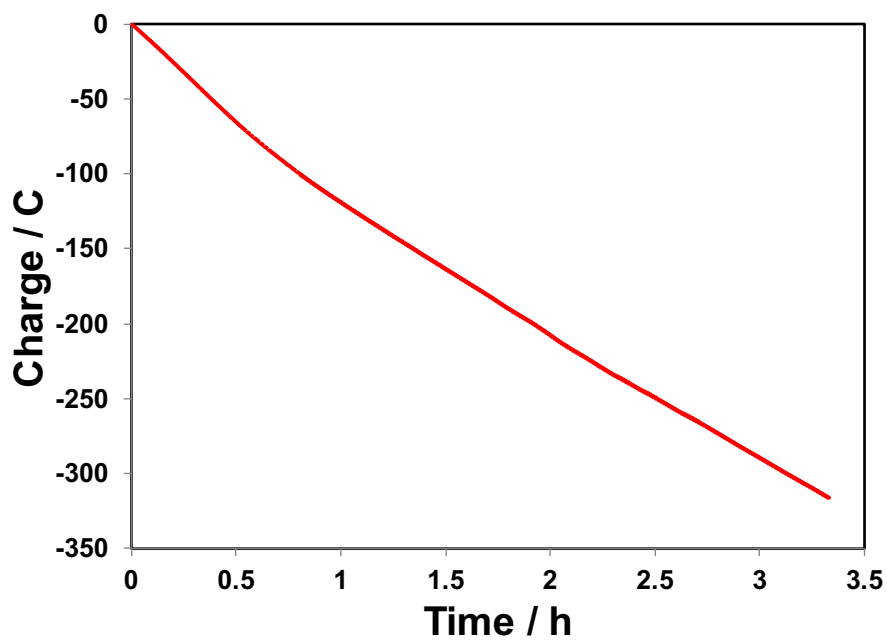


Figure S81. CPE plot for attempted hydrogenation of **1d** using a Pt mesh working electrode.

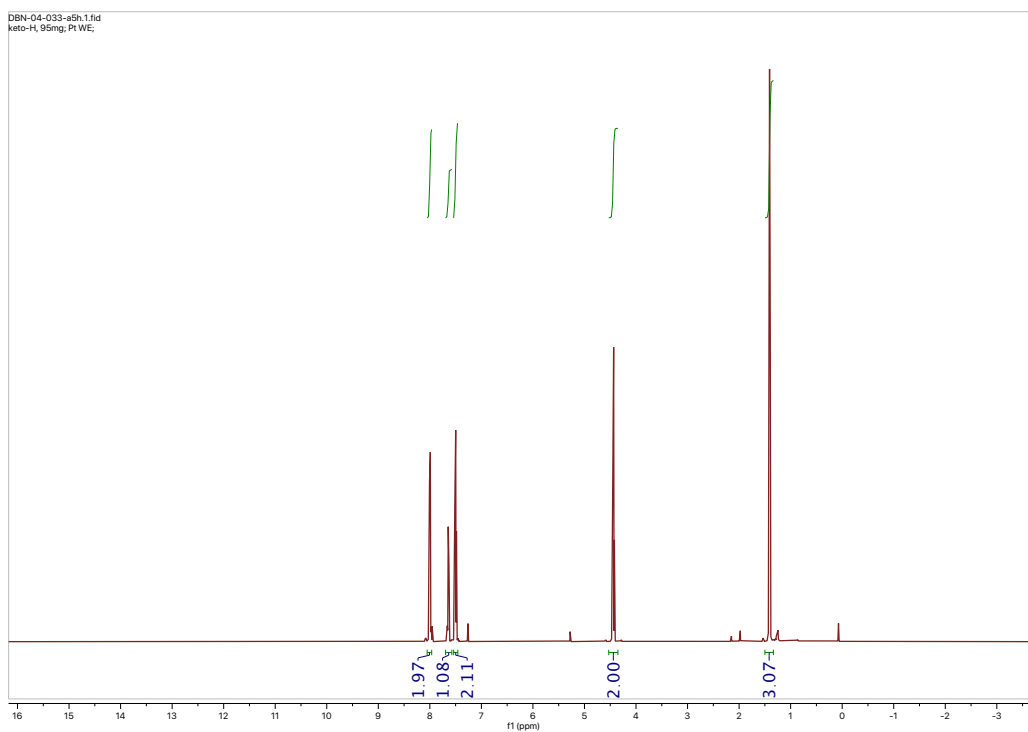


Figure S82. ^1H NMR (300 MHz, 22 °C, CDCl_3) of **1d** using a Pt mesh working electrode. No conversion to product is observed.

Electrochemical Hydrogenation of **1d** in Neat CH₃CN

The general procedure was followed but in neat CH₃CN (no added water) using LiClO₄ (1.285 g, 12.07 mmol), ethyl-benzoylformate (**1d**; 0.095 g, 0.533 mmol), and acetic acid (150 μL, 2.62 mmol); $E_{app} = -0.9$ V vs. Ag/AgCl, 3.3 h. Slightly-yellow oil. NMR conversion to **1d-H₂** = 64 %. Yield = 0.069 g (46 % yield). Charge passed = 183 C (%FE = 26 %).

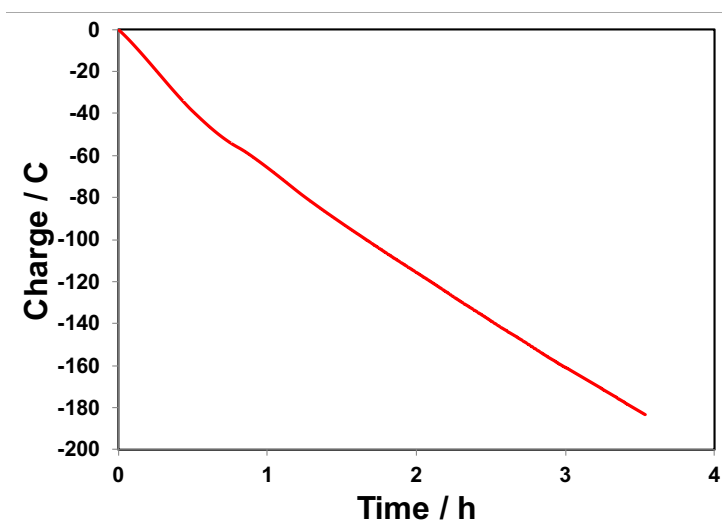


Figure S83. CPE plot for hydrogenation of **1d** in neat CH₃CN.

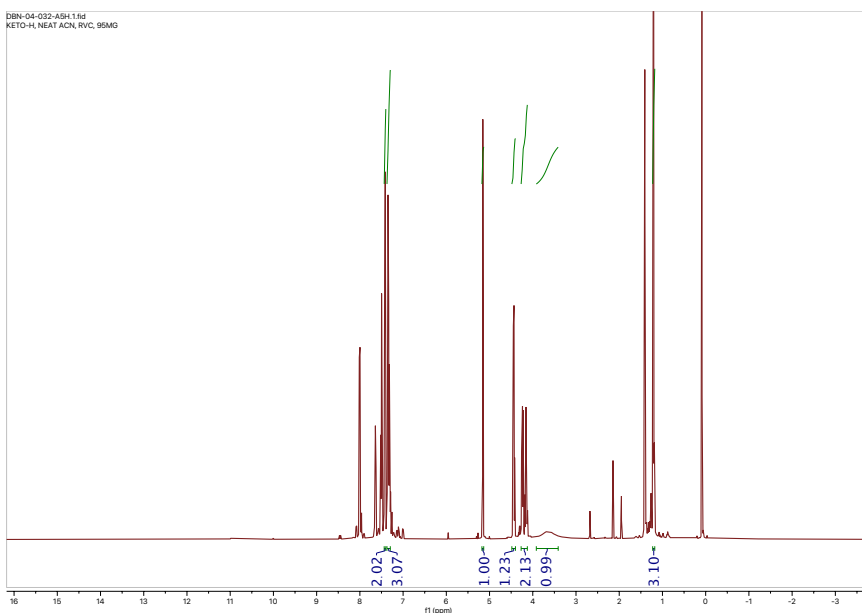


Figure S84. ¹H NMR (500 MHz, 22 °C, CDCl₃) of **1d-H₂** produced in neat CH₃CN.

pH Changes During Electrolytic Hydrogenation of **1b**

For the bulk electrolysis of **1b** performed using the standard hydrogenation conditions noted above, the pH was measured before and after the run using a digital pH meter. The initial pH was measured to be $\text{pH}_{\text{initial}} = 2.60$ and had risen to $\text{pH}_{\text{final}} = 6.20$ after the electrolysis was stopped. The difference in solution pH can be used to estimate proportion of the charge that led to the consumption of additional protons for hydrogen gas evolution. While the pK_a of an acid is dependent on the solution conditions, the measured pH for the mixed $\text{CH}_3\text{CN}/\text{H}_2\text{O}$ medium used here is on the order of what would be expected for in water alone.¹¹ After accounting for the protons consumed in the hydrogenation of the organic substrate, the difference between initial protons added to solution (in the form of acetic acid) and the excess protons remaining in solution upon completion of electrolysis was calculated using the observed pH changes. This can be done through summing the proton containing molecules on both sides of the acetic acid equilibrium (pH measurement and Henderson-Hasselbalch equation). This calculation indicates that for the hydrogenation of **1b** (%FE for production of **1b-H₂** = 25 %, Table 1), 193 C (or 72.5 % of the overall charge passed) can be attributed to the consumption of H^+ in an HER type process, in excellent agreement with the unassigned charge of 200 C.

Electrochemical Hydrogenation of **1a at Lower Electrolyte Concentration**

Using a lower concentration of electrolyte (1.1 M), but otherwise following the general procedure, electrochemical hydrogenation was performed using LiClO_4 (1.000 g, 9.4 mmol), **1a** (0.088 g, 0.0410 mmol), acetic acid (150 μl , 2.62 mmol); $E_{\text{app}} = -0.9$ V vs. Ag/AgCl , 3.2 h. ^1H NMR analysis shows 73% conversion to hydrogenated product **1a-H₂**. Charge passed = 252 C.

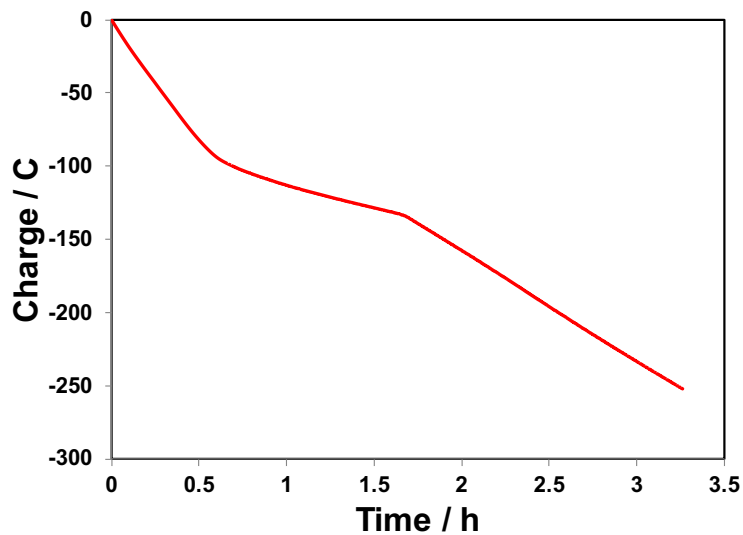


Figure S85. CPE plot for electrochemical hydrogenation of **1a** using the standard electrochemical hydrogenation conditions but with 1.1 M LiClO₄.

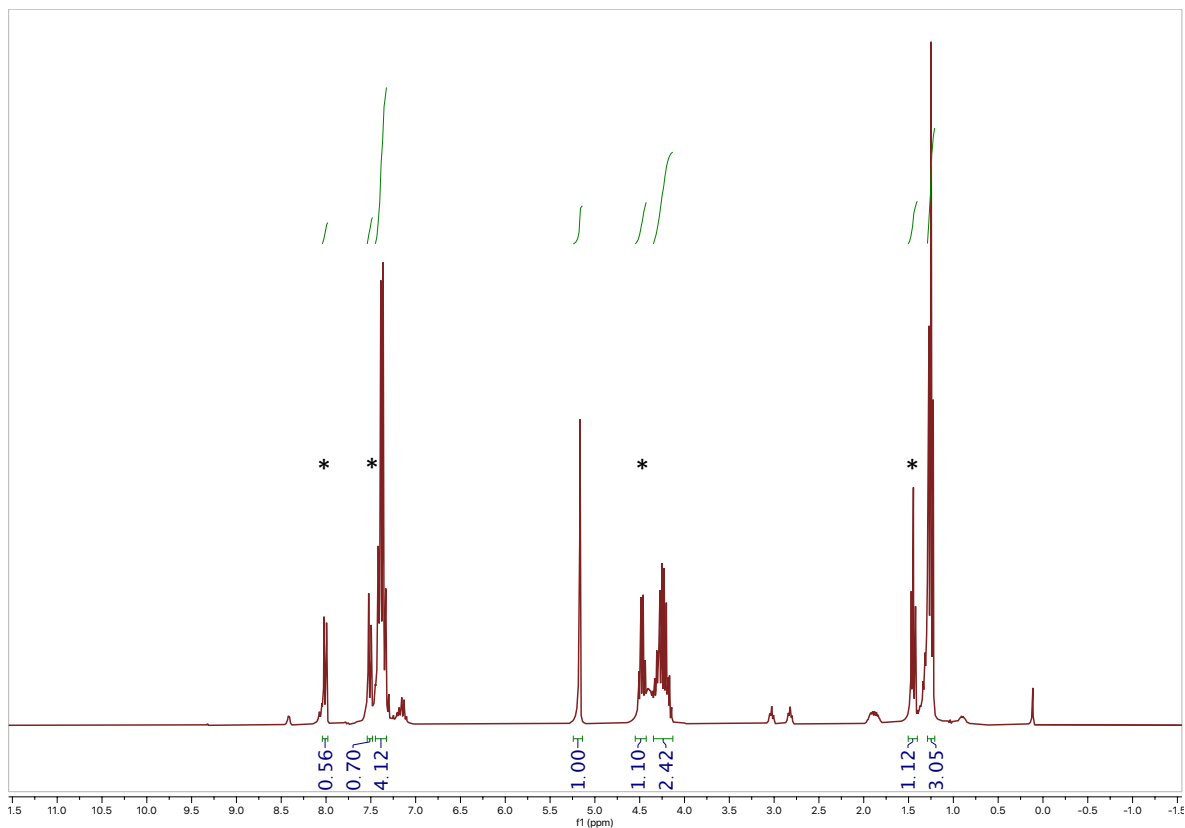


Figure S86. ¹H NMR (300 MHz, 22 °C, CDCl₃) of **1a**, using the standard electrochemical hydrogenation conditions but with 1.1 M LiClO₄. Unreacted starting material **1a** is denoted with an asterisk (*).

Electrochemical Hydrogenation Using Alternative Electrolytes

Using electrochemical grade LiCl as electrolyte in place of LiClO₄, the CH₃CN and water fractions of the solution were observed to partition and become immiscible, resulting in insufficient charge passage within the electrochemical cell for meaningful electrochemistry to occur. We also attempted replacing LiClO₄ with the common organic electrolyte [nBu₄N][PF₆]. Under otherwise identical general experimental conditions, the run of **2d** was replicated. In comparison with the general conditions, 32% lower conversion to **2d-H₂** was observed, and isolation of the hydrogenated product was complicated by the similar solubility of [nBu₄N][PF₆] and substrate/product.

Electrochemical Production of 2d-H₂ Using Alternate Electrolyte: Using [nBu₄N][PF₆] instead of LiClO₄ as the electrolyte, but otherwise following the general procedure a bulk electrolysis was performed using [nBu₄N][PF₆] (3.250 g, 8.390 mmol), 3-phenyl-2H-benzo[*b*][1,4]oxazin-2-one (0.120 g, 0.538 mmol), acetic acid (150 μl, 2.62 mmol); $E_{app} = -0.9$ V vs. Ag/AgCl, 3.2 h. ¹H NMR analysis shows 66% conversion to hydrogenated product. Charge passed = 340 C.

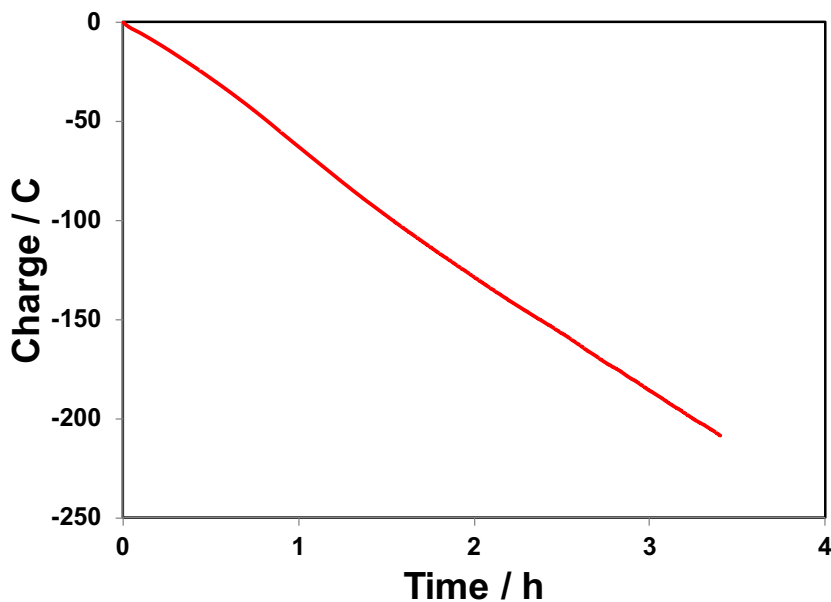


Figure S87. CPE plot of **2d**, using the standard electrochemical hydrogenation conditions but with $[n\text{Bu}_4\text{N}][\text{PF}_6]$ as the electrolyte.

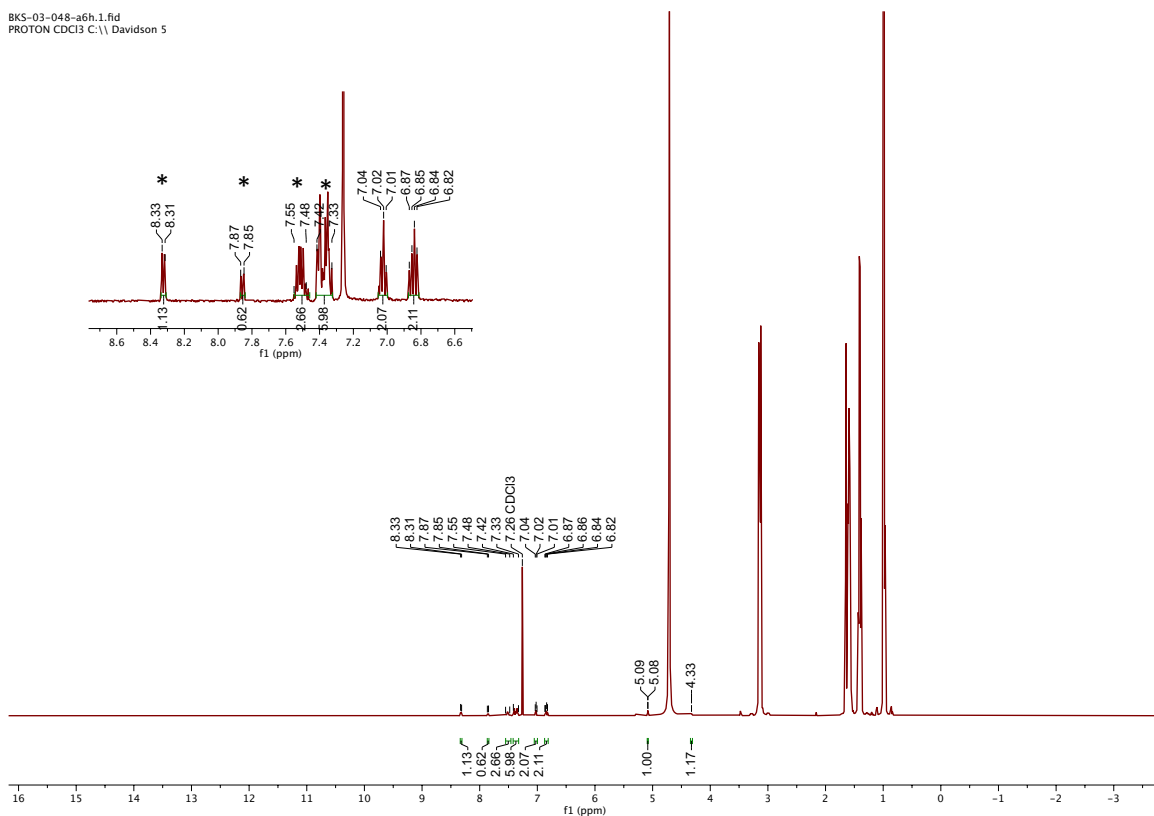


Figure S88. ¹H NMR (500 MHz, 22 °C, CDCl₃) of **2d**, using the standard electrochemical hydrogenation conditions but with $[n\text{Bu}_4\text{N}][\text{PF}_6]$ as the electrolyte. Unreacted starting material **1a** is denoted with an asterisk (*). The major species present is $[n\text{Bu}_4\text{N}][\text{PF}_6]$.

Attempted Electrochemical Hydrogenation of Alkylated Ketoester **1k**

The general procedure was followed using LiClO₄ (1.30 g, 12.2 mmol), *tert*-butyl 2-oxopropanoate (**1k**; 0.065 g, 0.451 mmol), and acetic acid (0.146 mL, 2.54 mmol); $E_{app} = -0.9$ V vs. Ag/AgCl, 6.0 h. No significant amount of hydrogenated product could be observed in, nor isolated from, the crude reaction mixture. Charge passed = 515 C.

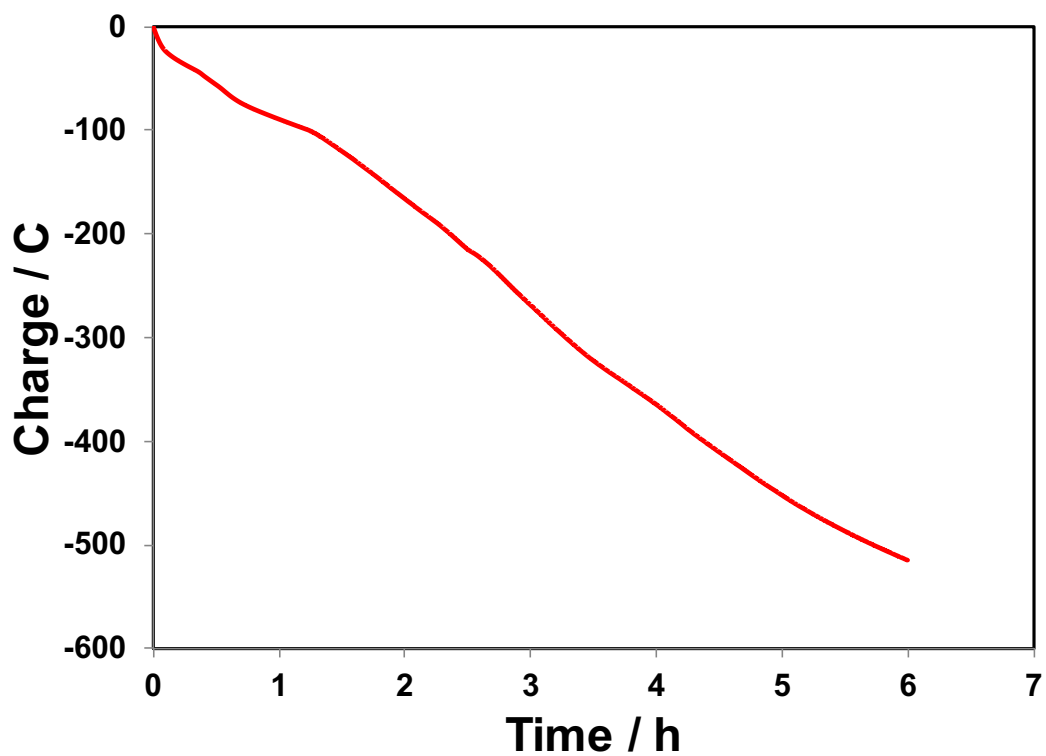
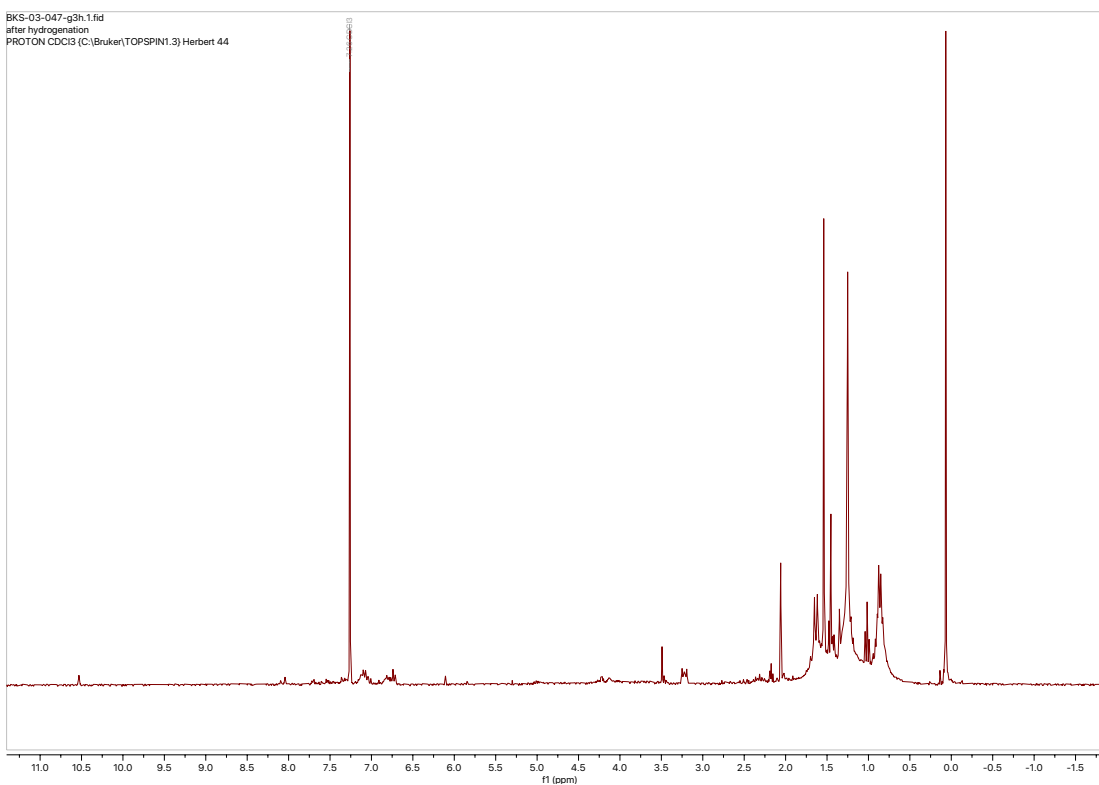
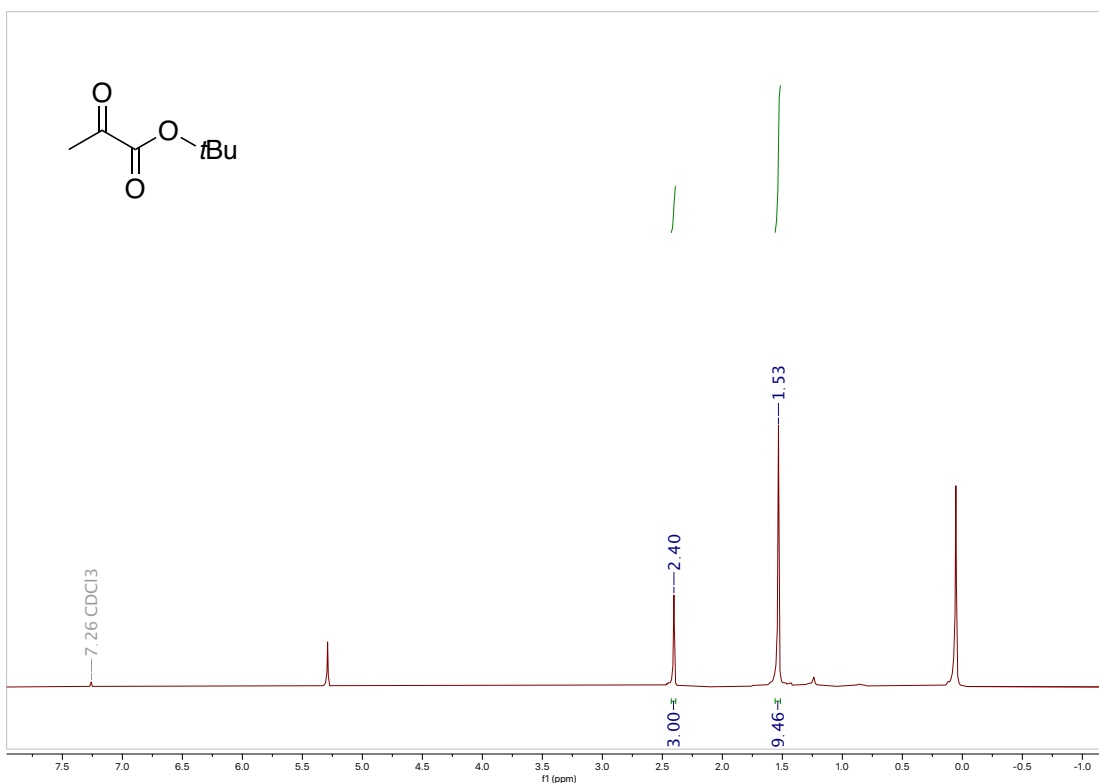


Figure S89. CPE plot of the attempted formation of *tert*-butyl 2-hydroxypropanoate **1k**.



X-RAY CRYSTALLOGRAPHY EXPERIMENTAL

Crystal structure data was using collected from multi-faceted crystals of suitable size and quality selected from a representative sample of crystals of the same habit using an optical microscope. In each case, crystals were mounted on MiTiGen loops and data collection carried out in a cold stream of nitrogen (150 K; Bruker D8 QUEST ECO). All diffractometer manipulations were carried out using Bruker APEX3 software.¹² Absorption corrections were applied using SADABS.¹³ Structure solution and refinement was carried out using XS, XT and XL programs,¹⁴ embedded within the OLEX2 software suite.¹⁵ For each structure, the absence of additional symmetry was confirmed using ADDSYM incorporated in the PLATON program.¹⁶ CCDC Nos. 2024461-2024463 and 2026013-2026014 contain the supplementary crystallographic data for this paper. The data can be obtained free of charge from The Cambridge Crystallographic Data Centre via www.ccdc.cam.ac.uk/structures.

Crystal structure data for **2g** (CCDC 2024461): X-ray quality crystals were grown by slow evaporation of a chloroform solution. Crystal structure parameters: colourless plate; $C_{15}H_8F_3NO_2$ 291.22 g mol⁻¹, monoclinic, space group $P2_1/n$; $a = 7.6065(4)$ Å, $b = 5.8376(3)$ Å, $c = 27.3880(14)$ Å, $\alpha = \gamma = 90^\circ$, $\beta = 96.766(2)^\circ$, $V = 1207.66(11)$ Å³; $Z = 4$, $\rho_{\text{calcd}} = 1.602$ g cm⁻³; crystal dimensions 0.450 x 0.160 x 0.060 mm; $2\theta_{\text{max}} = 55.88^\circ$; 36910 reflections, 2889 independent ($R_{\text{int}} = 0.0690$, intrinsic phasing; absorption coeff ($\mu = 0.138$ mm⁻¹), absorption correction semi-empirical from equivalents (SADABS); refinement (against F_o^2) with SHELXTL V6.1, 190 parameters, 0 restraints, $R_I = 0.0443$ ($I > 2\sigma$) and $wR_2 = 0.1108$ (all data), Goof = 1.027, residual electron density 0.29/−0.37 Å⁻³.

Crystal structure data for **2g-H₂** (CCDC 2024462): X-ray quality crystals were grown by slow evaporation of a chloroform solution. Crystal structure parameters: Colourless blocks; C₁₅H₁₀F₃NO₂ 293.24 g mol⁻¹, monoclinic, space group *Cc*; *a* = 24.5598(16) Å, *b* = 4.6673(3) Å, *c* = 11.1063(7) Å, $\alpha = \gamma = 90^\circ$, $\beta = 92.835(2)^\circ$, *V* = 1271.53(14) Å³; *Z* = 4, $\rho_{\text{calcd}} = 1.532 \text{ g cm}^{-3}$; crystal dimensions 0.310 x 0.120 x 0.030 mm; $2\theta_{\text{max}} = 55.034^\circ$; 18036 reflections, 2901 independent ($R_{\text{int}} = 0.0565$), intrinsic phasing; absorption coeff ($\mu = 0.131 \text{ mm}^{-1}$), absorption correction semi-empirical from equivalents (SADABS); refinement (against F_o^2) with SHELXTL V6.1, 222 parameters, 2 restraints, $R_I = 0.0395$ ($I > 2\sigma$) and $wR_2 = 0.0830$ (all data), Goof = 1.063, residual electron density 0.18/−0.21 Å⁻³.

Crystal structure data for **1j** (CCDC 2024463): X-ray quality crystals were grown by the layering of a CH₂Cl₂ solution with diethylether solution. Colourless needles; C₁₆H₂₀O₃ 260.32 g/mol, monoclinic, space group *P2₁/c*; *a* = 8.0826(3) Å, *b* = 22.3489(9) Å, *c* = 8.0949(3) Å, $\alpha = \gamma = 90^\circ$, $\beta = 107.167(2)^\circ$, *V* = 1397.09(9) Å³; *Z* = 4, $\rho_{\text{calcd}} = 1.238 \text{ g cm}^{-3}$; crystal dimensions 0.210 x 0.150 x 0.120 mm; $2\theta_{\text{max}} = 48.12^\circ$; 31846 reflections, 2489 independent ($R_{\text{int}} = 0.0680$), intrinsic phasing; absorption coeff ($\mu = 0.084 \text{ mm}^{-1}$), absorption correction semi-empirical from equivalents (SADABS); refinement (against F_o^2) with SHELXTL V6.1, 174 parameters, 0 restraints, $R_I = 0.0373$ ($I > 2\sigma$) and $wR_2 = 0.0874$ (all data), Goof = 1.044, residual electron density 0.13/−0.19 Å⁻³.

Crystal structure data for **2a** (CCDC 2026013): X-ray quality crystals were grown by slow evaporation of a CHCl₃ solution. Colourless blocks; C₁₄H₈ClNO₂ 257.66 g/mol, monoclinic, space group *P2₁/n*; *a* = 3.8058(2) Å, *b* = 21.9865(13) Å, *c* = 13.2467(8) Å, *α* = *γ* = 90°, *β* = 94.488(2)°, *V* = 1105.04(11) Å³; *Z* = 4, *ρ*_{calcd} = 1.549 g cm⁻³; crystal dimensions 0.630 x 0.180 x 0.160 mm; 2*θ*_{max} = 55.15°; 2522 reflections, 2522 independent (*R*_{int} = 0.1095, intrinsic phasing; absorption coeff (*μ* = 0.336 mm⁻¹), absorption correction semi-empirical from equivalents (SADABS); refinement (against *F*_o²) with SHELXTL V6.1, 164 parameters, 0 restraints, *R*_I = 0.0695 (*I* > 2*σ*) and *wR*₂ = 0.1556 (all data), Goof = 1.299, residual electron density 0.37/−0.36 Å⁻³. A two-component twin was found (79:21) and treated with the appropriate twin law found using TWINROTMAT embedded in the PLATON program.¹⁷

Crystal structure data for **2b** (CCDC 2026014): X-ray quality crystals were grown by slow evaporation of a CHCl₃ solution. Pink needles; C₁₅H₁₁NO₂ 237.25 g/mol, orthorhombic, space group *P2₁2₁2₁*; *a* = 7.0081(3) Å, *b* = 12.2782(6) Å, *c* = 13.4697(6) Å, *α* = *β* = *γ* = 90°, *V* = 1159.03(9) Å³; *Z* = 4, *ρ*_{calcd} = 1.360 g cm⁻³; crystal dimensions 0.490 x 0.110 x 0.070 mm; 2*θ*_{max} = 55.546°; 30662 reflections, 2728 independent (*R*_{int} = 0.0726, intrinsic phasing; absorption coeff (*μ* = 0.091 mm⁻¹), absorption correction semi-empirical from equivalents (SADABS); refinement (against *F*_o²) with SHELXTL V6.1, 164 parameters, 0 restraints, *R*_I = 0.0410 (*I* > 2*σ*) and *wR*₂ = 0.0921 (all data), Goof = 1.040, residual electron density 0.24/−0.21 Å⁻³.

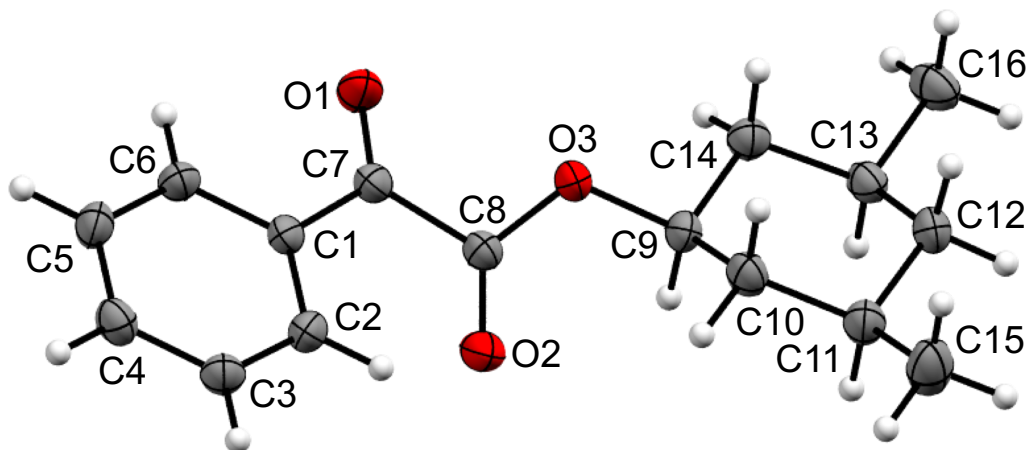


Figure S92. Solid-state structure of **1j** (CCDC 2024463) with thermal ellipsoids shown at 50% probability levels. Selected bond distances (Å) and angles (°): C1-C7 1.4789(19), C7-C8 1.531(2), C7-O1 1.2147(17), C8-O2 1.1999(17), C8-O3 1.3290(16), C9-O3 1.4728(17); C1-C7-C8 119.33(12), O1-C7-C1 122.85(13), O1-C7-C8 117.73(13), O2-C8-C7 122.96(13), O2-C8-O3 126.18(13), O3-C8-C7 110.67(11).

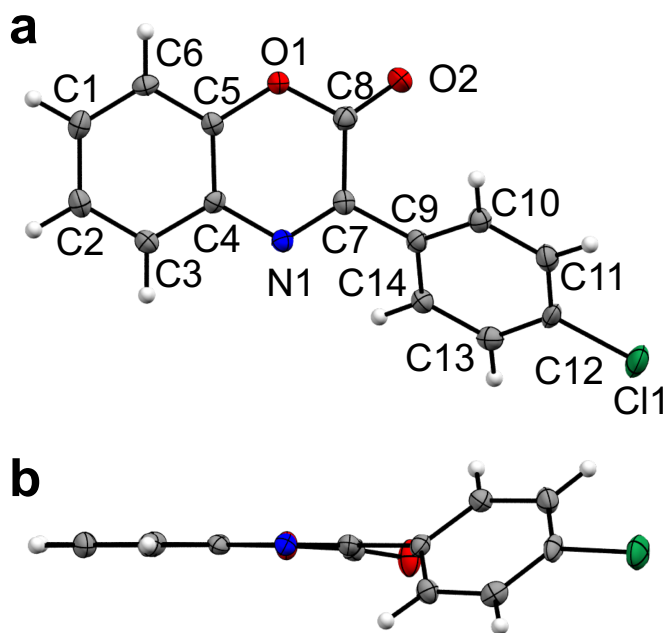


Figure S93. (a) Solid-state structure of **2a** (CCDC 2026013) with thermal ellipsoids shown at 50% probability levels. Selected bond distances (Å) and angles (°): N(1)-C(7) 1.292(5), N(1)-C(4) 1.394(5), C(7)-C(8) 1.494(5), C(7)-C(9) 1.475(6); C(4)-N(1)-C(7) 118.2(3), N(1)-C(7)-C(8) 122.9(3), N(1)-C(7)-C(9) 119.8(3), C(9)-C(7)-C(8) 117.3(3). (b) View along N1-O1 vector showing the 43° angle between the plane formed by C1-C8/O1/N1 and the plane formed by C9-C14.

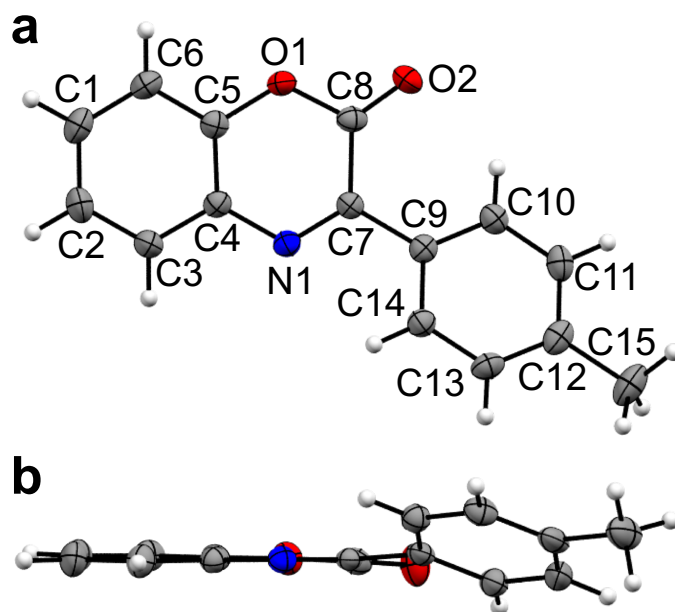


Figure S94. (a) Solid-state structure of **2b** (CCDC 2026014) with thermal ellipsoids shown at 50% probability levels. Selected bond distances (Å) and angles (°): N(1)-C(7) 1.290(3), N(1)-C(4) 1.393(3), C(7)-C(8) 1.500(3), C(7)-C(9) 1.484(3); C(4)-N(1)-C(7) 119.27(18), N(1)-C(7)-C(8) 122.43(19), N(1)-C(7)-C(9) 118.47(19), C(9)-C(7)-C(8) 119.07(19). (b) View along N1-O1 vector showing the 29° angle between the plane formed by C1-C8/O1/N1 and the plane formed by C9-C14.

REFERENCES

- 1 M. Hayashi and S. Nakamura, Catalytic Enantioselective Protonation of α -Oxygenated Ester Enolates Prepared through Phospha-Brook Rearrangement, *Angew. Chem., Int. Ed.*, 2011, **50**, 2249–2252.
- 2 J. Zhu, Y. Yuan, S. Wang and Z.-J. Yao, Synthesis of 2,3-Dialkylated Tartaric Acid Esters via Visible Light Photoredox-Catalyzed Reductive Dimerization of α -Ketoesters, *ACS Omega*, 2017, **2**, 4665–4677.
- 3 Z. Han, G. Liu, R. Wang, X.-Q. Dong and X. Zhang, Highly efficient Ir-catalyzed asymmetric hydrogenation of benzoxazinones and derivatives with a Brønsted acid cocatalyst, *Chem. Sci.*, 2019, **10**, 4328–4333.
- 4 N. G. Connelly and W. E. Geiger, Chemical Redox Agents for Organometallic Chemistry., *Chem. Rev.*, 1996, **96**, 877–910.
- 5 L.-Q. Lu, Y. Li, K. Junge and M. Beller, Iron-Catalyzed Hydrogenation for the In Situ Regeneration of an NAD(P)H Model: Biomimetic Reduction of α -Keto/ α -Iminoesters, *Angew. Chem., Int. Ed.*, 2013, **52**, 8382–8386.
- 6 M. Sugaya, T. Yamamoto and H. Shinozaki, Palladium catalyzed synthesis of mandelate derivatives from arylboronic acids and glyoxylate hemiacetals, *Tetrahedron Lett.*, 2017, **58**, 2495–2497.
- 7 H. H. San, S.-J. Wang, M. Jiang and X.-Y. Tang, Boron-Catalyzed O–H Bond Insertion of α -Aryl α -Diazoesters in Water, *Org. Lett.*, 2018, **20**, 4672–4676.
- 8 Y. Motoyama, K. Morii, S. Ishizuka, S. Inomoto, Z. Zhang and S.-H. Yoon, Specific Inhibition of the Hydrogenolysis of Benzylic C–O Bonds Using Palladium Nanoparticles Supported on Nitrogen-Doped Carbon Nanofibers, *ChemCatChem*, 2018, **10**, 505–509.
- 9 Z.-Y. Xue, Y. Jiang, X.-Z. Peng, W.-C. Yuan and X.-M. Zhang, The First General, Highly Enantioselective Lewis Base Organo-catalyzed Hydrosilylation of Benzoxazinones and Quinoxalinones, *Adv. Synth. Catal.*, 2010, **352**, 2132–2136.
- 10 X. Zhang, B. Xu and M.-H. Xu, Rhodium-catalyzed asymmetric arylation of N- and O-containing cyclic aldimines: facile and efficient access to highly optically active 3,4-dihydrobenzo[1,4]oxazin-2-ones and dihydroquinoxalinones, *Org. Chem. Front.*, 2016, **3**, 944–948.
- 11 Y. M. Kwon, Y. Lee, G. E. Evenson, T. A. Jackson and D. Wang, Crystal Structure and C–H Bond-Cleaving Reactivity of a Mononuclear Co^{IV}–Dinitrate Complex, *J. Am. Chem. Soc.*, 2020, **142**, 13435–13441.
- 12 Bruker-AXS, *APEX3 v2016.1-0*, Madison, Wisconsin, USA, 2016.
- 13 G. M. Sheldrick, *SADABS, Program for Absorption Correction for Data from Area Detector Frames*, University of Göttingen, Göttingen, Germany, 2008.
- 14 G. M. Sheldrick, A Short History of SHELX, *Acta Cryst.*, 2008, **A64**, 112–122.
- 15 O. V. Dolomanov, L. J. Bourhis, R. J. Gildea, J. A. K. Howard and H. Puschmann, OLEX2: a complete structure solution, refinement and analysis program, *J. Appl. Crystallogr.*, 2009, **42**, 339–341.
- 16 A. L. Spek, Structure Validation in Chemical Crystallography, *Acta Cryst.*, 2009, **D65**, 148–155.
- 17 A. L. Spek, *PLATON, A Multipurpose Crystallographic Tool*, Utrecht University, Utrecht, The Netherlands, 1998.